Refined topological vertex for a 5D $Sp(N)$ gauge theories with antisymmetric matter

Shi Cheng[1,2,*] and Sung-Soo Kim[1,†]

[1]*School of Physics, University of Electronic Science and Technology of China, No. 2006 Xiyuan Avenue, West Hi-Tech Zone, Chengdu, Sichuan 611731, China*

[2]*Faculty of Physics, University of Warsaw, ulica Pasteura 5, 02-093 Warsaw, Poland*

(Received 25 April 2021; accepted 3 September 2021; published 4 October 2021)

We consider type IIB 5-brane web diagrams for a 5D $Sp(N)$ gauge theory with an antisymmetric hypermultiplet and N_f fundamental hypermultiplets. The corresponding 5-branes can be obtained by Higgsing a 5-brane web for quiver gauge theory. We use the refined topological vertex formalism to compute Nekrasov partition functions of 5D $Sp(2)$ theories with one antisymmetric hypermultiplet and flavors. Our results agree with the known results obtained from the Atiyah-Drinfeld-Hitchin-Manin method. We also discuss a particular tuning of Kähler parameters associated with this Higgsing.

DOI: 10.1103/PhysRevD.104.086004

I. INTRODUCTION

A large class of five-dimensional (5D) $\mathcal{N}=1$ supersymmetric gauge theories [1] can be constructed in type IIB 5-brane webs [2,3] or in M theory on Calabi-Yau threefolds [4–7]. The duality between a 5-brane web in type IIB string theory and a toric Calabi-Yau threefold in M theory [8] enables one to utilize the topological string partition function on a toric Calabi-Yau threefold to obtain the Bogomol'nyi-Prasad-Sommerfield partition function of a 5D gauge theory on the dual 5-brane web [9–14]. The topological string method known as (refined) topological vertex [15–19] thus provides another powerful tool for computing the partition function of 5D $\mathcal{N}=1$ gauge theories.

In recent years, there has been much progress on understanding 5D $\mathcal{N}=1$ gauge theories from the perspective of type IIB 5-brane webs [20–28], revealing that an even larger class of 5D $\mathcal{N}=1$ theories can be realized by 5-brane webs. For instance, 5D $SU(2)$ theories with $5 \leq N_f \leq 7$ hypermultiplets in the fundamental representation (flavors) can be obtained by Higgsing of a 5-brane web for T_3, T_4, and T_6 theories, respectively [29]. It is straightforwardly generalized to a 5D $SU(N)$ theory with $2N+1 \leq N_f \leq 2N+3$ flavors. The dual diagrams for these 5-brane webs are generically nontoric, as they can be understood as a Higgsed diagram of certain quiver theories [22,23,30]. 5D $SO(N)/Sp(N)$ (quiver) gauge theories with the number of hypermultiplets in the fundamental representation exceeding the bound in Ref. [7] can also be constructed from 5-brane webs with the orientifold planes by Higgsing [24,31]. Moreover, $Sp(N)$ gauge theories with the hypermultiplet in the antisymmetric representation [24] and $SO(N)$ gauge theories with hypermultiplets in the spinor representation [32] are also constructed. Even G_2 gauge theories with $N_f \leq 6$ flavors are represented by 5-brane webs [33]. Dual diagrams for such 5-brane webs are generically nontoric, as they can be obtained by a Higgsing of some certain quiver theory and also by introduction of the orientifolds, implying that the corresponding Calabi-Yau threefolds are nontoric.

The topological vertex formalism also has been implemented to nontoric Calabi-Yau threefolds [20,34,35] by tuning Kähler parameters [36–39]. Even for a nontoric diagram with an $O5$ plane, (unrefined) topological vertex formalism was newly proposed [40], which enables one to compute the partition function for 5D G_2 gauge theories based on a 5-brane web with an $O5$ plane [33], which agrees with the field theory results up to two instanton contributions [41–46]. Though the topological vertex formalism is applicable to 5D gauge theories of various gauge groups, application of the topological vertex to theories with a hypermultiplet other than the fundamental hypermultiplet is still limited.

In this paper, we utilize the topological vertex to compute the partition function for a 5D $Sp(N)$ theory with an antisymmetric hypermultiplet and $N_f \leq 7$ flavors. The theory has the fixed point at UV where the global symmetry is enhanced to $E_{N_f+1} \times SU(2)$ [1,4–7]. The partition function for a 5D $Sp(N)$ theory with a massless antisymmetric hypermultiplet and $5 \leq N_f \leq 7$ flavors was

*scheng@fuw.edu.pl
†sungsoo.kim@uestc.edu.cn

already computed based on web diagrams of Higgsed T_N theories [35]. Here, we consider 5D $Sp(N)$ theories with a *massive* antisymmetric hypermultiplet and N_f flavors, whose diagrams are obtained from Higgsing of a certain quiver gauge theory [24,26]. To obtain the Nekrasov partition function from the corresponding nontoric diagram, one needs to properly tune Kähler parameters associated with the Higgsing. We find a proper tuning for the Kähler parameters by comparing the partition function obtained from the topological vertex result with the known result from localization. As such Higgsed parts of the 5-brane web are locally a T_2 diagram, such tuning can be also determined by considering tuning of a T_2 diagram (T_2 tuning). Following Ref. [47], global symmetry enhancement can be shown by redefining the gauge theory parameters to make the fiber-base duality manifest.

The paper is organized as follows. In Sec. II, we discuss 5-brane configurations for 5D $Sp(N)$ gauge theories with one antisymmetric hypermultiplet and flavors. In Sec. III, we review the refined topological vertex formalism and discuss a special tuning of Kähler parameters for a 5-brane diagram for a T_2 theory, which is associated with the Higgsing of 5-brane webs giving rise to $Sp(N)$ gauge theories with an antisymmetric hypermultiplet. In Sec. IV, we compute the instanton partition function for $Sp(2)$ gauge theories with an antisymmetric hypermultiplet and $N_f \leq 4$ flavors and also discuss $Sp(3)$ gauge theory as an example of generalization to a higher rank gauge group. We then conclude with some remarks in Sec. V.

A *Mathematica* package for a refined topological vertex for generic toric diagrams is accompanied and available at the arXiv Web site or Ref. [48]. The package would be used for more complicated toric diagrams.

II. 5-BRANE CONFIGURATIONS FOR $Sp(N)$ GAUGE THEORY WITH ANTISYMMETRIC MATTER

From the perspective of type I′ string theory, 5D $Sp(N)$ gauge theories with N_f hypermultiplets in the fundamental representation (flavors) and one hypermultiplet in the antisymmetric representation are realized as N D4-branes near the N_f D8-branes on top of a single $O8^-$ orientifold plane. The theory has a superconformal fixed point that arises in the infinite coupling limit of the gauge theory. It exhibits $SO(2N_f) \times U(1)_I \times SU(2)_{\text{antisym}}$ global symmetry of flavors, instanton number, and an antisymmetric hypermultiplet. At the UV fixed point, the global symmetry is enhanced to [1]

$$E_{N_f+1} \times SU(2)_{\text{antisym}} \supset SO(2N_f) \times U(1)_I \times SU(2)_{\text{antisym}}, \tag{2.1}$$

where E_n refer to E_8, E_7, and E_6; $E_5 = Spin(10)$, $E_4 = SU(5)$, $E_3 = SU(3) \times SU(2)$, $E_2 = SU(2) \times U(1)$, and $E_1 = SU(2)$. The enhancement of global symmetry is explicitly checked from the superconformal index based on the Atiyah-Drinfeld-Hitchin-Manin (ADHM) method [49,50]. Without any flavors, $Sp(N)$ gauge theory with or without antisymmetric hypers has the discrete theta parameters (angles) associated with $\pi_4(Sp(N)) = \mathbb{Z}_2$, referred to as $\theta = 0, \pi$. Hence, there are two inequivalent pure $Sp(N)$ gauge theories: one with $\theta = 0$, denoted as $Sp(N)_0$, and the other with $\theta = \pi$, denoted as $Sp(N)_\pi$. The origin of the discrete theta parameters from type I′ theory is discussed in Ref. [51]. We note that $Sp(N)_0$ theory with an antisymmetric hypermultiplet enjoys enhanced global symmetry $SU(2)_I \times SU(2)_{\text{antisym}}$ at the UV fixed point, while $Sp(N)_\pi$ theory with an antisymmetric hypermultiplet has $U(1)_I \times SU(2)_{\text{antisym}}$. Without antisymmetric matter, both theories have only $U(1)_I$ global symmetry, except for the $Sp(1)$ theory, where the global symmetry is enhanced to $SU(2)_I \supset U(1)_I$.

A 5D $Sp(N)$ gauge theory can also be understood from type IIB string theory. In fact, a wide range of 5D $\mathcal{N} = 1$ theories can be described by type IIB string theory, which provides not only qualitative understanding but also quantitative aspects for 5D gauge theories. To describe a 5D $Sp(N)$ gauge theory in type IIB string theory, one can introduce an $O5$ plane or an $O7^-$ plane. As a representative example, 5-brane webs for pure $Sp(N)$ gauge theory are depicted in Fig. 1. In 5-brane webs with an $O5$ plane, when one changes the coupling of the pure $Sp(N)$ theory, the brane configurations are deformed in two different ways. These two different phases distinguish the discrete theta angles for the pure $Sp(N)$ theory [52]. One can also compute the (unrefined) partition function of $Sp(N)$ theory with $N_f \leq 2N + 6$ flavors based on a 5-brane web using the topological vertex method [40].

5-brane configurations with an $O7^-$ plane are, in particular, interesting. An $O7^-$ plane can be resolved into a pair of two 7-branes of the same monodromy [53]. For instance, suppose one resolves an $O7^-$ plane in Fig. 2(a), and then the resulting 5-brane configuration becomes a 5-brane configuration for an $SU(N+1)_\kappa$ theory with the Chern-Simons level $\kappa = 2N + 6 - 2|\kappa|$ as depicted in Fig. 2(b) and, hence, provides a diagrammatical account for the duality between 5D $Sp(N)$ gauge theory with

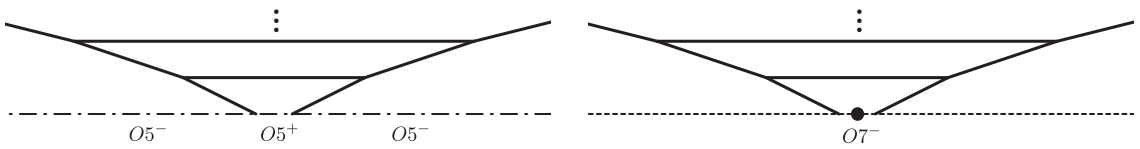

FIG. 1. (a) A 5-brane web for $Sp(N)$ with an $O5$ plane. (b) A 5-brane web for $Sp(N)$ with an $O7^-$ plane.

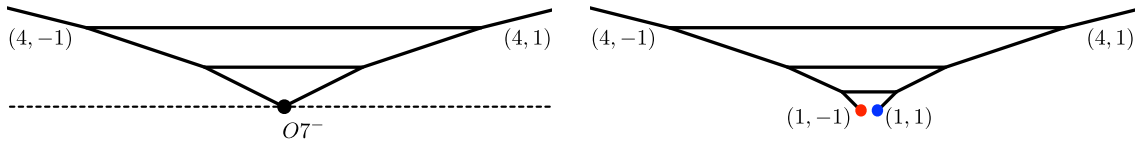

FIG. 2. (a) A deformation of a 5-brane web with an $O7^-$ plane for pure $Sp(2)$. (b) Resolution of an $O7^-$ plane into a pair of 7-branes of the charge (1,1) and $(1,-1)$. The resulting diagram is pure $SU(5)$ theory of Chern-Simons level -5.

$N_f \leq 2N+6$ flavors and $SU(N+1)$ gauge theory with the same number of N_f flavors [23,54], where flavors in 5-brane webs are represented by D7-branes.

For $Sp(N)$ gauge theory with an antisymmetric hypermultiplet, it is still a challenge to describe the theory based on 5-brane webs with an $O5$ plane. It is, however, possible to describe antisymmetric matter of an $Sp(N)$ theory using $O7^-$ planes. To realize an $Sp(N)$ theory with an antisymmetric hypermultiplet, one introduces two $O7^-$ planes horizontally separated on a 5-brane web, and N D5-branes are placed parallel to two $O7^-$ planes as depicted in Fig. 3. An alternative description is to introduce a half NS 5-brane stuck on one of the $O7^-$ planes [24] as in Fig. 4. While the 5-brane description in Fig. 3 corresponds to an $Sp(N)$ theory with a massless antisymmetric hypermultiplet [29], the 5-brane in Fig. 4 describes an $Sp(N)$ theory with a massive antisymmetric hypermultiplet, where the mass of an antisymmetric hypermultiplet is parameterized by the vertical distance between two $O7^-$ planes.

The discrete theta parameters for $Sp(N)$ gauge theory in this 5-brane web with $O7^-$-planes are realized as two different resolutions of an $O7^-$ plane into a pair of 7-branes [24]. For instance, $O7^-$ can be resolved either into a pair of 7-branes of the charges $[1,-1]$ and [1, 1] or into a pair of 7-branes of the charges $[2,-1]$ and [0, 1]. If one resolves two $O7^-$ planes into the same types of 7-brane pairs, then it

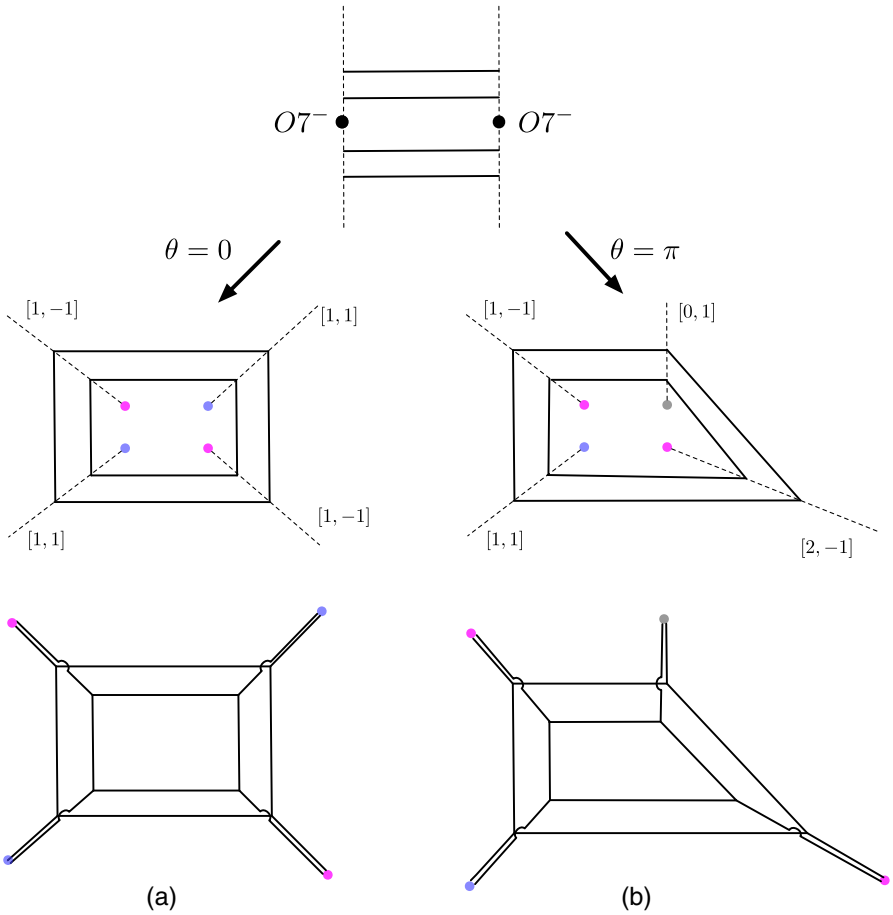

FIG. 3. Massless case: (a) 5-brane configuration for $Sp(2)_0 + 1\mathbf{AS}$, where resolving two $O7^-$ planes into the same types of a 7-brane pair (in this case, those of the 7-brane charges [1, 1] and $[1,-1]$) yields the discrete theta angle $\theta = 0$. (b) 5-brane configuration for $Sp(2)_\pi + 1\mathbf{AS}$, where resolving two $O7^-$ planes into the different types of 7-brane pairs [in this case, $([1,1],[1,-1])$ and $([2,-1],[0,1])$] yields the discrete theta angle $\theta = 0$.

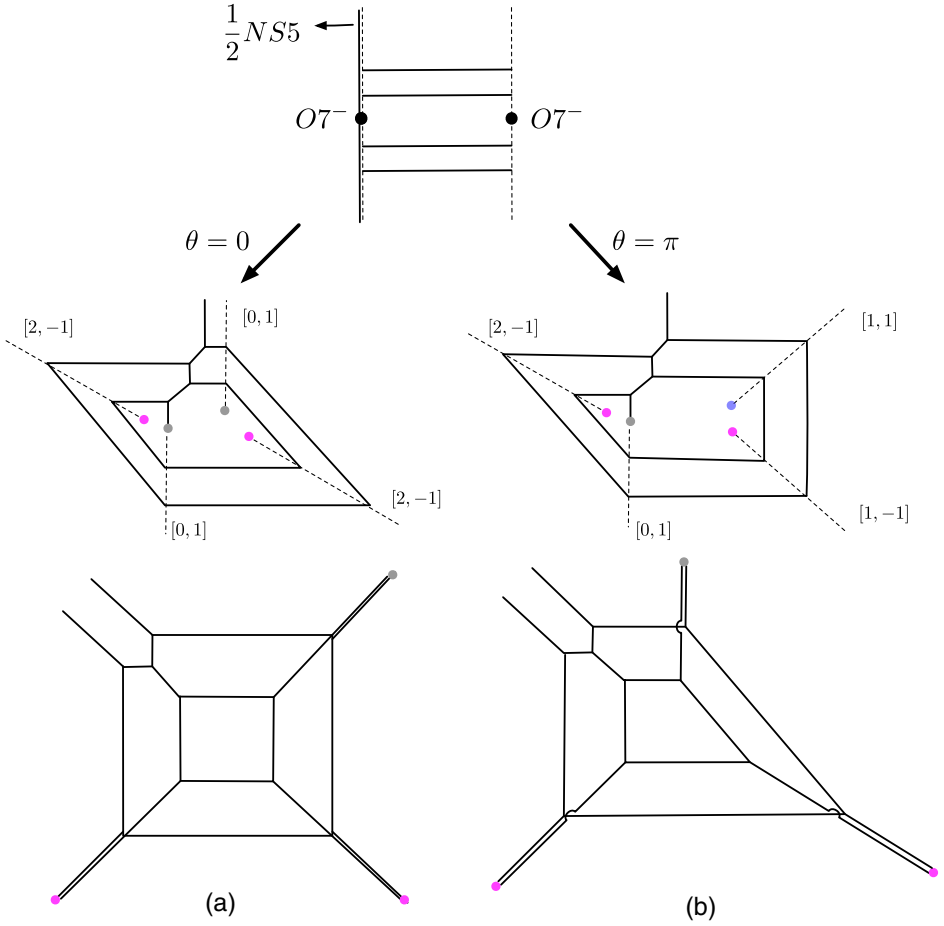

FIG. 4. Massive cases: (a) A 5-brane configuration for $Sp(2)_0 + 1\mathbf{AS}$. (b) A 5-brane configuration for $Sp(2)_\pi + 1\mathbf{AS}$. The 5-brane diagrams in the bottom are obtained after pulling out 7-branes from 5-brane loops and performing $SL(2,\mathbb{Z})$ transformations.

gives the discrete theta angle $\theta = 0$, while the resolution into two different types of 7-brane pairs leads to the discrete theta angle $\theta = \pi$. One can summarize 5-brane configurations for $Sp(N)$ theory with an antisymmetric hypermultiplet with the discrete theta angle $\theta = 0$ $(Sp(N)_0 + 1\mathbf{AS})$ and that with the discrete theta angle $\theta = \pi$ $(Sp(N)_\pi + 1\mathbf{AS})$ as follows: For a massless antisymmetric hypermultiplet, it is depicted in Fig. 3. For a massive antisymmetric hypermultiplet, it is depicted in Fig. 4.

Flavors can be introduced by adding D7-branes. We list some representative 5-brane webs for 5D $Sp(N)$ gauge theory with one antisymmetric hypermultiplet and N_f flavors $[Sp(N) + 1\mathbf{AS} + N_f\mathbf{F}]$ in Fig. 5. For web diagrams for $Sp(2) + 1\mathbf{AS} + N_f(\leq 8)\mathbf{F}$, see the Appendix in Ref. [55].

As one can see, 5-brane web diagrams for 5D $Sp(N)$ theories with an antisymmetric hypermultiplet have jumps on the (p, q) plane. In other words, the corresponding dual diagrams are nontoric. Such a 5-brane web can be regarded as a Higgsed web diagram from some other (quiver) gauge theories. For instance, as we will see in the later sections, a 5-brane web for 5D $Sp(2)_0$ theory with an antisymmetric hypermultiplet can be obtained from a Higgsing of a $SU(2) \times SU(4) \times SU(2)$ quiver theory as shown in Fig. 6. Another example that we will discuss is a 5-brane web for 5D $Sp(3)_0$ theory with an antisymmetric hypermultiplet which can be obtained from a Higgsing of a $SU(2) \times SU(4) \times SU(6) \times SU(4) \times SU(2)$ quiver theory. Likewise, 5D $Sp(N)_0$ theory with an antisymmetric hypermultiplet can be obtained from a Higgsing of an $SU(2) \times SU(4) \times \cdots \times SU(2N) \times \cdots \times SU(4) \times SU(2)$ quiver theory.

III. TOPOLOGICAL VERTEX AND T_2 TUNING

In this section, we set up our convention and very briefly review the refined topological vertex formalism, which enables one to compute the Nekrasov partition function for 5D $\mathcal{N} = 1$ gauge theories, via geometric engineering [13,17]. We also discuss Higgsing procedures associated with $Sp(2)$ gauge theories with antisymmetric matter. Our convention closely follows that used in Ref. [56].

A. Brief review of topological vertex

5D $\mathcal{N} = 1$ gauge theory in a general Ω background can be engineered by some local toric Calabi-Yau

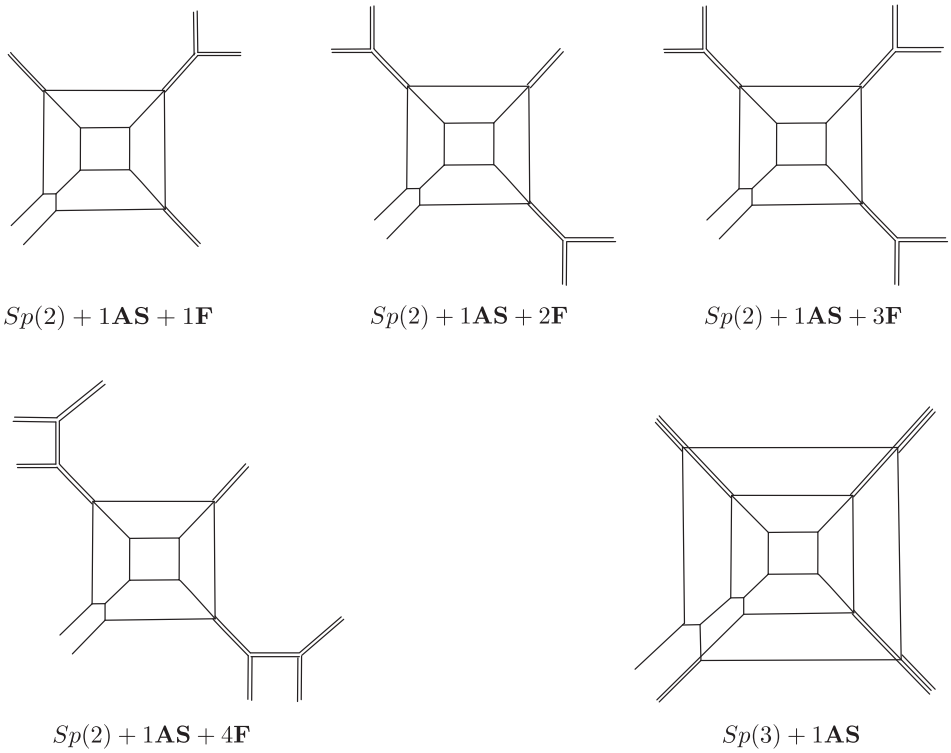

FIG. 5. Some representative examples of 5-brane web $Sp(N)$ gauge theories with one antisymmetry hypermultiplet and flavors, which are also considered in Sec. IV.

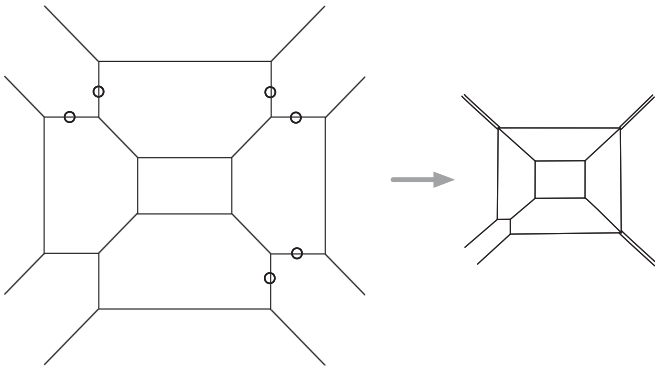

FIG. 6. A 5-brane web diagram for 5D $SU(2) \times SU(4) \times SU(2)$ quiver gauge theory and its Higgsed diagram giving rise to a 5-brane web for 5D $Sp(N)_0 + 1\mathbf{AS}$.

threefold [13]. It is also described by type IIB 5-brane web diagrams. Through various dualities, such 5-brane webs are equivalent to toric diagrams for local Calabi-Yau threefold in an A model [8]. The Nekrasov partition functions can, thus, be given by topological string partition functions. In what follows, we may use 5-brane webs and toric diagrams in an interchangeable way. In the topological vertex utilizing toric diagrams, one chooses the preferred direction denoted by $\|$, assign Young diagram $(\mu, \nu, \ldots)$ and Kähler parameter $Q_\bullet$ to edges, and the vertex factor to vertices and then glues and performs the Young diagrams to get the topological string partition functions

$$Z^{\text{top}} = \sum_{\lambda_i} \prod (\text{edge factor}) \cdot \prod (\text{vertex factor}). \quad (3.1)$$

The assignment of the vertex factor and the edge factor is illustrated in Figs. 7 and 8. With the Ω deformation parameters $q = e^{-\epsilon_2}$ and $t = e^{\epsilon_1}$, the vertex factor is defined as

$$C_{\lambda\mu\nu}(t,q) \coloneqq q^{\frac{\|\mu\|^2+\|\nu\|^2}{2}} t^{-\frac{\|\mu^T\|^2}{2}} \tilde{Z}_\nu(t,q) \sum_\eta \left(\frac{q}{t}\right)^{\frac{|\eta|+|\lambda|-|\mu|}{2}} s_{\lambda^T/\eta}(t^{-\rho}q^{-\nu}) s_{\mu/\eta}(q^{-\rho}t^{-\nu^T}), \quad (3.2)$$

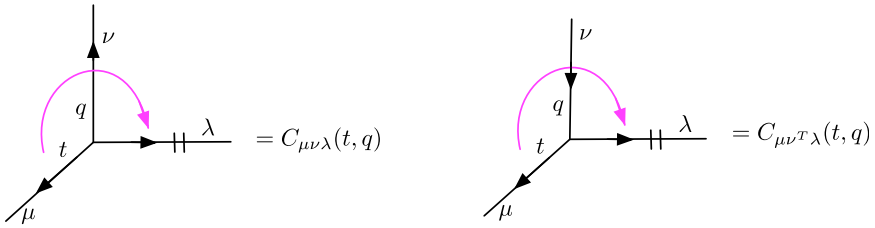

FIG. 7. Vertex factor assignment. The direction of the arrow on the edges can be chosen arbitrary, and the associated Young diagrams get transposed when the arrow is flopped. Here q, t are the Ω deformation parameters $q = e^{-\epsilon_2}, t = e^{\epsilon_1}$.

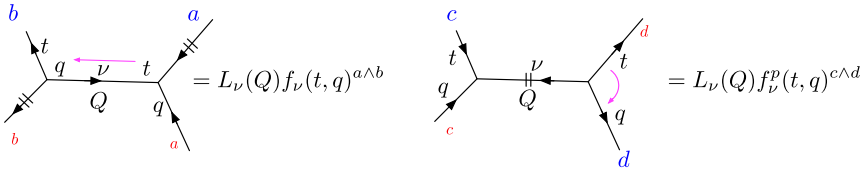

FIG. 8. The left figure is for nonpreferred edges and the second for preferred edges. The colors of letters do not matter, as the blue framing number $a \wedge b$ equals red $a \wedge b$, and blue $c \wedge d$ equals red $c \wedge d$.

where

$$\tilde{Z}_\nu(t,q) \coloneqq \prod_{(i,j)\in\nu} (1 - q^{\nu_i - j} t^{\nu_j^T - i + 1})^{-1} \tag{3.3}$$

and $s_{\lambda/\eta}$ are skew Schur functions. The edge factor is defined as

$$f_\nu^\bullet(t,q)^{\text{framing num}} L_\nu(Q), \tag{3.4}$$

with

$$f_\nu^p(t,q) \coloneqq (-1)^{|\nu|} t^{\frac{||\nu^T||^2}{2}} q^{-\frac{||\nu||^2}{2}},$$
$$f_\nu(t,q) \coloneqq \left(\frac{q}{t}\right)^{-\frac{|\nu|}{2}} f_\nu^p(t,q), \qquad L_\nu(Q) \coloneqq (-Q)^{|\nu|}, \tag{3.5}$$

where $f^p(t,q)$ is for the edges along the preferred direction and $f(t,q)$ for other edges for nonpreferred directions.

After summing over Young diagrams along nonpreferred directions by Cauchy identities (A1) and (A2), topological string partition function (3.1) generically takes the following form:

$$Z^{\text{top}}(Q_i,t,q) = Z^M \cdot Z^{\text{sum}}, \tag{3.6}$$

where Z^M is a product of $M(Q_i,t,q)$'s:

$$Z^M = \frac{\prod M(Q_i,t,q)}{\prod M(Q_j,t,q)}, \tag{3.7}$$

with

$$M(Q,t,q) \coloneqq \prod_{i,j=1}^{\infty} (1 - Q q^i t^{j-1}) \tag{3.8}$$

and Z^{sum} is the terms which contain the Young diagram sum along the preferred directions, which has the following structure:

$$Z^{\text{sum}} = \sum_{\mu_\cdot} Q_i^{|\mu_\cdot|} \prod_{\mu_\cdot} ||\tilde{Z}_{\mu_\cdot}(t,q)||^2 \times \frac{\prod N_{\nu_\cdot}^{\text{half},-}(Q_i,t^{-1},q^{-1}) N_{\mu_\cdot\nu_\cdot}(Q_i,t^{-1},q^{-1})}{\prod N_{\mu_\cdot\nu_\cdot}(Q_i,t^{-1},q^{-1})}, \tag{3.9}$$

where

$$||\tilde{Z}_\mu(t,q)||^2 \coloneqq \tilde{Z}_{\mu^T}(t,q)\tilde{Z}_\mu(q,t), \tag{3.10}$$

$$N_{\mu\nu}(Q;t,q) \coloneqq \prod_{i,j=1}^{\infty} \frac{1 - Q q^{\nu_i - j} t^{\mu_j^T - i + 1}}{1 - Q q^{-j} t^{-i+1}}, \tag{3.11}$$

and

$$N_\nu^{\text{half},-}(Q;t,q) \coloneqq N_{\nu\emptyset}\left(Q\sqrt{\frac{q}{t}},t,q\right), \tag{3.12}$$

$$N_\nu^{\text{half},+}(Q;t,q) \coloneqq N_{\emptyset\nu}\left(Q\sqrt{\frac{q}{t}},t,q\right). \tag{3.13}$$

One can also think of Z^M as the overall factor multiplied to the terms which have the Young diagram sum. In other words, Z^M is the term that is obtained by setting the Young diagrams along the preferred directions to $\emptyset$, or $Z^{\text{top}}|_{\mu_i=\emptyset}$.

B. T_2 diagram and T_2 tuning

As an instructive example, the 5-brane web or toric diagram for 5D T_2 theory is depicted in Fig. 9. The topological string partition function for the T_2 theory is

straightforward to compute and is given by

$$Z^{\text{top}}_{T_2}(Q_1,Q_2,Q_3;t,q) = Z^{M}_{T_2}\cdot Z^{\text{sum}}_{T_2}, \tag{3.14}$$

where

$$Z^{M}_{T_2} = \frac{M(Q_1\sqrt{\frac{t}{q}},t,q)M(Q_2\sqrt{\frac{t}{q}},t,q)}{M(Q_1Q_2,q,t)}. \tag{3.15}$$

T_2 theory is, in fact, special in that the Young diagram sum part $Z^{\text{sum}}_{T_2}$ can be performed, yielding a compact form:

$$\begin{aligned} Z^{\text{sum}}_{T_2} &= \sum_{\nu}(-Q_3)^{|\nu|}q^{\frac{||\nu||^2}{2}}t^{\frac{||\nu^T||^2}{2}}||\tilde{Z}_\nu(q,t)||^2 N^{\text{half},-}_{\nu^T}(Q_1;t^{-1},q^{-1})N^{\text{half},+}_{\nu^T}(Q_2;t^{-1},q^{-1}) \\ &= \frac{M(Q_3\sqrt{\frac{t}{q}},t,q)M(Q_1Q_2Q_3\sqrt{\frac{t}{q}},t,q)}{M(Q_1Q_3,t,q)M(Q_2Q_3,q,t)}. \end{aligned} \tag{3.16}$$

We thus have

$$Z^{\text{top}}_{T_2} = \frac{M(Q_1\sqrt{\frac{t}{q}},t,q)M(Q_2\sqrt{\frac{t}{q}},t,q)M(Q_3\sqrt{\frac{t}{q}},t,q)M(Q_1Q_2Q_3\sqrt{\frac{t}{q}},t,q)}{M(Q_1Q_3,t,q)M(Q_2Q_3,q,t)M(Q_1Q_2,q,t)}. \tag{3.17}$$

We note that the partition function $Z^{\text{top}}_{T_2}$ is $SL(2,\mathbb{Z})$ invariant; hence, T_2 diagrams with different preferred directions in Fig. 10 have the same partition function.

As discussed in Sec. II, 5D $Sp(2)$ gauge theories with an antisymmetric hypermultiplet can be obtained by Higgsing a quiver gauge theory. The Higgsing here is locally the Higgsing of a T_2 diagram which serves as building blocks. When the preferred direction is chosen, there are four possible Higgsings on a T_2 diagram. For convenience, we call them cases A, B, C, and D as shown in Fig. 11. In particular, case D is a typical configuration when flavors are added. With the assignment of Kähler parameters in Fig. 9, case A is achieved by tuning the Kähler parameters Q_1 and Q_2 to a special value, case B by tuning Q_1 and Q_3, and case C by tuning Q_2 and Q_3. Case D requires tuning of all three Kähler parameters Q_1, Q_2, and Q_3.

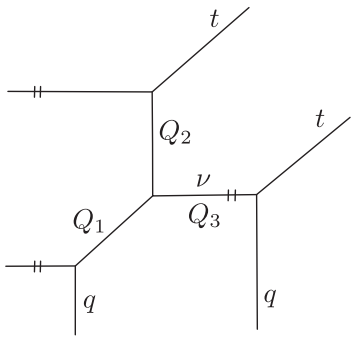

FIG. 9. A T_2 diagram. The preferred directions are denoted by $\|$ along the horizontal edges. Q_i are the Kähler parameters assigned to the internal edges, and ν is the Young diagram along the edge associated with Q_i. The empty Young diagram is given to six external edges.

This Higgsing procedure corresponds to certain geometric transitions [36–39], and the Kähler parameters responsible for the Higgsings are tuned to be either $\sqrt{\frac{q}{t}}$ or $\sqrt{\frac{t}{q}}$ [20,35]. We found the suitable choices for tuning Kähler parameters that reproduce the partition functions for 5D $Sp(N)+1\mathbf{AS}+N_f\mathbf{F}$:

$$\begin{aligned} &\text{Case A: } Q_1 = Q_2 = \sqrt{\frac{q}{t}} \quad \text{or} \quad \sqrt{\frac{t}{q}}, \\ &\text{Case B: } Q_1 = Q_3 = \sqrt{\frac{t}{q}}, \\ &\text{Case C: } Q_2 = Q_3 = \sqrt{\frac{q}{t}}, \\ &\text{Case D: } Q_1 = Q_2 = Q_3, \end{aligned} \tag{3.18}$$

which is consistent with the result obtained from the ADHM method. Here, for case A, either choice of Kähler parameters $\sqrt{\frac{q}{t}}$ or $\sqrt{\frac{t}{q}}$ is allowed and leads to the same result. As the 5-brane configuration in case D needs to be glued to either of case A, B, or C Higgsed diagrams, the tuning of Kähler parameter for case D is the same as the

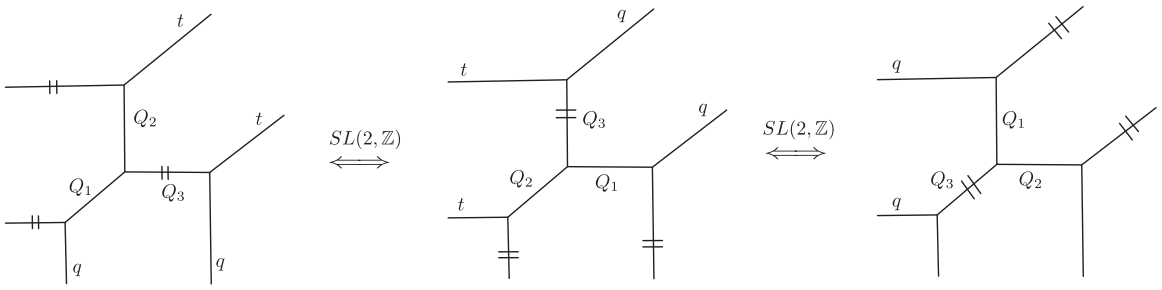

FIG. 10. T_2 diagrams related through $SL(2,\mathbb{Z})$ transformation.

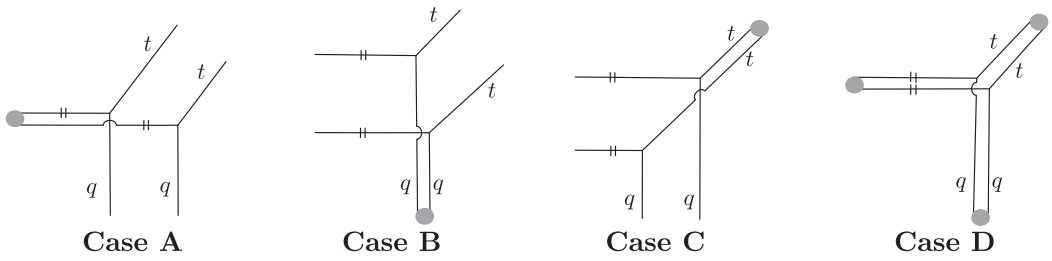

FIG. 11. Four possible Higgsed T_2 diagrams. Each jump on a T_2 diagram denotes a particular tuning of the Kähler parameters for Higgsing.

value of the Kähler parameter for the Higgsed diagram to which case D is connected. As we will frequently refer to when we compute the partition function in the next section, we call these special tunings of Kähler parameters (3.19) collectively "T_2 tuning." A pictorial version of the T_2 tuning is presented in Fig. 12.

We remark that the Young diagram sum part of the partition function, $Z^{\text{num}}_{T_2}$ should be trivial for the Higgsed T_2 diagrams depicted in Fig. 11, and indeed T_2 tuning satisfies

$$Z^{\text{sum}}_{T_2}|_{\text{case A,B,C,D}} = 1. \tag{3.19}$$

When applying the T_2 tuning to the partition function computations, we found the following identities related to geometric transitions [36] useful:

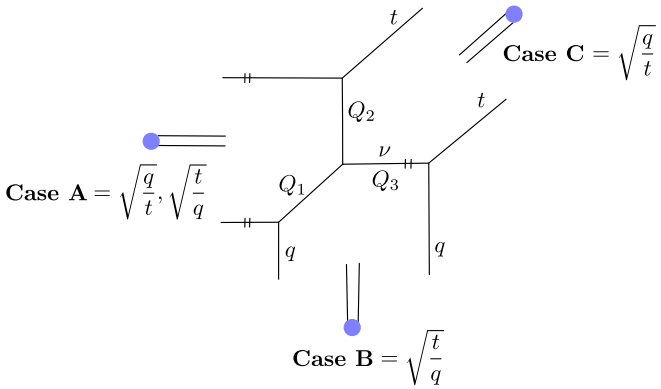

FIG. 12. T_2 tuning: cases A, B, and C.

$$N^{\text{half},+}_{\nu}\left(\sqrt{\frac{q}{t}};t^{-1},q^{-1}\right) = \begin{cases} 1 & \nu=\emptyset, \\ 0 & \nu\neq\emptyset, \end{cases} \quad N^{\text{half},-}_{\nu^T}\left(\sqrt{\frac{t}{q}};t^{-1},q^{-1}\right) = \begin{cases} 1 & \nu=\emptyset, \\ 0 & \nu\neq\emptyset, \end{cases} \tag{3.20}$$

and many simplifications take place due to the following relations:

$$\begin{aligned} &N_{\mu\alpha}(1;t^{-1},q^{-1}) \neq 0, \quad \text{only if } \mu \succcurlyeq \alpha, \\ &N_{\mu\alpha}\left(\frac{t}{q};t^{-1},q^{-1}\right) \neq 0, \quad \text{only if } \mu \preccurlyeq \alpha. \end{aligned} \tag{3.21}$$

It follows that in the unrefined limit $t = q$, as illustrated in Fig. 13, Eq. (3.21) becomes

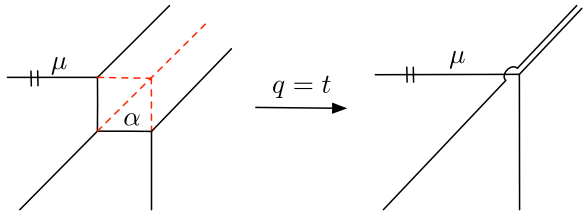

FIG. 13. A un-Higgsed diagram in the unrefined limit reproduces the jump. In the diagram on the left, the Young diagram sum is constrained such that $\mu \succcurlyeq \alpha$, while $\mu = \alpha$, in the unrefined limit.

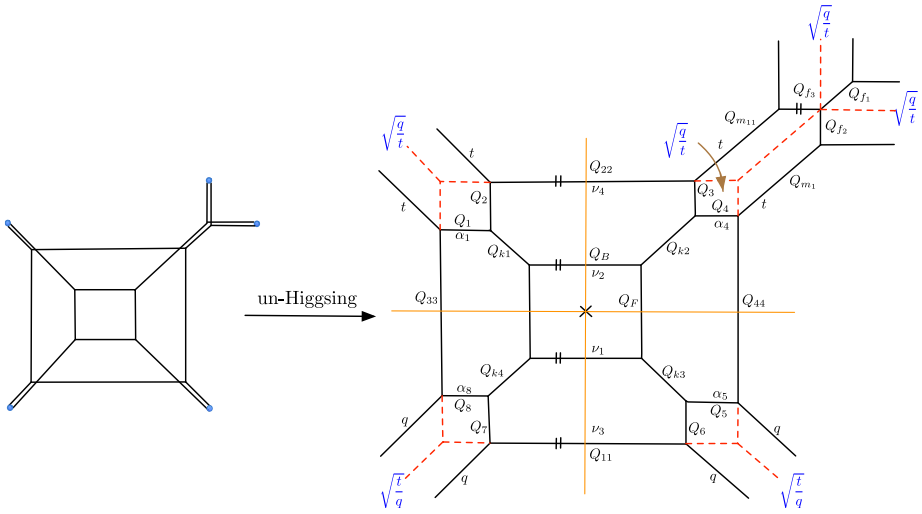

FIG. 14. Un-Higgsing procedure for a 5-brane web for $Sp(2) + 1\mathbf{AS} + 1\mathbf{F}$. Following T_2 tuning in Eq. (3.19), one can assign values to Higgsed edges, where $\sqrt{\frac{q}{t}}$ or $\sqrt{\frac{t}{q}}$ in blue are tuned Kähler parameters.

$$N_{\mu\alpha}(1; t^{-1}, t^{-1}) \neq 0, \quad \text{only if } \mu = \alpha, \tag{3.22}$$

and, thus, further simplifies Z^{sum} so that the partition functions for 5D $Sp(2)$ theories with one massless antisymmetric hypermultiplet are written as a product of two $Sp(1)$ theories [57].

In summary, 5-brane web diagrams for 5D $Sp(2) + 1\mathbf{AS} + 1\mathbf{F}$ can be understood as a Higgsed web diagram of a 5-brane web for the quiver gauge theory discussed in Sec. II. To compute topological string partition function, we consider the corresponding un-Higgsed 5-brane web diagrams and implement a refined topological vertex. We then perform the Higgsing on the un-Higgsed 5-brane web diagrams by tuning Kähler parameters via T_2 tuning (3.19), which yields that the topological string partition function as a Young diagram sum over the preferred directions $Z^{\text{top}} = Z^M Z^{\text{sum}}$. Finally, by properly identifying Kähler parameters with 5D gauge theory parameters, we obtain the Nekrasov partition function as an expansion of the instanton fugacity. In Fig. 14, we depict this procedure of un-Higgsing and T_2 tuning for a typical 5-brane web of $Sp(2)$ gauge theory with one antisymmetric hypermultiplet and one flavor $[Sp(2) + 1\mathbf{AS} + 1\mathbf{F}]$. We note that one can easily associate Kähler parameters with gauge theory parameters by introducing auxiliary lines which are projected lines when an un-Higgsed diagram is Higgsed back. For instance, the instanton fugacity for $Sp(2) + 1\mathbf{AS} + 1\mathbf{F}$ is obtained in the conventional way as $L_{\text{up}} \times L_{\text{down}} = u^2$, as illustrated in Fig. 15.

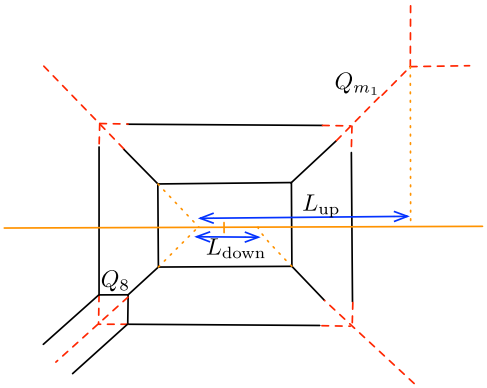

FIG. 15. Auxiliary lines (in red) and instanton fugacity which are projected lines when all edges are Higgsed. The instanton fugacity u is then obtained via the conventional way as $L_{\text{up}} \times L_{\text{down}} = u^2$.

IV. INSTANTON PARTITION FUNCTIONS

In this section, we use the topological vertex method to obtain the refined Nekrasov partition function for $Sp(2)$ theory with one antisymmetric hypermultiplet and N_f flavors $[Sp(2) + 1\mathbf{AS} + N_f\mathbf{F}]$. As the corresponding 5-brane web diagrams are nontoric, we properly apply the un-Higgsing and T_2-tuning procedure discussed in Sec. III.

Recall that the topological string partition function obtained through the topological vertex factorizes into the perturbative part Z^M, written in terms of $M(Q_\bullet, t, q)$, and the summation part Z^{sum}, summing over Young diagrams along preferred edges:

$$Z^{\text{top}} = Z^M \cdot Z^{\text{sum}}, \tag{4.1}$$

where each term contains a part of the field theory perturbative contribution or instanton (nonperturbative) contribution, in general:

$$Z^M = Z^{\text{pert-I}}(A_i, y_i) \cdot Z^{\text{nonpert-I}}(A_i, y_i, u), \tag{4.2}$$

$$Z^{\text{sum}} = Z^{\text{pert-II}}(A_i, y_i) \cdot Z^{\text{nonpert-II}}(A_i, y_i, u). \quad (4.3)$$

Here u is instanton fugacity, A_i Coulomb branch parameters, and y_i fugacity for hypermultiplet fields. Nekrasov partition function Z^{Nek} is then obtained as topological string partition function Z^{top} divided by the extra factor Z^{extra} that does not explicitly depend on the Coulomb branch parameters A_i. The resulting Nekrasov partition function factorizes into the perturbative contribution and the instanton contribution:

$$Z^{\text{Nek}} = \frac{Z^{\text{top}}(A_i, y_i, u)}{Z^{\text{extra}}(y_i, u)} = Z^{\text{pert}}(A_i, y_i) \cdot Z^{\text{instanton}}(A_i, y_i, u). \quad (4.4)$$

By factorizing the extra part,

$$Z^{\text{extra}} = Z^{\text{pert extra}}(y_i) \cdot Z^{\text{inst extra}}(y_i, u), \quad (4.5)$$

one can do the recombination and find that the full perturbative and instanton parts are obtained as

$$Z^{\text{pert}} = \frac{Z^{\text{pert-I}} \cdot Z^{\text{pert-II}}}{Z^{\text{pert extra}}}, \quad (4.6)$$

$$\begin{aligned} Z^{\text{instanton}} &= \frac{Z^{\text{nonpert-I}} \cdot Z^{\text{nonpert-II}}}{Z^{\text{inst extra}}} \\ &= \frac{Z^{\text{nonpert-I}}}{Z^{\text{inst extra}}} \cdot \frac{Z^{\text{sum}}}{Z^{\text{pert-II}}} \\ &= 1 + \sum_{k=1}^{\infty} Z_k(A_i, y_i) u^k, \end{aligned} \quad (4.7)$$

respectively, where $Z_k(A_i, y_i)$ is the k-instanton partition function. Typically, it is computationally demanding to find higher-instanton partition functions. Here, we also present the results up to two instanton order.

We note that, for a given number of flavors, one can have various 5-brane web configurations via Hanany-Witten transitions as well as flop transitions. Applying the topological vertex method, hence, may give seemingly different partition functions. The partition functions are, however, related by extra factors. After removing such extra factors, one obtains the unique Nekrasov partition function for the gauge theory. One can therefore choose a representative 5-brane configuration for $Sp(N) + 1\mathbf{AS} + N_f\mathbf{F}$ and compute the refined partition function as an expansion of the instanton fugacity. Here, we, however, consider only $Sp(2) + 1\mathbf{AS} + N_f\mathbf{F}$ ($N_f = 0, 1, 2, 3, 4$) and $Sp(3) + 1\mathbf{AS}$, as the partition functions for higher ranks or higher number of flavors takes a lot of time.

A. $Sp(2)_0 + 1\mathbf{AS}$

As depicted in Fig. 16, the 5-brane web for $Sp(2)_0 + 1\mathbf{AS}$ has three jumps associated with Higgsing of the external edges. There are also two edges that are not Higgsed, which are responsible for the mass of the hypermultiplet in the antisymmetric representation, given as the separation between these two edges.

The 5-brane web can be obtained by Higgsing of a 5-brane web of a $SU(2) \times SU(4) \times SU(2)$ quiver gauge theory depicted in Fig. 17.

On each edge of the un-Higgsed web diagram in Fig. 17, we assigned the Young diagrams α_i and the Kähler parameters $Q_i = e^{-iL_i}$, where L_i is the length of the corresponding edge. It is easy to see that not all Kähler parameters are independent. With the convention that

$$Q_{i,i,\ldots,l} \coloneqq Q_i Q_j \ldots Q_l, \quad (4.8)$$

we denote ten independent Kähler parameters by Q_i ($i = 1, \ldots, 6, 8, k4, F, B$). Then other Kähler parameters are expressed as

$$\begin{aligned} Q_{k1} &= \frac{Q_{8,k4}}{Q_1}, \qquad Q_{k2} = \frac{Q_{2,8,k4}}{Q_{1,3}}, \\ Q_{k3} &= \frac{Q_{2,4,8,k4}}{Q_{1,3,5}}, \qquad Q_7 = \frac{Q_{2,4,6,8}}{Q_{1,3,5}}, \\ Q_{11} &= \frac{Q_{2,4,8,B,k4,k4}}{Q_{1,3,5}}, \qquad Q_{22} = \frac{Q_{2,8,8,B,k4,k4}}{Q_{1,1,3}}, \\ Q_{33} &= \frac{Q_{8,F,k4,k4}}{Q_1}, \qquad Q_{44} = \frac{Q_{2,2,4,8,8,F,k4,k4}}{Q_{1,1,3,3,5}}. \end{aligned} \quad (4.9)$$

To obtain the Nekrasov partition function for $Sp(2)_0 + 1\mathbf{AS}$, one first needs to properly tune the Kähler parameters associated with the external edges, which reduces the un-Higgsed diagram in Fig. 17 to the 5-brane web for $Sp(2)_0 + 1\mathbf{AS}$ given in Fig. 16. Recalling the T_2 tuning in Sec. III, we found that the correct tuning of the Kähler parameters is given by

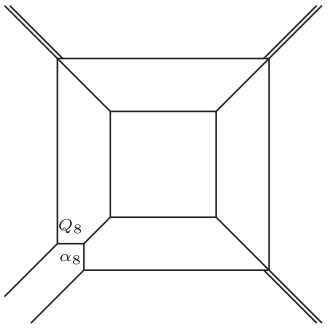

FIG. 16. A 5-brane web diagram for $Sp(2)_0 + 1\mathbf{AS}$. The Kähler parameter Q_8 assigned on an edge with the Young diagram α_8 is the mass fugacity for the antisymmetric hypermultiplet.

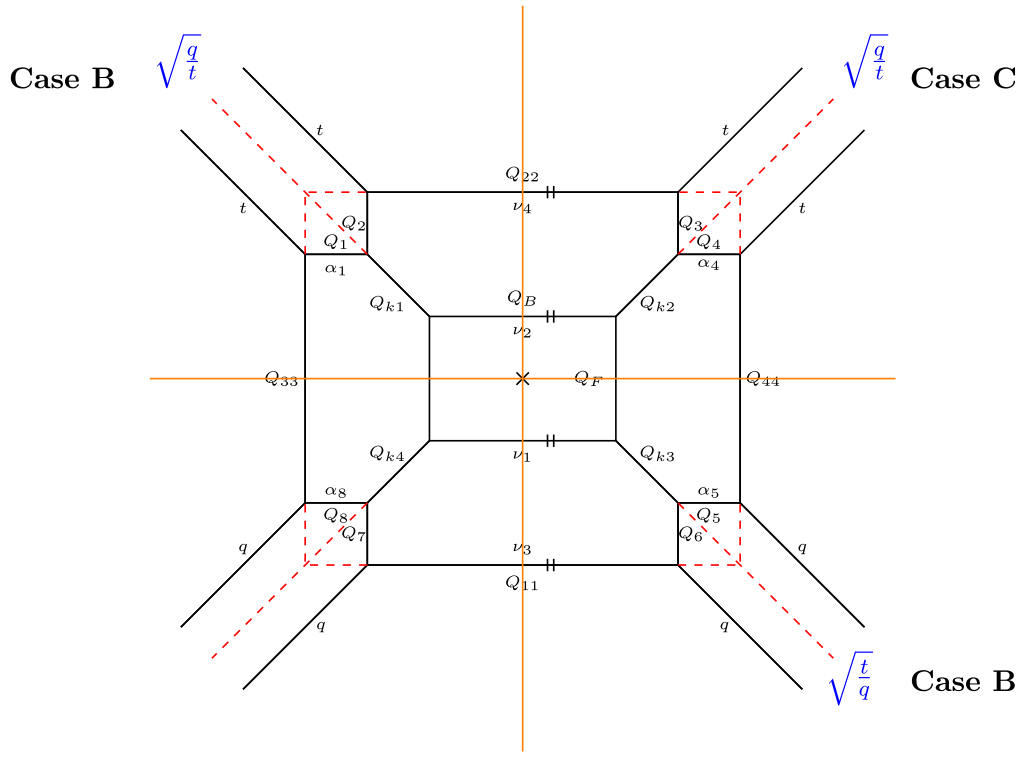

FIG. 17. An un-Higgsed diagram for $Sp(2)+1\mathbf{AS}$, which is a 5-brane web for an $SU(2)\times SU(4)\times SU(2)$ quiver gauge theory. By Higgsing or tuning the Kähler parameters associated with external edges, one reproduces the 5-brane web given in Fig. 16.

$$Q_1=Q_2=Q_3=Q_4=\sqrt{\frac{q}{t}},\quad Q_5=Q_6=\sqrt{\frac{t}{q}}, \tag{4.10}$$

which correspond to two case B and one case C. Next, the gauge theory parameters, two Coulomb branch parameters A_1 and A_2, the instanton fugacity u, and the mass fugacity for an antisymmetric hypermultiplet Q_8 are assigned to the following Kähler parameters:

$$Q_F=A_2{}^2,\qquad Q_{k4}=\frac{A_1}{A_2Q_8},\qquad Q_B=uA_2{}^2. \tag{4.11}$$

$Z^{\rm sum}_{Sp(2)_0+1\mathbf{AS}}$ as the summation over the Young diagrams along preferred edges is given by

$$\begin{aligned}Z^{\rm sum}_{Sp(2)_0+1\mathbf{AS}}&=\sum_{\substack{\nu_1,\nu_2,\\ \nu_3,\nu_4}}\sum_{\substack{\alpha_1,\alpha_4\\ \alpha_5,\alpha_8}}Z^{\mathbf{sum}}_{\mathbf{Sp(2)}+1\mathbf{AS}}\\&=\sum_{\substack{\nu_1,\nu_2,\\ \nu_3,\nu_4}}\sum_{\substack{\alpha_1,\alpha_4\\ \alpha_5,\alpha_8}}Z[\nu_1,\nu_2,\nu_3,\nu_4;\alpha_1,\alpha_4,\alpha_5,\alpha_8],\end{aligned} \tag{4.12}$$

with shorthand notation

$$\begin{aligned}Z^{\mathbf{sum}}_{\mathbf{Sp(2)}+1\mathbf{AS}}&:=Z[\nu_1,\nu_2,\nu_3,\nu_4;\alpha_1,\alpha_4,\alpha_5,\alpha_8]\\&=u^{|\nu_1|+|\nu_2|+|\nu_3|+|\nu_4|}{A_2}^{2|\nu_1|+2|\nu_2|}{A_1}^{2|\nu_3|+2|\nu_4|}Q_8^{-|\nu_3|}\prod_{i=1}^{4}\tilde{Z}_{\nu_i}(q,t)\tilde{Z}_{\nu_i^T}(t,q)q^{||\nu_2||^2+\frac{|\nu_3|}{2}|\nu_4|+||\nu_4||^2}t^{||\nu_1||^2-\frac{|\nu_3|}{2}+|\nu_4|+||\nu_3||^2}\\&\times\frac{1}{N_{\nu_2\nu_1^T}(A_2{}^2)N_{\nu_2\nu_1^T}(\frac{A_2{}^2t}{q})N_{\nu_2\nu_3^T}(A_1A_2)N_{\nu_2\nu_3^T}(\frac{A_1A_2t}{q})N_{\nu_4\nu_2}(\frac{A_1}{A_2})N_{\nu_4\nu_2}(\frac{A_1t}{A_2q})}\\&\times\frac{1}{N_{\nu_4\nu_1^T}(A_1A_2)N_{\nu_4\nu_1^T}(\frac{A_1A_2t}{q})N_{\nu_4\nu_3^T}(\frac{A_1}{A_2})N_{\nu_4\nu_3^T}(\frac{A_1t}{A_2q})N_{\nu_1^T\nu_3^T}(\frac{A_1}{A_2})N_{\nu_1^T\nu_3^T}(\frac{A_1t}{A_2q})}\end{aligned}$$

$$\times (-1)^{|\alpha_1|+|\alpha_4|+|\alpha_5|+|\alpha_8|} Q_8^{|\alpha_8|} \prod_{j=1,4,5,8} \tilde{Z}_{\alpha_j}(q,t)\tilde{Z}_{\alpha_j^T}(t,q)$$
$$\times q^{\frac{|\alpha_1|+||\alpha_1||^2+|\alpha_4|+||\alpha_4||^2-|\alpha_5|+||\alpha_5^T||^2+||\alpha_8^T||^2}{2}} t^{\frac{-|\alpha_1|+||\alpha_1^T||^2-|\alpha_4|+||\alpha_4^T||^2+|\alpha_5|+||\alpha_5||^2+||\alpha_8||^2}{2}}$$
$$\times \frac{N_{\alpha_1\nu_2}(\frac{A_1 t}{A_2 q})N_{\alpha_1\nu_1^T}(\frac{A_1A_2 t}{q})N_{\alpha_1\nu_3^T}(\frac{{A_1}^2 t}{q})N_{\alpha_4\nu_2}(\frac{A_1 t}{A_2 q})N_{\alpha_4\nu_1^T}(\frac{A_1A_2 t}{q})N_{\alpha_4\nu_3^T}(\frac{{A_1}^2 t}{q})N_{\nu_2\alpha_5^T}(A_1A_2)}{N_{\alpha_1\alpha_8^T}(\frac{{A_1}^2}{Q_8}\sqrt{\frac{t}{q}})N_{\alpha_1\alpha_8^T}(\frac{{A_1}^2 t}{Q_8 q}\sqrt{\frac{t}{q}})}$$
$$\times \frac{N_{\nu_2\alpha_8^T}(\frac{A_1A_2}{Q_8}\sqrt{\frac{t}{q}})N_{\nu_4\alpha_5^T}({A_1}^2)N_{\nu_4\alpha_8^T}(\frac{{A_1}^2}{Q_8}\sqrt{\frac{t}{q}})N_{{\alpha_8}^T\nu_3^T}(Q_8\sqrt{\frac{t}{q}})N_{\nu_1^T\alpha_5^T}(\frac{A_1}{A_2})N_{\nu_1^T\alpha_8^T}(\frac{A_1}{A_2 Q_8}\sqrt{\frac{t}{q}})}{N_{\alpha_4\alpha_5^T}(A_1^2)N_{\alpha_4\alpha_5^T}(A_1^2\frac{t}{q})}$$
$$\times N_{\nu_4\alpha_1}(1)N_{\nu_4\alpha_4}(1)N_{\alpha_5\nu_3}\left(\frac{t}{q}\right), \tag{4.13}$$

where we used a shorthand notation $N_{\bullet\bullet}(Q)$ for $N_{\bullet\bullet}(Q;t^{-1},q^{-1})$, and it follows from Eq. (3.21) that the Young diagrams of $N_{\nu_4\alpha_1}(1)N_{\nu_4\alpha_4}(1)N_{\alpha_5\nu_3}(\frac{t}{q})$ in the last line satisfy $\nu_4 \succcurlyeq \alpha_1$, $\nu_4 \succcurlyeq \alpha_4$, and $\nu_3 \succcurlyeq \alpha_5$.

1. Perturbative contribution

With these assignments of Kähler parameters, we can express the topological string partition function

$$Z^{\text{top}}_{Sp(2)_0+1\mathbf{AS}} = Z^{M}_{Sp(2)_0+1\mathbf{AS}} \cdot Z^{\text{sum}}_{Sp(2)_0+1\mathbf{AS}}, \tag{4.14}$$

where $Z^{M}_{Sp(2)_0+1\mathbf{AS}}$ takes the following form:

$$Z^{M}_{Sp(2)_0+1\mathbf{AS}} = Z^{\text{pert-I}}_{Sp(2)_0+1\mathbf{AS}} \cdot Z^{\text{nonpert-I}}_{Sp(2)_0+1\mathbf{AS}}, \tag{4.15}$$

where

$$Z^{\text{pert-I}}_{Sp(2)_0+1\mathbf{AS}} = \frac{M(\frac{A_1}{A_2Q_8}\sqrt{\frac{t}{q}},t,q)M(\frac{A_1A_2}{Q_8},t,q)M(Q_8\sqrt{\frac{t}{q}},t,q)}{M({A_1}^2,t,q)M(\frac{A_1}{A_2},t,q)M(A_1A_2,t,q)M({A_2}^2,t,q)M({A_2}^2,q,t)M(\frac{{A_1}^2}{Q_8}\sqrt{\frac{t}{q}},q,t)},$$
$$Z^{\text{nonpert-I}}_{Sp(2)_0+1\mathbf{AS}} = 1. \tag{4.16}$$

Here we neglected unimportant factors like $M(1,t,q)$ on the right-hand side of Eq. (4.15). We note that, in general, Z^M contains terms depending on the instanton fugacity u, but, in this case, Z^M is independent of u. We found, in fact, that $Z^{\text{nonpert-I}} = 1$ even with flavors up to $N_f = 3$.

The perturbative contribution from the summation part of partition function is also independent of instanton fugacity and is obtained by setting $\nu_1 = \nu_2 = \nu_3 = \nu_4 = \emptyset$:

$$Z^{\text{pert-II}}_{Sp(2)_0+1\mathbf{AS}} = \sum_{\alpha_1,\alpha_4,\alpha_5,\alpha_8} Z[\emptyset,\emptyset,\emptyset,\emptyset;\alpha_1,\alpha_4,\alpha_5,\alpha_8], \tag{4.17}$$

where it follows from Eqs. (3.20) and (3.21) that $\alpha_{1,4} \preccurlyeq \nu_4 = \emptyset$ and $\alpha_5 \preccurlyeq \nu_3 = \emptyset$, which yields

$$Z^{\text{pert-II}}_{Sp(2)_0+1\mathbf{AS}} = \sum_{\alpha_8} \underbrace{(-1)^{|\alpha_8|} q^{\frac{||\alpha_8^T||^2}{2}} t^{\frac{||\alpha_8||^2}{2}} ||\tilde{Z}_{\alpha_8^T}(q,t)||^2 N^{\text{half},-}_{\alpha_8^T}(Q_8) N^{\text{half},+}_{\alpha_8}(Q_8)}_{T_2 \text{ partition function}} \frac{N^{\text{half},+}_{\alpha_8^T}(Q_{F,k4})}{N^{\text{half},+}_{\alpha_8^T}(Q_{8,F,k4}\frac{t}{q})}$$
$$= \frac{M(Q_8\sqrt{\frac{q}{t}},q,t)M(\frac{Q_8A_1}{A_2}\sqrt{\frac{q}{t}},q,t)M(Q_8A_1A_2\sqrt{\frac{q}{t}},q,t)M(\frac{{A_1}^2}{Q_8}\sqrt{\frac{t}{q}},q,t)}{M({A_1}^2,q,t)M(\frac{A_1}{A_2},q,t)M(A_1A_2,q,t)M({Q_8}^2,t,q)}, \tag{4.18}$$

where we reorganized $M(\bullet,t,q)$ to express $Z^{\text{pert-II}}$ as a compact form. We note that, even though we add flavors, $Z^{\text{pert-II}}$ is unaltered at least for $N_f \leq 4$. Taking into account the extra factor associated with an antisymmetric hypermultiplet, the stringy contribution from two parallel external edges in Fig. 16 is given by

$$Z^{\text{extra}}_{Q_8} = \frac{1}{M(Q_8{}^2,t,q)}. \tag{4.19}$$

One obtains from Eq. (4.6) that the full perturbative part of the partition function

$$\begin{aligned} Z^{\text{pert}}_{Sp(2)_0+1\mathbf{AS}} &= \frac{Z^{\text{pert-I}}_{Sp(2)_0+1\mathbf{AS}} \cdot Z^{\text{pert-II}}_{Sp(2)_0+1\mathbf{AS}}}{Z^{\text{extra}}_{Q_8}} \\ &= \frac{M(Q_8A_1A_2\sqrt{\frac{t}{q}},t,q)M(\frac{A_1A_2}{Q_8}\sqrt{\frac{t}{q}},t,q)M(\frac{Q_8A_1}{A_2}\sqrt{\frac{t}{q}},t,q)}{M(A_1A_2,t,q)M(A_1A_2,q,t)M(\frac{A_1}{A_2},t,q)M(\frac{A_1}{A_2},q,t)} \frac{M(\frac{A_1}{Q_8A_2}\sqrt{\frac{t}{q}},t,q)M(Q_8\sqrt{\frac{t}{q}},t,q)^2}{M(A_1{}^2,t,q)M(A_1{}^2,q,t)M(A_2{}^2,t,q)M(A_2{}^2,q,t)}, \end{aligned} \tag{4.20}$$

which exactly agrees with the result obtained from the localization computation (B1). With a proper normalization, the full perturbative part can be expressed as

$$\begin{aligned} Z^{\text{pert}'}_{Sp(2)_0+1\mathbf{AS}} &= \frac{Z^{\text{pert}}_{Sp(2)_0+1\mathbf{AS}}}{M(Q_8\sqrt{\frac{t}{q}},t,q)^2} \\ &= 1 + \frac{q+t}{(1-q)(1-t)}A_2{}^2 + \frac{q+t-\sqrt{qt}\chi_2^{SU(2)}[Q_8]}{(1-q)(1-t)}\frac{A_1}{A_2} \\ &\quad + \frac{(1+qt)(q+t-\sqrt{qt}\chi_2^{SU(2)}[Q_8])}{(1-q)^2(1-t)^2}A_1A_2 + \mathcal{O}(A_1{}^1;A_2{}^1), \end{aligned}$$

where $\chi_2^{SU(2)}[Q_8] = Q_8 + Q_8{}^{-1}$ is the character associated with the mass fugacity of the antisymmetric hypermultiplet. From here on, we use the following simpler notation $\chi_n^{SU(2)} = \chi_n^{SU(2)}[Q_8]$ for the character associated with the mass of an antisymmetric hypermultiplet in the n-dimensional representation of $SU(2)$.

2. Instanton contribution

The instanton contribution is obtained from Eq. (4.9). For n-instanton partition function Z_n, one restricts the power of the instanton fugacity to be n; in other words, $u^{|\nu_1|+|\nu_2|+|\nu_3|+|\nu_4|} = u^n$. As $Z^{\text{nonpert-I}}_{Sp(2)_0+1\mathbf{AS}}(u,A_i,y_i) = 1$, the one-instanton contribution is given by

$$Z^{\text{one-instanton}}_{Sp(N)+1\mathbf{AS}} = \frac{\sum_{\substack{\nu_1,\nu_2,\nu_3,\nu_4\in\{\square,\emptyset\}\\ \text{and}\,|\nu_1|+|\nu_2|+|\nu_3|+|\nu_4|=1}} \sum_{\alpha_1,\alpha_4,\alpha_5,\alpha_8} Z[\nu_1,\nu_2,\nu_3,\nu_4,\alpha_1,\alpha_4,\alpha_5,\alpha_8]}{Z^{\text{pert-II}}_{Sp(2)_0+1\mathbf{AS}}}, \tag{4.21}$$

which actually is already quite lengthy if one sums over the contributions of $|\alpha_1|+|\alpha_4|+|\alpha_5|+|\alpha_8| \leq 6$. Since Eq. (3.21) leads to constraints $\alpha_1,\alpha_4 \preccurlyeq \nu_4$ and $\alpha_5 \preccurlyeq \nu_3$, and other terms do not satisfy this constraint just equal to zero, Z_1 can be further simplified:

$$\begin{aligned} Z^{\text{one-instanton}}_{Sp(N)+1\mathbf{AS}} \cdot Z^{\text{pert-II}} = \sum_{\alpha_8} Z[\underbrace{\{1\},\emptyset,\emptyset,\emptyset}_{\nu_1,\nu_2,\nu_3,\nu_4};\underbrace{\emptyset,\emptyset,\emptyset,\alpha_8}_{\alpha_1,\alpha_4,\alpha_5,\alpha_8}] &+ Z[\emptyset,\{1\},\emptyset,\emptyset;\emptyset,\emptyset,\emptyset,\alpha_8] + Z[\emptyset,\emptyset,\{1\},\emptyset;\emptyset,\emptyset,\emptyset,\alpha_8] \\ &+ Z[\emptyset,\emptyset,\{1\},\emptyset;\emptyset,\emptyset,\{1\},\alpha_8] + Z[\emptyset,\emptyset,\emptyset,\{1\};\emptyset,\emptyset,\emptyset,\alpha_8] + Z[\emptyset,\emptyset,\emptyset,\{1\};\emptyset,\{1\},\emptyset,\alpha_8] \\ &+ Z[\emptyset,\emptyset,\emptyset,\{1\};\{1\},\emptyset,\emptyset,\alpha_8] + Z[\emptyset,\emptyset,\emptyset,\{1\};\{1\},\{1\},\emptyset,\alpha_8], \end{aligned} \tag{4.22}$$

where $\{1\}$ stands for Young diagram $\square$. By expanding Eq. (4.21) with respect to the Coulomb branch parameters, we get

$$Z^{\text{one-instanton}}_{Sp(N)+1\mathbf{AS}} = \frac{q+t}{(1-q)(1-t)}(A_1^2+A_2^2) + \frac{q+t-\sqrt{qt}\chi_2^{SU(2)}}{(1-q)(1-t)}A_2A_1 + \frac{(q^2+qt+t^2)(q+t-\sqrt{qt}\chi_2^{SU(2)})}{(1-q)q(1-t)t}(A_1A_2^3+A_1^3A_2) + \frac{(q+t)^2(q+t\sqrt{qt}\chi_2^{SU(2)})}{(1-q)q(1-t)t}A_2^2A_1^2 + \frac{(q^2+qt+t^2)^2(q+t-\sqrt{qt}\chi_2^{SU(2)})}{(1-q)q^2(1-t)t^2}A_2^3A_1^3 + \mathcal{O}(A_1^4;A_2^4). \tag{4.23}$$

We now compare the one-instanton contribution with the known result, which we summarized in Eq. (B5). The relevant part ($N_f = 0$) is given as follows:

$$Z^{\text{one-instanton}}_{Sp(N)+1\mathbf{AS}} = \frac{1}{2}\left(\frac{1}{2\sinh\frac{\epsilon_+\pm\epsilon_-}{2}}\frac{2\sinh\frac{m\pm\alpha_1}{2}2\sinh\frac{m\pm\alpha_2}{2}-2\sinh\frac{\pm\alpha_1+\epsilon_+}{2}2\sinh\frac{\pm\alpha_2+\epsilon_+}{2}}{2\sinh\frac{\pm\alpha_1+\epsilon_+}{2}2\sinh\frac{\pm\alpha_2+\epsilon_+}{2}2\sinh\frac{m\pm\epsilon_+}{2}} + \frac{1}{2\sinh\frac{\epsilon_+\pm\epsilon_-}{2}}\frac{2\cosh\frac{m\pm\alpha_1}{2}2\cosh\frac{m\pm\alpha_2}{2}-2\cosh\frac{\pm\alpha_1+\epsilon_+}{2}2\cosh\frac{\pm\alpha_2+\epsilon_+}{2}}{2\cosh\frac{\pm\alpha_1+\epsilon_+}{2}2\cosh\frac{\pm\alpha_2+\epsilon_+}{2}2\sinh\frac{m\pm\epsilon_+}{2}}\right). \tag{4.24}$$

With the identification $A_1 := e^{\alpha_1}$, $A_2 := e^{\alpha_2}$, and $Q_8 := e^m$ with m being the mass of the antisymmetric hypermultiplet and the Omega deformation parameters $q = e^{-\epsilon_2}$, $t = e^{\epsilon_1}$, and $\epsilon_\pm = \frac{\epsilon_1\pm\epsilon_2}{2}$, the expansion of Eq. (4.24) in terms of A_1 and A_2 agrees with our result (4.23).

Similarly, the two-instanton contribution is given by

$$Z^{\textbf{two-instanton}}_{Sp(N)+1\mathbf{AS}} = \frac{\sum_{\alpha_1,\alpha_4,\alpha_5,\alpha_8}\ \sum_{\substack{\nu_1,\nu_2,\nu_3,\nu_4\in\{\square,\ \square\square,\ \square,\ \emptyset\}\\ |\nu_1|+|\nu_2|+|\nu_3|+|\nu_4|=2}} Z[\nu_1,\nu_2,\nu_3,\nu_4;\alpha_1,\alpha_4,\alpha_5,\alpha_8]}{Z^{\textbf{pert-II}}_{Sp(N)+1\mathbf{AS}}}, \tag{4.25}$$

which can also be reduced by constraints $\alpha_1,\alpha_4 \preccurlyeq \nu_4$ and $\alpha_5 \preccurlyeq \nu_3$. With the assignment of Kähler parameters in terms of (A_i, u, y_i), the two-instanton contribution can be expanded as

$$Z^{\text{two-instanton}}_{Sp(N)+1\mathbf{AS}} = \frac{(q+t)(q+t-\sqrt{qt}\chi_2^{SU(2)})}{(1-q)^2(1-t)^2}(A_2^3A_1+A_2A_1^3) + \frac{(q+t)(qt\chi_3^{SU(2)}-\sqrt{qt}(1+q)(1+t)\chi_2^{SU(2)}+2(q+t)(1+qt)+3qt+q^2+t^2)}{(1-q)^2(1+q)(1-t)^2(1+t)}A_2^2A_1^2 + \mathcal{O}(A_1^3;A_2^3), \tag{4.26}$$

where $\chi_3^{SU(2)} = Q_8{}^2 + 1 + Q_8{}^{-2}$.

3. Enhancement of global symmetry

With a proper normalization, the partition function for $Sp(2)+1\mathbf{AS}+n\mathbf{F}$ with enhancement symmetry can be expressed as

$$Z := \frac{Z^{\text{pert}}(A_i,y_i)}{M(Q_8\sqrt{\frac{t}{q}},t,q)^2}\cdot\left(1+\sum_{k=1}^{\infty}Z_k(A_i,y_i)u^k\right) = 1+\sum_{m,n}f(\chi[\tilde{u},\tilde{y}_i],t,q)\tilde{A}_1^m\tilde{A}_2^n, \tag{4.27}$$

where $\chi[\tilde{u},\tilde{y}_i]$ is some characters for the enhanced global symmetry written in terms of the redefined fugacities of instanton and hypermultiplets and $\widetilde{A}_i$ are redefined parameters.

As $Sp(2)_0+1\mathbf{AS}$ is rank 2 E_1 theory, its global symmetry is enhanced to $SU(2)$ at the UV fixed point which was explicitly shown through superconformal index computation [49]. At the level of partition function, the enhancement of global symmetry can also be shown by taking into account the fiber-base duality. Following Ref. [47], we redefine the

Coulomb branch parameters

$$\tilde{A}_1 = A_1 u^{\frac{1}{4}}, \qquad \tilde{A}_2 = A_2 u^{\frac{1}{4}}, \tag{4.28}$$

to make the fiber-base duality manifest

$$u \leftrightarrow u^{-1}, \qquad Q_B \leftrightarrow Q_F, \qquad Q_8 \leftrightarrow Q_8. \tag{4.29}$$

For $Sp(2)_0 + 1\mathbf{AS}$, we indeed find that Eq. (4.27) is expressed in terms of the characters of the enhanced $SU(2)$ global symmetry:

$$\begin{aligned} Z_{Sp(2)_0+1\mathbf{AS}} = 1 &+ \frac{(q+t)\chi_2[u]}{(1-q)(1-t)}\tilde{A}_2{}^2 + \frac{q+t-\sqrt{qt}\chi_3^{SU(2)}}{(1-q)(1-t)}\frac{\tilde{A}_1}{\tilde{A}_2} + \frac{(1+qt)\chi_2[u](q+t-\sqrt{qt}\chi_3^{SU(2)})}{(1-q)^2(1-t)^2}\tilde{A}_1\tilde{A}_2 \\ &+ \frac{(q+t)(qt\chi_3^{SU(2)} - \sqrt{qt}(1+q)(1+t)\chi_2^{SU(2)} + (q+t)(1+qt)+qt)}{(1-q)^2(1+q)(1-t)^2(1+t)}\frac{\tilde{A}_1^2}{\tilde{A}_2^2} + \mathcal{O}(\tilde{A}_1{}^2;\tilde{A}_2{}^2), \end{aligned} \tag{4.30}$$

where $\chi_2[u] = \sqrt{u} + \frac{1}{\sqrt{u}}$ is the character of the enhanced $SU(2)$ global symmetry and $\chi_n^{SU(2)}$ are the characters for the antisymmetric hypermultiplet. From Eq. (4.30), one sees the enhancement of global symmetry is $SU(2)_u \times SU(2)_{Q_8}$, as expected.

B. $Sp(2)_\pi + 1\mathbf{AS}$

We now discuss $Sp(2)$ gauge theory with the discrete theta angle $\theta = \pi$ and an antisymmetric hypermultiplet. A 5-brane web configuration is given in Fig. 18, from which one can read off the relations between Kähler parameters:

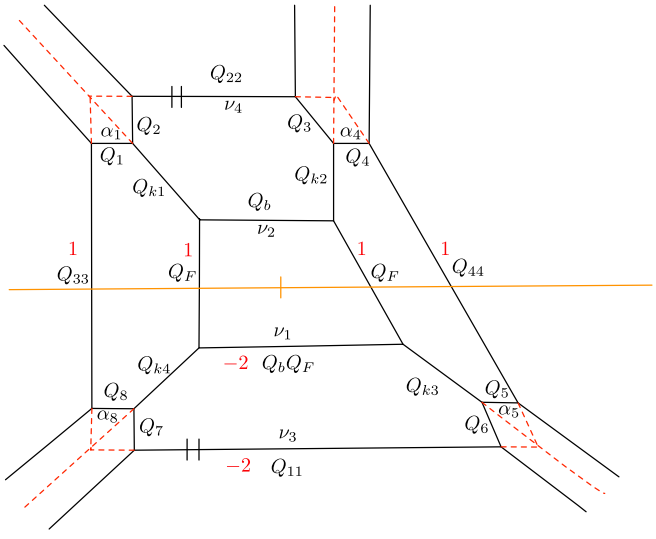

FIG. 18. An un-Higgsed 5-brane web diagram for $Sp(2)_\pi + 1\mathbf{AS}$. The numbers in red denote framing numbers associated with edges.

$$\begin{aligned} &Q_{k1} = \frac{Q_{8,k4}}{Q_1}, \quad Q_{k2} = \frac{Q_{2,8,k4}}{Q_{1,3}}, \quad Q_{k3} = \frac{Q_{2,4,8,k4}}{Q_{1,3,5}}, \\ &Q_7 = \frac{Q_{2,4,6,8}}{Q_{1,3,5}}, \quad Q_{22} = \frac{Q_{8,b,k4}}{Q_{1,3}}, \quad Q_{33} = \frac{Q_{8,F,k4,k4}}{Q_1}, \\ &Q_{44} = \frac{Q_{2,2,4,8,8,F,k4,k4}}{Q_{1,1,3,3,5}}, \quad Q_{11} = \frac{Q_{2,2,4,4,6,8,8,b,F,k4,k4,k4}}{Q_{1,1,3,3,5,5}}. \end{aligned} \tag{4.31}$$

By the T_2 tuning, the correct tuning for Kähler parameter given is as follows:

$$Q_1 = Q_2 = Q_3 = Q_4 = \sqrt{\frac{q}{t}}, \qquad Q_5 = Q_6 = \sqrt{\frac{t}{q}}. \tag{4.32}$$

Independent Kähler parameters are assigned with gauge theory parameters

$$Q_F = A_2{}^2, \qquad Q_{k4} = \frac{A_1}{A_2 Q_8}, \qquad Q_b = uA_2. \tag{4.33}$$

It is then straightforward to compute $Z^{\text{pert-I}}$ and $Z^{\text{pert-II}}$, which shows that the full perturbative part $Z^{\text{pert}}_{Sp(2)_\pi+1\mathbf{AS}}$ is the same as that of $Sp(2)_0 + 1\mathbf{AS}$, as expected.

1. Instanton contribution

We now consider the instanton contribution for $Sp(2)_\pi + 1\mathbf{AS}$. To obtain the instanton contributions, the summation part of the topological string partition function is needed:

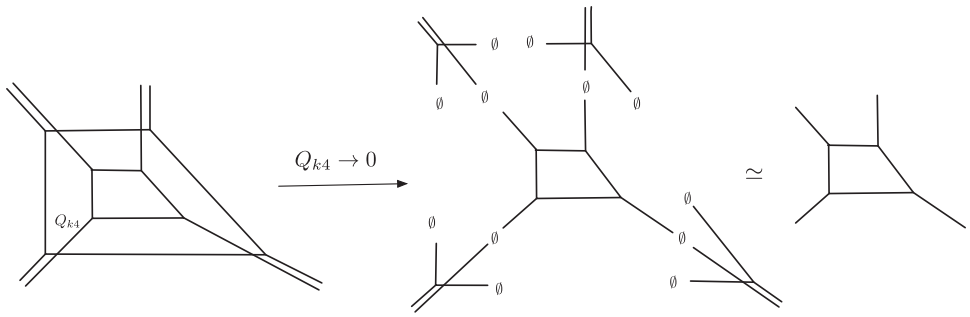

FIG. 19. Sending $Q_{k4} \to 0$ implies $A_1 \to 0$. According to T_2 tuning, each jump on the four corners of the middle diagram provides a trivial contribution, namely, 1, or extra factors if the **AS** is massive, so $Sp(2)_\pi + 1\mathbf{AS}$ reduces to $SU(2)_\pi$.

$$Z^{\text{sum}}_{Sp(2)_\pi+1\mathbf{AS}} = \sum_{\nu_1,\nu_2,\nu_3,\nu_4} \sum_{\alpha_1,\alpha_4,\alpha_5,\alpha_8} Z^{\mathbf{sum}}_{\mathbf{Sp(2)}+1\mathbf{AS}} \cdot \mathbf{terms}_\pi,$$
$$\mathbf{terms}_\pi := (-1)^{|\nu_1|+|\nu_2|+|\nu_3|+|\nu_4|} A_1^{|\nu_3|-|\nu_4|} A_2^{|\nu_1|-|\nu_2|} q^{-\frac{\|\nu_1^T\|^2+\|\nu_2\|^2+\|\nu_3^T\|^2+\|\nu_4\|^2}{2}} t^{\frac{\|\nu_1\|^2+\|\nu_2^T\|^2+\|\nu_3\|^2+\|\nu_4^T\|^2}{2}}, \tag{4.34}$$

where $Z^{\mathbf{sum}}_{\mathbf{Sp(2)}+1\mathbf{AS}}$ is defined in Eq. (4.13).

The one- and two-instanton contributions then take the form

$$Z^{\text{one-instanton}}_{Sp(2)_\pi+1\mathbf{AS}} = -\frac{\sqrt{qt}}{(1-q)(1-t)}(A_1 + A_2) + \frac{q+t}{(1-q)(1-t)}\left(\chi_2^{SU(2)}(Q_8) + \frac{q+t}{\sqrt{qt}}\right) A_1 A_2 (A_1 + A_2) + \mathcal{O}({A_1}^2; {A_2}^2). \tag{4.35}$$

$$Z^{\text{two-instanton}}_{Sp(2)_\pi+1\mathbf{AS}} = -\frac{qt(q+t)}{(1-q)^2(1+q)(1-t)^2(1+t)}({A_1}^2 + {A_2}^2) + \frac{qt}{(1-q)^2(1-t)^2} A_1 A_2 + \frac{2(q+t)\sqrt{qt}}{(1-q)^2(1-t)^2}\left(\chi_2^{SU(2)}(Q_8) + \frac{q+t}{qt}\right) {A_1}^2 {A_2}^2 + \mathcal{O}({A_1}^2; {A_2}^2). \tag{4.36}$$

2. Reduction to $SU(2)_\pi$

When the antisymmetric matter **AS** is massless, the corresponding 5-brane web becomes two copies of $Sp(1)_\pi$ theories as depicted in Fig. 3. This means that the corresponding partition function factorizes to

$$Z^{\text{sum}}_{Sp(2)_\pi+1\mathbf{AS}} = Z_{\text{inner layer}} \cdot Z_{\text{outer layer}} = Z_{SU(2)_\pi} \cdot Z_{SU(2)_{\pi'}}. \tag{4.37}$$

In fact, by applying the T_2 tuning, one can check that the partition $Sp(N) + 1\mathbf{AS} + N_f\mathbf{F}$ also factorizes to N copies of $Sp(N) + 1\mathbf{AS} + N_f\mathbf{F}$ in the massless limit of antisymmetric hypermultiplet **AS**.

Regardless of the antisymmetric matter being massless or massive, brane webs of $Sp(2)_{0,\pi} + 1\mathbf{AS}$ are reduced to the webs of $SU(2)_{0,\pi}$ as the Coulomb branch parameter $A_1 \to 0$ or, equivalently, $Q_{k4} \to 0$. This is because, in the topological vertex, each internal edge is associated with $(-Q)^{|\nu|}$ and so, if $Q \to 0$, only trivial Young diagram $\nu = \emptyset$ contributes.[1] This reduction is illustrated in Fig. 19. By taking the Coulomb branch parameter $A_1 \to 0$ or $Q_{k4} \to 0$, one gets the constraints[2] $\nu_3 = \emptyset$, $\nu_4 = \emptyset$, $\alpha_1 = \emptyset$, $\alpha_4 = \emptyset$, and $\alpha_5 = \emptyset$ for the un-Higgsed diagram in Fig. 18. Hence, $Z_{SU(2)_{\pi'}} \to 1$ and $Z \to Z_{SU(2)_\pi}$. Through this reduction, we reproduce the partition function for $SU(2)_\pi$:

[1]This means (length of line $\to \infty$) $\simeq$ ($Q \to 0$) $\simeq$ ($\nu \to \emptyset$) $\simeq$ (cut internal line).

[2]$\nu_3 = \emptyset$ and $\nu_4 = \emptyset$ force $\alpha_1 = \emptyset$, $\alpha_4 = \emptyset$, and $\alpha_5 = \emptyset$ through Eq. (3.20).

$$
\begin{aligned}
Z^{\mathrm{Nek}}_{SU(2)_\pi} &= Z^{\mathrm{pert}}_{SU(2)_\pi} \cdot Z^{\mathrm{instanton}}_{SU(2)_\pi}, \\
Z^{\mathrm{instanton}}_{SU(2)_\pi} &= \sum_{\nu_1,\nu_2} (-1)^{|\nu_1|+|\nu_2|} Q_b^{|\nu_1|+|\nu_2|} q^{\frac{-||\nu_1^T||^2+||\nu_2||}{2}} t^{\frac{3||\nu_1||^2+||\nu_2^T||^2}{2}} ||\tilde{Z}_{\nu_1}(t,q)||^2 ||\tilde{Z}_{\nu_2}(t,q)||^2 \\
&\quad \times \frac{1}{N_{\nu_2,\nu_1^T}(Q_F; t^{-1}, q^{-1}) N_{\nu_2,\nu_1^T}(Q_F \frac{t}{q}; t^{-1}, q^{-1})}, \\
Z^{\mathrm{pert}}_{SU(2)_\pi} &= \frac{1}{M(Q_F; t, q) M(Q_F; q, t)},
\end{aligned}
\tag{4.38}
$$

which is the same as the result in Ref. [17]. This is a trivial consistency check for the partition function of the $Sp(2)$ theory to satisfy. If an antisymmetric hypermultiplet is massive, one, of course, needs to remove the extra factor arising from the mass of an antisymmetric hypermultiplet.

C. $Sp(2)$ + 1AS + 1F

Three equivalent webs related through Hanany-Witten moves were depicted in Fig. 20. We choose the first web in Fig. 20 for computation, as it shows fiber-base duality. Its un-Higgsed diagram is depicted in Fig. 21. The relations between Kähler parameters are given by

$$
\begin{aligned}
&Q_{k1} = \frac{Q_{8,k4}}{Q_1}, \qquad Q_{k2} = \frac{Q_{2,8,k4}}{Q_{1,3}}, \qquad Q_{k3} = \frac{Q_{k4,2,4,8}}{Q_{1,3,5}}, \qquad Q_7 = \frac{Q_{2,3,6,8}}{Q_{1,3,5}}, \\
&Q_{11} = \frac{Q_{2,4,5,B,k_4,k_4}}{Q_{1,3,5}}, \qquad Q_{22} = \frac{Q_{2,8,8,B,k_4,k_4}}{Q_{1,1,3}}, \qquad Q_{33} = \frac{Q_{8,F,k_4,k_4}}{Q_1}, \qquad Q_{44} = \frac{Q_{2,2,4,8,8,F,k_4,k_4}}{Q_{1,1,3,3,5}}, \\
&Q_{m_{11}} = \frac{Q_{f_2,m_1}}{Q_3}, \qquad Q_{f_3} = \frac{Q_{3,4}}{Q_{f_2}}.
\end{aligned}
\tag{4.39}
$$

Following T_2 tuning, we assign values to tuned Kähler parameters

$$
Q_1 = Q_2 = Q_3 = Q_4 = \sqrt{\frac{q}{t}}, \qquad Q_5 = Q_6 = \sqrt{\frac{t}{q}}, \qquad Q_{f_1} = Q_{f_2} = Q_{f_3} = \sqrt{\frac{q}{t}},
\tag{4.40}
$$

which corresponds to two case B, one case C, and one case D. Next, we apply the conventional method on auxiliary lines to find the relations between Kähler parameters and instanton fugacity u, and L_{up} and L_{down} can be read off from the diagram, as discussed in Fig. 15:

$$
\begin{aligned}
L_{\mathrm{up}} &= \frac{Q_B}{\sqrt{Q_F}} \cdot Q_{k2} Q_4 Q_{m_1} = \frac{Q_B}{\sqrt{Q_F}} \cdot Q_8 Q_{k4} Q_{m_1}, \qquad L_{\mathrm{down}} = \frac{Q_B}{Q_F}, \\
L_{\mathrm{up}} \cdot L_{\mathrm{down}} &= u^2 \Rightarrow Q_B = \frac{Q_F^{3/4} u}{\sqrt{Q_8 Q_{k4} Q_{m_1}}}.
\end{aligned}
\tag{4.41}
$$

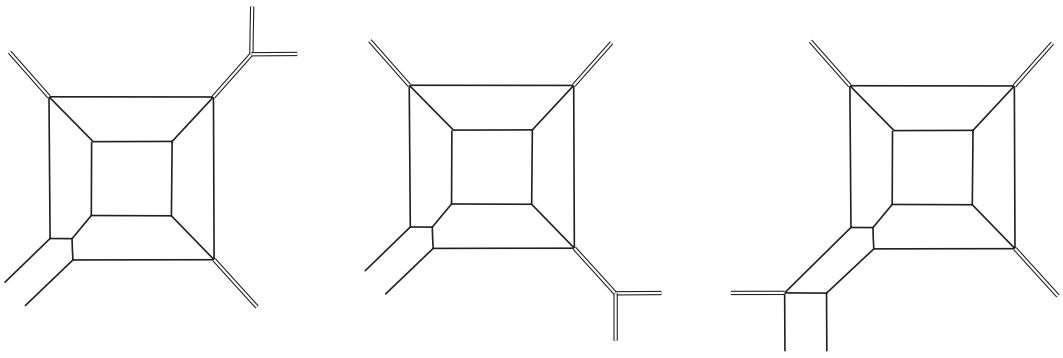

FIG. 20. Some equivalent webs for $Sp(2) + 1\mathbf{AS} + 1\mathbf{F}$.

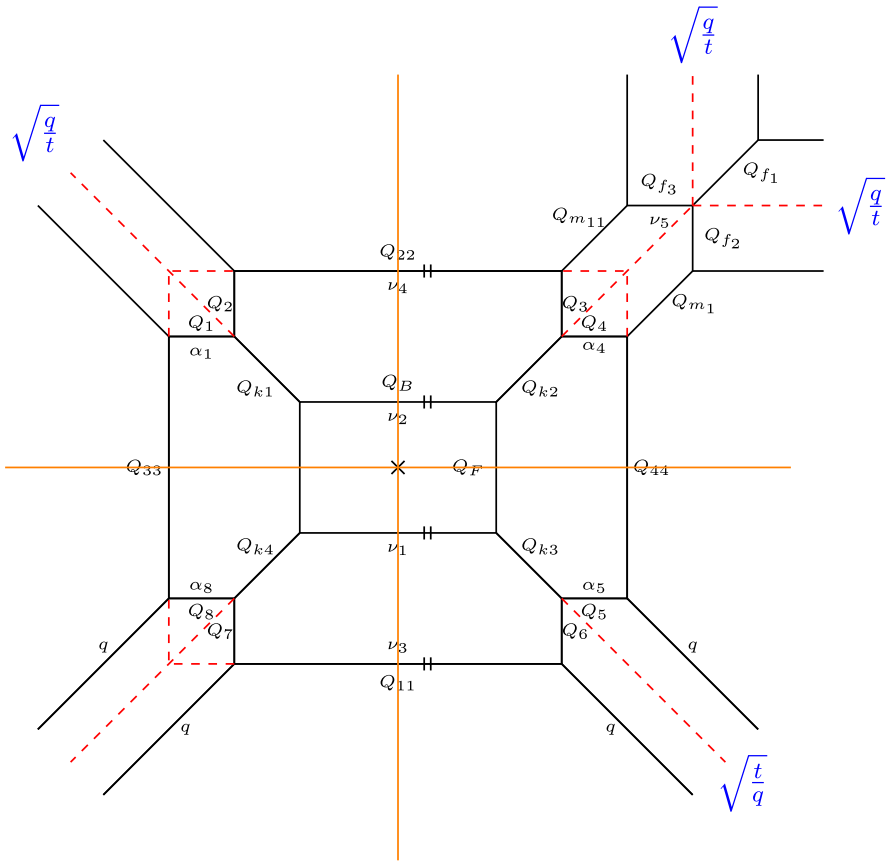

FIG. 21. An un-Higgsed diagram for $Sp(2) + 1\mathbf{AS} + 1\mathbf{F}$.

Hence, in order to reproduce the Nekrasov partition function, independent Kähler parameters should be assigned with

$$Q_F = {A_2}^2, \qquad Q_{k4} = \frac{A_1}{A_2 Q_8}, \qquad Q_B = \frac{u{A_2}^2}{\sqrt{y_1}}, \qquad Q_{m_1} = \frac{y_1}{A_1}, \tag{4.42}$$

where $y_1 = e^{-im_1}$ and m_1 is the mass of the flavor.

In this case, case D comes from adding flavor **F** and leads to a geometric transition-related term (3.20) in the partition function, which gives the constraint $\nu_5 = \emptyset$. Thus, the summation part Z^{sum} can be reduced:

$$\begin{aligned} Z^{\text{sum}}_{Sp(2)+1\mathbf{AS}+1\mathbf{F}} &= \sum_{\nu_1,\nu_2,\nu_3,\nu_4,\nu_5} \sum_{\alpha_1,\alpha_2,\alpha_3,\alpha_4} Z[\nu_1,\nu_2,\nu_3,\nu_4,\nu_5;\alpha_1,\alpha_4,\alpha_5,\alpha_8] \\ &= \sum_{\nu_1,\nu_2,\nu_3,\nu_4} \sum_{\alpha_1,\alpha_2,\alpha_3,\alpha_4} Z[\nu_1,\nu_2,\nu_3,\nu_4,\emptyset;\alpha_1,\alpha_4,\alpha_5,\alpha_8], \end{aligned} \tag{4.43}$$

which differs from the summation part of $Sp(2) + 1\mathbf{AS}$ by a term $\mathbf{terms}[\mathbf{y_1}]$:

$$\begin{aligned} Z^{\text{sum}}_{Sp(2)+1\mathbf{AS}+1\mathbf{F}} &= \sum_{\nu_1,\nu_2,\nu_3,\nu_4} \sum_{\alpha_1,\alpha_4,\alpha_5,\alpha_8} Z^{\mathbf{sum}}_{\mathbf{Sp(2)}+1\mathbf{AS}} \cdot \mathbf{terms}[y_1], \\ \mathbf{terms}[y_1] &:= y_1^{-\frac{|\nu_1|+|\nu_2|+|\nu_3|+|\nu_4|}{2}} N^{\text{half},-}_{\nu_2}\left(\frac{y_1}{A_2}\right) N^{\text{half},-}_{\nu_4}\left(\frac{y_1}{A_1}\right) N^{\text{half},-}_{\nu_1^T}(A_2 y_1) N^{\text{half},-}_{\nu_3^T}(A_1 y_1), \end{aligned} \tag{4.44}$$

where $Z^{\mathbf{sum}}_{\mathbf{Sp(2)}+1\mathbf{AS}}$ is defined in Eq. (4.13).

1. Perturbative contribution

We find that the fundamental hypermultiplet does not contribute to $Z^{\text{pert-II}}$ but adds to $Z^{\text{pert-I}}$ the term $Z_{\mathbf{F}}^{\text{pert}}$:

$$Z^{\text{pert-II}}_{Sp(2)+1\mathbf{AS}+n\mathbf{F}} = Z^{\text{pert-II}}_{Sp(2)+1\mathbf{AS}}, \tag{4.45}$$

$$Z^{\text{pert-I}}_{Sp(2)+1\mathbf{AS}+n\mathbf{F}} = Z^{\text{pert-I}}_{Sp(2)+1\mathbf{AS}} \cdot \prod_{i=1}^{n} Z_{\mathbf{F}}^{\text{pert}}(Q_{m_i}), \tag{4.46}$$

$$Z_{\mathbf{F}}^{\text{pert}}(Q_{m_i}) = M\left(\frac{A_1}{y_1}\sqrt{\frac{t}{q}}, t, q\right) M\left(A_1 y_1 \sqrt{\frac{t}{q}}, t, q\right) M\left(\frac{A_2}{y_1}\sqrt{\frac{t}{q}}, t, q\right) M\left(A_2 y_1 \sqrt{\frac{t}{q}}, t, q\right), \tag{4.47}$$

where $Z_{\mathbf{F}}^{\text{pert}}(Q_{m_i})$ is the contribution of the flavor $\mathbf{F}$ to the perturbative part. In total, the fully perturbative part for $Sp(2) + 1\mathbf{AS} + 1\mathbf{F}$ is given by

$$Z^{\text{pert}}_{Sp(2)+1\mathbf{AS}+1\mathbf{F}} = \frac{Z^{\text{pert-I}}_{Sp(2)+1\mathbf{AS}+1\mathbf{F}} \cdot Z^{\text{pert-II}}_{Sp(2)_0+1\mathbf{AS}+1\mathbf{F}}}{Z^{\text{extra}}_{Q_8}} = Z^{\text{pert}}_{Sp(2)+1\mathbf{AS}} \cdot Z_{\mathbf{F}}^{\text{pert}}(Q_{m_1}), \tag{4.48}$$

which exactly agrees with localization computation (B1). With proper normalization, the perturbative part can be expanded as

$$\begin{aligned}\frac{Z^{\text{pert}}_{Sp(2)+1\mathbf{AS}+1\mathbf{F}}}{M(Q_8\sqrt{\frac{t}{q}}, t, q)^2} &= 1 - \frac{\sqrt{qt}\chi_2^{SU(2)}[y_1]}{(1-q)(1-t)}A_2 - \frac{(q^{\frac{3}{2}}t^{\frac{3}{2}} - qt\chi_2^{SU(2)} + \sqrt{qt})\chi_2^{SU(2)}[y_1]}{(1-q)^2(1-t)^2}A_1 \\ &+ \frac{(q+t) - \sqrt{qt}\chi_2^{SU(2)}}{(1-q)(1-t)}\frac{A_1}{A_2} + \frac{qt(q+t)\chi_3^{SU(2)}[y_1] + (qt(1+qt) - (q+t)(q^2+t^2-q^2t^2-1))}{(1-q)^2(1+q)(1-t)^2(1+t)}{A_2}^2 \\ &+ \mathcal{O}({A_1}^1; {A_2}^1),\end{aligned}$$

where $\chi_2^{SU(2)}[y_1] = y_1 + y_1^{-1}$, $\chi_3^{SU(2)}[y_1] = y_1^2 + 1 + y_1^{-2}$, and $\chi_2^{SU(2)} = Q_8 + Q_8^{-1}$.

2. Instanton contribution

The instanton contribution is obtained by Eq. (4.9). As $Z^{\text{nonpert-I}} = 1$ in this case, the one-instanton contribution is given by

$$Z^{\text{one-instanton}}_{Sp(2)+1\mathbf{AS}+1\mathbf{F}} = \frac{\sum_{\alpha_1,\alpha_4,\alpha_5,\alpha_8} \sum_{\substack{\nu_1,\nu_2,\nu_3,\nu_4 \in \{\square,\emptyset\} \\ |\nu_1|+|\nu_2|+|\nu_3|+|\nu_4|=1}} Z[\nu_1,\nu_2,\nu_3,\nu_4,\emptyset;\alpha_1,\alpha_4,\alpha_5,\alpha_8]}{Z^{\text{pert-II}}_{Sp(2)+1\mathbf{AS}+1\mathbf{F}}}. \tag{4.49}$$

By expanding it with respect to Coulomb branch parameters, we obtain

$$\begin{aligned}Z^{\text{one-instanton}}_{Sp(2)+1\mathbf{AS}+1\mathbf{F}} &= \frac{-\sqrt{qt}\sqrt{y_1}}{(1-q)(1-t)}(A_2 + A_1) + \frac{q+t}{(1-q)(1-t)\sqrt{y_1}}(A_2^2 + A_1^2) \\ &+ \frac{q+t-\sqrt{qt}\chi_2^{SU(2)}}{(1-q)(1-t)\sqrt{y_1}}A_2A_1 - \frac{(q+t)(q+t-\sqrt{qt}\chi_2^{SU(2)})\sqrt{y_1}}{(1-q)(1-t)\sqrt{qt}}(A_2^2A_1 + A_1A_2^2) \\ &+ \frac{(q+t)^2(q+t-\sqrt{qt}\chi_2^{SU(2)})}{(1-q)q(1-t)t\sqrt{y_1}}A_2^2A_1^2 + \mathcal{O}(A_1^3; A_2^3),\end{aligned} \tag{4.50}$$

which equals the localization result (B5) with $N_f = 1$, $y_1 \coloneqq e^{m_1}$, and $Q_8 \coloneqq e^m$.

Similarly, the two-instanton contribution is given by

$$Z^{\textbf{two-instanton}}_{Sp(2)+1\mathbf{AS}+1\mathbf{F}} = \frac{\sum_{\alpha_1,\alpha_4,\alpha_5,\alpha_8} \sum_{\substack{\nu_1,\nu_2,\nu_3,\nu_4 \in \{\square,\ \square\square,\ \square,\ \emptyset\} \\ |\nu_1|+|\nu_2|+|\nu_3|+|\nu_4|=2}} Z[\nu_1,\nu_2,\nu_3,\nu_4,\emptyset;\alpha_1,\alpha_4,\alpha_5,\alpha_8]}{Z^{\textbf{pert-II}}}, \tag{4.51}$$

which can be expanded in terms of A_1 and A_2:

$$\begin{aligned} Z^{\text{two-instanton}}_{Sp(2)+1\mathbf{AS}+1\mathbf{F}} &= \frac{qt(q+t)y_1}{(1-q)^2(1+q)(1-t)^2(1+t)}(A_2^2+A_1^2) + \frac{qty_1}{(1-q)^2(1-t)^2}A_1A_2 \\ &\quad - \frac{2\sqrt{qt}(q+t) - qt\chi_2^{SU(2)}}{(1-q)^2(1-t)^2}(A_2^2A_1 + A_2A_1^2) + \mathcal{O}(A_1^2;A_2^2). \end{aligned} \tag{4.52}$$

3. Enhancement of global symmetry

Nekrasov partition functions of $Sp(2)_0 + 1\mathbf{AS} + N_f\mathbf{F}$ enjoy global symmetry enhancement with properly shifting of parameters (A_i, u, y_i). With the help of fiber-base duality, this shift can be found. The exchanging symmetry between A_1 and A_2 preserves, so following the argument in Ref. [47] we shift

$$\tilde{A}_1 = A_1 u^{\frac{2}{7}}, \qquad \tilde{A}_2 = A_2 u^{\frac{2}{7}}. \tag{4.53}$$

According to the webs in Fig. 21, the global symmetry of $Sp(2) + 1\mathbf{AS} + 1\mathbf{F}$ is supposed to be $G = SU(2)_{Q_8} \times E_1 = SU(2)_{Q_8} \times SU(2) \times U(1)$. We define two new fugacities u_1 and u_2 for $SU(2)_{u_1} \times U(1)_{u_2}$, respectively. The fiber-base duality

$$Q_B \leftrightarrow Q_F, \qquad Q_8 \leftrightarrow Q_8, \qquad Q_{m_1} \leftrightarrow Q_{m_1}, \tag{4.54}$$

through shifts, becomes

$$u_1 \leftrightarrow u_1^{-1}, \qquad u_2 \leftrightarrow u_2, \qquad \tilde{A}_1 \leftrightarrow \tilde{A}_1, \qquad \tilde{A}_2 \leftrightarrow \tilde{A}_2, \tag{4.55}$$

which along with Eq. (4.53) determine the relations between u and fugacities $u_{1,2}$ as follows:

$$\tilde{A}_1 = u_1^{\frac{1}{2}}u_2^{-\frac{1}{14}}A_1, \qquad \tilde{A}_2 = u_1^{\frac{1}{2}}u_2^{-\frac{1}{14}}A_2, \qquad u = u_1^{\frac{7}{4}}u_2^{-\frac{1}{4}}, \qquad y_1 = \frac{1}{\sqrt{u_1u_2}}. \tag{4.56}$$

These relations are similar to relations for $SU(2) + 1\mathbf{F}$ in Ref. [47]. Once again, we note that $Sp(2) + 1\mathbf{AS} + N_f\mathbf{F}$ is similar to $SU(2) + N_f\mathbf{F}$. We indeed find that shifted partition functions can be expressed in terms of the characters of enhanced $SU(2)_{Q_8} \times E_1$ global symmetry as expected

$$\begin{aligned} Z_{Sp(2)+1\mathbf{AS}+1\mathbf{F}} &= 1 - \frac{\sqrt{qt}(u_2^{\frac{4}{7}} + u_2^{-\frac{3}{7}}\chi_2^{SU(2)}[u_1])}{(1-q)(1-t)}\tilde{A}_2 + \frac{q+t-\sqrt{qt}\chi_2^{SU(2)}}{(1-q)(1-t)}\frac{\tilde{A}_1}{\tilde{A}_2} \\ &\quad - \frac{\sqrt{qt}(u_2^{\frac{4}{7}} + u_2^{-\frac{3}{7}}\chi_2^{SU(2)}[u_1])(-\sqrt{qt}\chi_2^{SU(2)} + 1 + qt)}{(1-q)^2(1-t)^2}\tilde{A}_1 \\ &\quad + \frac{(q+t)(qt\chi_3^{SU(2)} - \sqrt{qt}(1+q)(1+t)\chi_2^{SU(2)} + (q+t)(1+qt) + qt)}{(1-q)^2(1+q)(1-t)^2(1+t)}\frac{\tilde{A}_1^2}{\tilde{A}_2^2} \\ &\quad + \mathcal{O}(\tilde{A}_1^2;\tilde{A}_2^2), \end{aligned} \tag{4.57}$$

where $\chi_2^{\mathrm{SU}(2)}[u_1] = u_1 + u_1^{-1}$.

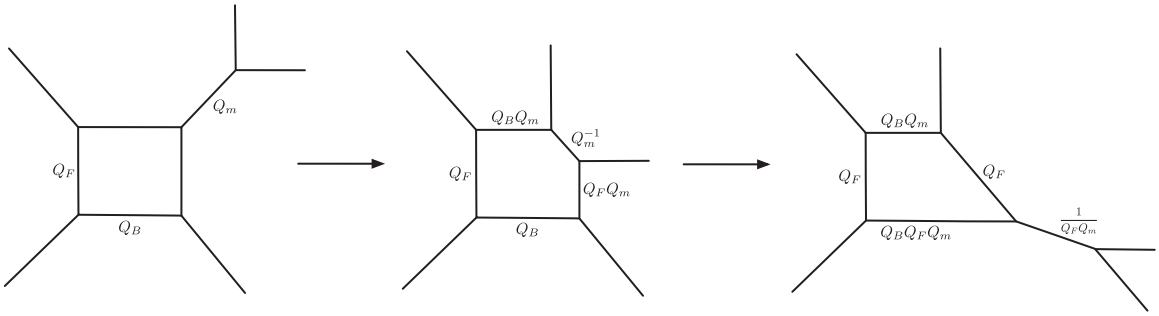

FIG. 22. $SU(2)_0 + 1\mathbf{F}$ and $SU(2)_\pi + 1\mathbf{F}$ are equivalent via two flops.

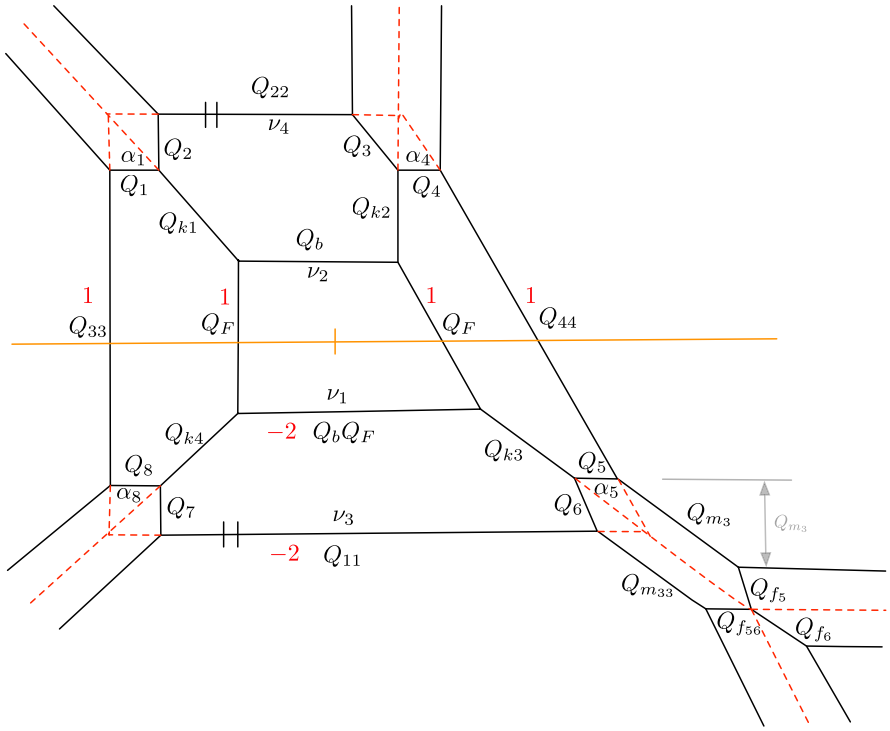

FIG. 23. The un-Higgsed diagram for $Sp(2)_\pi + 1\mathbf{AS} + 1\mathbf{F}$, with framing numbers in red assigned.

4. $Sp(2)_\pi + 1\mathbf{AS} + 1\mathbf{F}$

Just like the fact that $SU(2)_0 + 1\mathbf{F}$ and $SU(2)_\pi + 1\mathbf{F}$ are equivalent up to flops, there is equivalence

$$Sp(2)_0 + 1\mathbf{AS} + 1\mathbf{F} \backsimeq Sp(2)_\pi + 1\mathbf{AS} + 1\mathbf{F}, \tag{4.58}$$

related through flops. By taking the mass of $1\mathbf{F}$ to infinity to decouple flavor, one can obtain $Sp(2)_0 + 1\mathbf{AS}$ and $Sp(2)_\pi + 1\mathbf{AS}$, respectively. Similar to the flops illustrated in Fig. 22, Kähler parameters of $Sp(2)_0 + 1\mathbf{AS} + 1\mathbf{F}$ and of $Sp(2)_\pi + 1\mathbf{AS} + 1\mathbf{F}$ are related through transformation[3]

$$Q_F \to Q_F, \qquad Q_{k4} \to Q_{k4}, \qquad Q_B \to Q_8 Q_b Q_F Q_{k4} Q_{m_3}, \qquad Q_{m_1} \to (Q_8{}^2 Q_F Q_{k4} Q_{m_3})^{-1}. \tag{4.59}$$

Following T_2 tuning in Sec. III, we find the correct tuned Kähler parameters for the un-Higgsed diagram of $Sp(2)_\pi + 1\mathbf{AS} + 1\mathbf{F}$ depicted in Fig. 23 are given as follows:

[3]The parameters on the left-hand side of arrows are for $Sp(2)_0 + 1\mathbf{AS}$ and the right side for $Sp(2)_\pi + 11\mathbf{AS}$.

$$Q_1 = Q_2 = Q_3 = Q_4 = \sqrt{\frac{q}{t}}, \qquad Q_5 = Q_6 = Q_{f_5} = Q_{f_6} = Q_{f_{56}} = \sqrt{\frac{t}{q}}, \tag{4.60}$$

and independent Kähler parameters are assigned with gauge theory parameters

$$Q_F = {A_2}^2, \qquad Q_{k4} = \frac{A_1}{A_2 Q_8}, \qquad Q_b = \frac{uA_2}{\sqrt{y_3}}, \qquad Q_{m_3} = \frac{y_3}{A_1}, \tag{4.61}$$

where $y_3 = e^{-im_3}$.

We find the perturbative part is equal to Eq. (4.48), and the one-instanton contribution obtained from Eq. (4.49) can be expressed as

$$\begin{aligned} Z^{\text{one-instanton}}_{Sp(2)_\pi+1\mathbf{AS}+1\mathbf{F}} = & -\frac{\sqrt{qt}}{(1-q)(1-t)\sqrt{y_3}}(A_1+A_2) + \frac{(q+t)\sqrt{y_3}}{(1-q)(1-t)}({A_1}^2+{A_2}^2) \\ & + \frac{\sqrt{y_3}(q+t-\sqrt{qt}\chi_2^{SU(2)})}{(1-q)(1-t)}A_1A_2 - \frac{(q+t)(q+t-\sqrt{qt}\chi_2^{SU(2)})}{(1-q)(1-t)\sqrt{qt}\sqrt{y_3}}(A_1{A_2}^2+A_2{A_1}^2) \\ & + \frac{\sqrt{y_3}(q+t)^2(q+t-\sqrt{qt}\chi_2^{SU(2)})}{(1-q)(1-t)qt}{A_1}^2{A_2}^2 + \mathcal{O}(A_1,A_2), \end{aligned} \tag{4.62}$$

which equals Eq. (4.50) as expected. The two-instanton contribution was checked to agree with Eq. (4.52). The topological string partition functions between $Sp(2)_{0,\pi} + 1\mathbf{AS} + 1\mathbf{F}$ are equal through transformation (4.59). By taking the mass m_3 for flavor to infinity to decouple flavor, namely, $Q_{m_3} \to 0$, one can reproduce the topological string partition function for $Sp(2)_\pi + 1\mathbf{AS}$.

D. $Sp(2) + 1\mathbf{AS} + 2\mathbf{F}$

For $Sp(2) + 1\mathbf{AS} + 2\mathbf{F}$, there are many equivalent web configurations related through Hanany-Witten moves, and some of them are depicted in Fig. 24. The Nekrasov partition functions for web configurations in Fig. 24 become equivalent, once extra factors were removed:

$$\begin{aligned} Z^{\text{Nek}}_{Sp(2)+1\mathbf{AS}+2\mathbf{F}} &= \frac{Z^{\text{top}}_{Sp(2)+1\mathbf{AS}+2\mathbf{F}\backslash\backslash}}{Z^{\text{extra}}_{Q_8}} = \frac{Z^{\text{top}}_{Sp(2)+1\mathbf{AS}+2\mathbf{F}^{=}}}{Z^{\text{extra}}_{=}\cdot Z^{\text{extra}}_{Q_8}} = \frac{Z^{\text{top}}_{Sp(2)+1\mathbf{AS}+2\mathbf{F}^{\parallel}}}{Z^{\text{extra}}_{\parallel}\cdot Z^{\text{extra}}_{Q_8}} = \frac{Z^{\text{top}}_{Sp(2)+1\mathbf{AS}+2\mathbf{F}^{=//}}}{Z^{\text{extra}}_{=//}\cdot Z^{\text{extra}}_{Q_8}} \\ &= \underbrace{Z^{\mathbf{pert}}_{Sp(2)+1\mathbf{AS}}\prod_{i=1}^{N_f=2} Z^{\text{pert}}_{\mathbf{F}}(Q_{m_i})}_{Z^{\text{pert}}_{Sp(2)+1\mathbf{AS}+2\mathbf{F}}} \cdot \underbrace{\left(1+\sum_{k=1}^{\infty}u^k Z_k(A_i,y_i)\right)}_{Z^{\mathbf{instanton}}_{Sp(2)+1\mathbf{AS}+2\mathbf{F}}}. \end{aligned} \tag{4.63}$$

We checked this equivalence up to two-instanton contributions, which is consistent with the fact that Nekrasov partition functions are insensitive to Hanany-Witten moves.

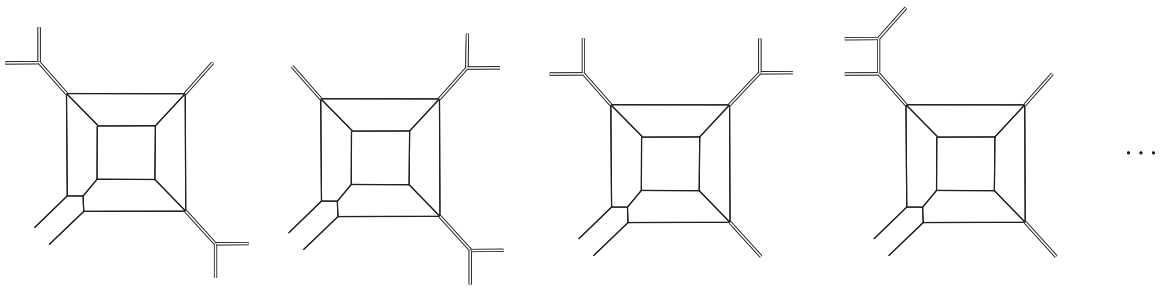

FIG. 24. Some equivalent webs related through Hanany-Witten moves for $Sp(2) + 1\mathbf{AS} + 2\mathbf{F}$.

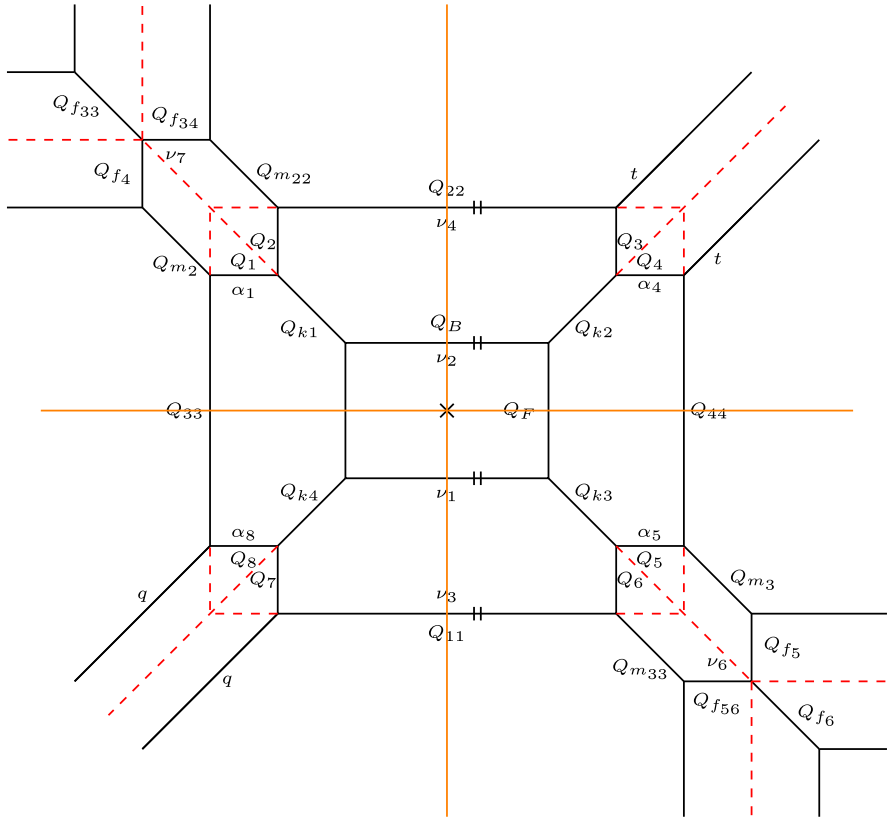

FIG. 25. The un-Higgsed diagram for $Sp(2) + 1\mathbf{AS} + 2\mathbf{F}^{//}$.

As a representative example, consider the first web in Fig. 24. This contains no extra factor other than $Z_{Q_8}^{\text{extra}}$ and also of reflection symmetry. For its un-Higgsed diagram depicted in Fig. 25, the associated tuned Kähler parameters are found to be the following:

$$Q_1 = Q_2 = Q_3 = Q_4 = Q_{f_{33}} = Q_{f_4} = Q_{f_{34}} = \sqrt{\frac{q}{t}}, \qquad Q_5 = Q_6 = Q_{f_5} = Q_{f_6} = Q_{f_{56}} = \sqrt{\frac{t}{q}}. \tag{4.64}$$

The relations between independent Kähler parameters and (A_i, u, y_i) are

$$Q_F = {A_2}^2, \qquad Q_{k4} = \frac{A_1}{A_2 Q_8}, \qquad Q_B = \frac{u{A_2}^2}{\sqrt{y_2}\sqrt{y_3}}, \qquad Q_{m_2} = \frac{y_2}{A_1}, \qquad Q_{m_3} = \frac{y_3}{A_1}. \tag{4.65}$$

Similar to $Sp(2)_0 + 1\mathbf{AS} + 1\mathbf{F}$, geometric transition relevant terms (3.20) caused by tuned parameters (4.64) give rise to constraints on Young diagrams: $\nu_6 = \emptyset$ and $\nu_7 = \emptyset$. Hence, the summation part of the topological string partition function can be reduced to

$$\begin{aligned} Z^{\text{sum}}_{Sp(2)+1\mathbf{AS}+2\mathbf{F}} &= \sum_{\substack{\nu_1,\nu_2,\nu_3,\nu_4,\\ \alpha_1,\alpha_2,\alpha_3,\alpha_4}} Z^{\mathbf{sum}}_{\mathbf{Sp(2)}+1\mathbf{AS}} \cdot \mathbf{terms}[y_1] \cdot \mathbf{terms}[y_2], \\ \mathbf{terms}[y_2] &:= y_2^{\frac{|\nu_1|+|\nu_2|+|\nu_3|+|\nu_4|}{2}} N^{\text{half},-}_{\nu_2}\left(\frac{y_2}{A_2}\right) N^{\text{half},-}_{\nu_4}\left(\frac{y_2}{A_1}\right) N^{\text{half},-}_{\nu_1^T}(A_2 y_2) N^{\text{half},-}_{\nu_3^T}(A_1 y_2), \end{aligned} \tag{4.66}$$

where $\mathbf{terms}[y_1]$ is defined in Eq. (4.44).

1. Perturbative and instanton contributions

The normalized perturbative part can be expressed as

$$\frac{Z^{\text{pert}}_{Sp(2)+1\mathbf{AS}+2\mathbf{F}}}{M(Q_8\sqrt{\frac{t}{q}},t,q)^2} = 1 - \frac{\sqrt{qt}(\chi_2^{SU(2)}[y_2]+\chi_2^{SU(2)}[y_3])}{(1-q)(1-t)}A_2 + \frac{(q+t)-\sqrt{qt}\chi_2^{SU(2)}}{(1-q)(1-t)}\frac{A_1}{A_2} - \frac{\sqrt{qt}(1+qt-\sqrt{qt}\chi_2^{SU(2)})(\chi_2^{SU(2)}[y_2]+\chi_2^{SU(2)}[y_3])}{(1-q)^2(1-t)^2}A_1 + \mathcal{O}(A_1^2;A_2^2),$$

where $\chi_2^{SU(2)}[y_i] = y_i + \frac{1}{y_i}$, $\chi_2^{SU(2)} = Q_8 + Q_8^{-1}$, and $\chi_3^{SU(2)} = Q_8^2 + 1 + Q_8^{-2}$.

2. Instanton contributions

The one-instanton contribution can be expanded:

$$\begin{aligned} Z^{\text{one-instanton}}_{Sp(2)+1\mathbf{AS}+2\mathbf{F}} = {} & \frac{-\sqrt{qt}}{(1-q)(1-t)}\chi_2[y_{2/3}](A_2+A_1) + \frac{q+t}{(1-q)(1-t)}\chi_2[y_{23}](A_2^2+A_1^2) \\ & + \frac{q+t-\sqrt{qt}\chi_3^{SU(2)}}{(1-q)(1-t)}\chi_2[y_{23}]A_1A_2 - \frac{(q+t)(q+t-\sqrt{qt}\chi_2^{SU(2)})}{(1-q)(1-t)\sqrt{qt}}\chi_2[y_{2/3}](A_2^2A_1+A_1A_2^2) \\ & + \frac{(q+t)^2(q+t-\sqrt{qt}\chi_2^{SU(2)})}{(1-q)q(1-t)t}\chi_2[y_{23}]A_2^2A_1^2 + \mathcal{O}(A_1^3;A_2^3), \end{aligned} \tag{4.67}$$

where we define $\chi_2[y_\cdot] = \sqrt{y_\cdot} + \frac{1}{\sqrt{y_\cdot}}$, $y_{23} := y_2y_3$, and $y_{2/3} := \frac{y_2}{y_3}$. To match the one-instanton contribution with localization result when $N_f = 2$, we define $y_2 = e^{m_2}$, $y_3 = e^{m_3}$, $Q_8 = e^m$, $A_1 = e^{\alpha_1}$, and $A_2 = e^{\alpha_2}$ for Eq. (B5).

Similarly, the two-instanton contribution can be obtained and expanded as

$$\begin{aligned} Z^{\text{two-instanton}}_{Sp(2)+1\mathbf{AS}+2\mathbf{F}} = {} & \frac{qt(1+qt+(q+t))(1+\chi_2[y_{2/3}])}{(1-q)^2(1+q)(1-t)^2(1+t)}(A_2^2+A_1^2) + \frac{qt(2+\chi_2[y_{2/3}])}{(1-q)^2(1-t)^2}A_2A_1 \\ & - \frac{2\sqrt{qt}(q+t)-qt\chi_2^{SU(2)}}{(1-q)^2(1-t)^2}(\chi_2[y_2]+\chi_2[y_3])(A_2^2A_1+A_2A_1^2) + \mathcal{O}(A_1^2,A_2^2), \end{aligned} \tag{4.68}$$

where $\chi_2[y_\cdot] = y_\cdot + \frac{1}{y_\cdot}$.

3. Enhancement of global symmetry

Because of enhancement, the Nekrasov partition function can be written in terms of characters of the global symmetry group. Following Ref. [47], the shifted Coulomb branch parameters for this theory are given by

$$\tilde{A}_1 = A_1u^{\frac{1}{3}}, \qquad \tilde{A}_2 = A_2u^{\frac{1}{3}}. \tag{4.69}$$

The global symmetry of $Sp(2)+1\mathbf{AS}+2\mathbf{F}$ should be $G = SU(2)_{Q_8}\times E_3 = SU(2)_{Q_8}\times SU(2)_{\tilde{u}}\times SU(3)_{\tilde{y}_1,\tilde{y}_2,\tilde{y}_3}$. We define new fugacities $\tilde{u}$ for $SU(2)_{\tilde{u}}$ and $\tilde{y}_1$, $\tilde{y}_2$, and $\tilde{y}_3$ for $SU(3)_{\tilde{y}_1,\tilde{y}_2,\tilde{y}_3}$,[4] respectively. The fiber-base duality for the diagram in Fig. 25 is

$$Q_B \leftrightarrow Q_F, \qquad Q_8 \leftrightarrow Q_8, \qquad Q_{m_2} \leftrightarrow Q_{m_3}, \tag{4.70}$$

which by new parameters $(\tilde{A}_i,\tilde{u},\tilde{y}_i)$ can be represented as

$$\tilde{u} \leftrightarrow \tilde{u}^{-1}, \qquad \tilde{y}_1 \leftrightarrow \tilde{y}_2, \qquad \tilde{y}_3 \leftrightarrow \tilde{y}_3, \qquad \tilde{A}_1 \leftrightarrow \tilde{A}_1, \qquad \tilde{A}_2 \leftrightarrow \tilde{A}_2. \tag{4.71}$$

[4]For $SU(3)$, $\tilde{y}_1\tilde{y}_2\tilde{y}_3 = 1$.

Then reparameterization can be fixed:

$$A_1 = \tilde{A}_1\sqrt{\tilde{y}_2\tilde{y}_3}, \qquad A_2 = \tilde{A}_2\sqrt{\tilde{y}_2\tilde{y}_3}, \qquad u = \tilde{y}_2^{-\frac{3}{2}}\tilde{y}_3^{-\frac{3}{2}}, \qquad y_2 = \sqrt{\frac{\tilde{u}\tilde{y}_2}{\tilde{y}_3}}, \qquad y_3 = \sqrt{\frac{\tilde{y}_2}{\tilde{u}\tilde{y}_3}}. \tag{4.72}$$

By taking these new parameters (4.72) into the normalized Nekrasov partition function, we indeed see the enhanced global symmetry:

$$\begin{aligned} Z_{Sp(2)+1\mathbf{AS}+2\mathbf{F}} = 1 &- \frac{\sqrt{qt}\chi_2^{SU(2)}[\tilde{u}]\chi_3^{SU(3)}[\tilde{y}]}{(1-q)(1-t)}\tilde{A}_2 + \frac{q+t-\sqrt{qt}\chi_2^{SU(2)}}{(1-q)(1-t)}\frac{\tilde{A}_1}{\tilde{A}_2} \\ &- \frac{\sqrt{qt}\chi_2^{SU(2)}[\tilde{u}]\chi_2^{SU(3)}[\tilde{y}](-\sqrt{qt}\chi_2^{SU(2)}+1+qt))}{(1-q)^2(1-t)^2}\tilde{A}_1 + \frac{(qt(q+t)\chi_3^{SU(2)}[\tilde{u}]+qt(1+qt))\chi_6^{SU(3)}[\tilde{y}]}{(1-q)^2(1+q)(1-t)^2(1+t)}\tilde{A}_2^2 \\ &+ \frac{((q+t)(1+q^2+t^2)-(q^3+t^3)+qt(1+qt)\chi_3^{SU(2)}[\tilde{u}])\chi_{\bar{3}}^{SU(3)}[\tilde{y}]}{(1-q)^2(1+q)(1-t)^2(1+t)}\tilde{A}_2^2 \\ &+ \frac{(q+t)(qt\chi_3^{SU(2)}-\sqrt{qt}(1+q)(1+t)\chi_2^{SU(2)}+(q+t)(1+qt)+qt)}{(1-q)^2(1+q)(1-t)^2(1+t)}\frac{\tilde{A}_1^2}{\tilde{A}_2^2} + \mathcal{O}(\tilde{A}_1^2;\tilde{A}_2^2), \end{aligned}$$

where

$$\chi_2^{SU(2)}[\tilde{u}] = \sqrt{\tilde{u}} + \frac{1}{\sqrt{\tilde{u}}}, \qquad \chi_3^{SU(2)}[\tilde{u}] = \tilde{u} + 1 + \tilde{u}^{-1}, \qquad \chi_3^{SU(3)}[\tilde{y}] = \tilde{y}_1 + \tilde{y}_2 + \tilde{y}_3,$$
$$\chi_{\bar{3}}^{SU(3)}[\tilde{y}] = \tilde{y}_1^{-1} + \tilde{y}_2^{-1} + \tilde{y}_3^{-1}, \qquad \chi_6^{SU(3)}[\tilde{y}] = \sum_{i=1}^{3}\frac{1}{\tilde{y}_i} + \tilde{y}_i.$$

4. Connected case D

Case D can be connected to other case D by adding fundamental flavors **F** or Hanany-Witten moving D7-branes on brane webs. For $Sp(2) + 1\mathbf{AS} + 2\mathbf{F}$, the fourth brane web shown in Fig. 24 is one typical example, whose un-Higgsed diagram is depicted in Fig. 26. Apart from the same tuned Kähler parameters in Eq. (4.64), there is one additional case D on the left top of the diagram in Fig. 26. According to the discussion in Sec. III B, the tuned Kähler parameters for case D should be determined by either of case A, B, C, or D it connects. We notice that for this diagram the tuned Kähler parameters for this case D are

$$Q_{f_9} = Q_{f_{10}} = Q_{f_{91}} = \sqrt{\frac{q}{t}}. \tag{4.73}$$

We observed that if we draw a horizontal line in orange on the web, all tuned Kähler parameters on the upper half-plane were given the value $\sqrt{\frac{q}{t}}$ and all tuned parameters on the lower half-plane $\sqrt{\frac{t}{q}}$ in this assignment of q and t on the diagram in Fig. 26. The associated gauge theory parameters for the un-Higgsed diagram in Fig. 26 are related to Kähler parameters by

$$Q_F = {A_2}^2, \qquad Q_{k4} = \frac{A_1}{A_2 Q_8}, \qquad Q_B = \frac{u{A_2}^2}{\sqrt{y_1}\sqrt{y_2}}, \qquad Q_{m_1} = \frac{y_1}{A_1}, \qquad Q_{m_2} = \frac{y_2}{A_1}. \tag{4.74}$$

The extra factors here are of the following:

$$Z^{\text{extra}}_{=//} = \frac{1}{M(\frac{y_1}{y_2},q,t)M(\frac{t}{q}\frac{y_1}{y_2},q,t)}\cdot\frac{1}{M(u\sqrt{y_1y_2},q,t)M(\frac{t}{q}u\sqrt{y_1y_2},q,t)}, \tag{4.75}$$

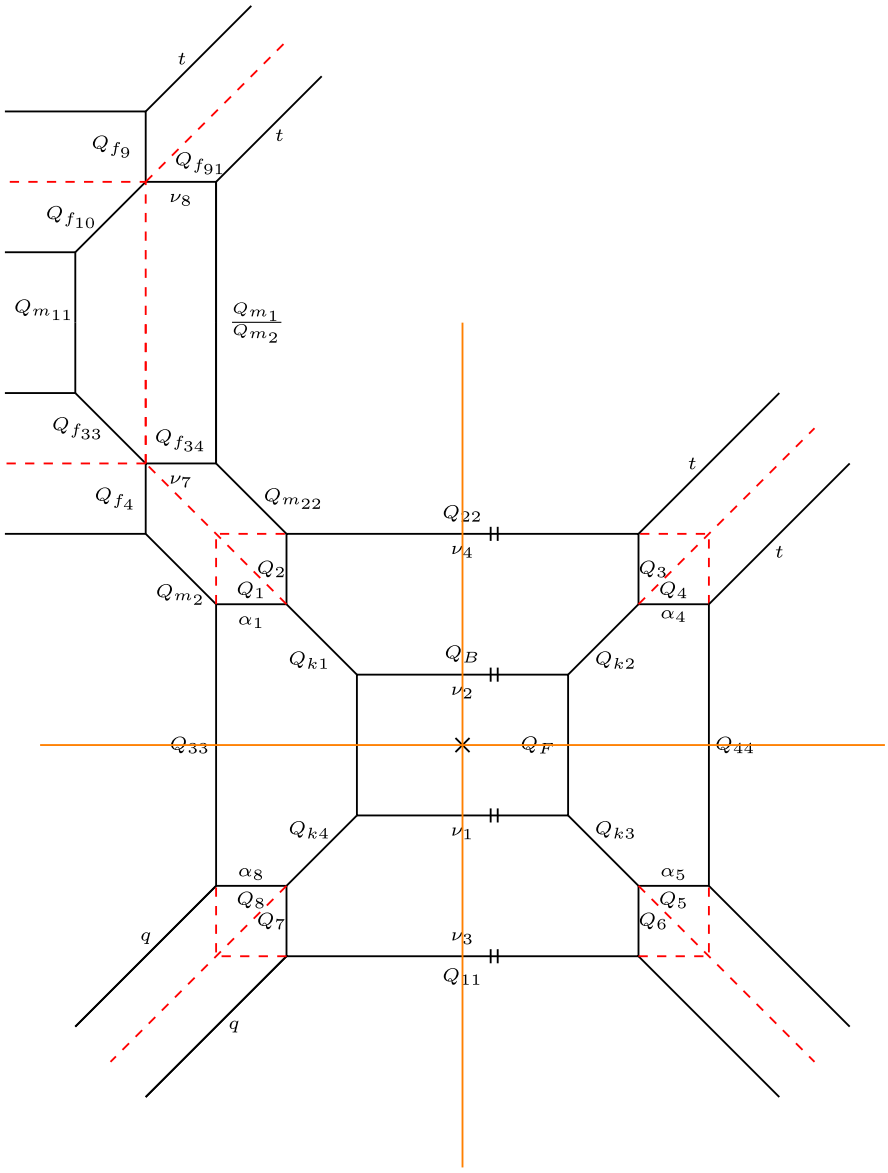

FIG. 26. The un-Higgsed diagram for $Sp(2) + 1\mathbf{AS} + 2\mathbf{F}^{=//}$.

where the instanton-dependent extra terms can be extracted by expanding the partition function and then picking up terms that break q, t-exchanging symmetry. The partition function obtained is the same as the web in Fig. 25, and, hence, we do not show the result again.

E. $Sp(2) + 1\mathbf{AS} + 3\mathbf{F}$

The un-Higgsed diagram for this theory is depicted in Fig. 27. Following the discussion in Sec. III B, the tuned Kähler parameters are determined to be

$$Q_1 = Q_2 = Q_3 = Q_4 = Q_{f_1} = Q_{f_2} = Q_{f_{33}} = Q_{f_4} = \sqrt{\frac{q}{t}},$$
$$Q_5 = Q_6 = Q_{f_5} = Q_{f_6} = \sqrt{\frac{t}{q}}. \tag{4.76}$$

The maps between Kähler parameters and gauge theory parameters (A_i, u, y_i) are

$$Q_F = {A_2}^2, \qquad Q_{k4} = \frac{A_1}{A_2 Q_8}, \qquad Q_B = \frac{u{A_2}^2}{\sqrt{y_2}\sqrt{y_3}},$$
$$Q_{m_1} = \frac{y_1}{A_1}, \qquad Q_{m_2} = \frac{y_2}{A_1}, \qquad Q_{m_3} = \frac{y_3}{A_1}, \tag{4.77}$$

where $y_i = e^{-im_i}$ are mass parameters. Similar to $Sp(2)_0 + 1\mathbf{AS} + N_f\mathbf{F}(N_f = 1, 2)$, constraints from Nekrasov factors (3.20) appear in the partition function and give rise to constraints on various Young diagrams: $\nu_5 = \emptyset$, $\nu_6 = \emptyset$, and $\nu_7 = \emptyset$. Hence, the summation part of topological string partition function Z^{sum} can be reduced to the following:

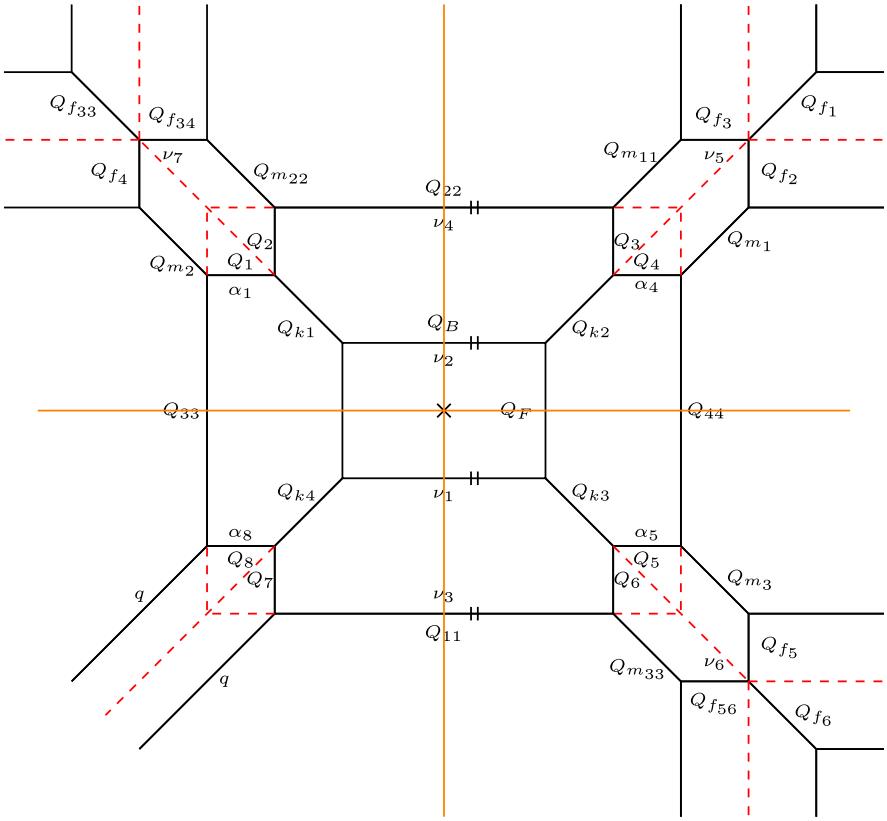

FIG. 27. The un-Higgsed diagram for $Sp(2) + 1\mathbf{AS} + 3\mathbf{F}$.

$$Z^{\text{sum}}_{Sp(2)+1\mathbf{AS}+3\mathbf{F}} = \sum_{\substack{\nu_1,\nu_2,\nu_3,\nu_4,\\ \alpha_1,\alpha_2,\alpha_3,\alpha_4}} Z^{\mathbf{sum}}_{\mathbf{Sp(2)}+1\mathbf{AS}} \cdot \mathbf{terms}[y_1] \cdot \mathbf{terms}[y_2] \cdot \mathbf{terms}[y_3],$$

$$\mathbf{terms}[y_3] := \frac{N^{\text{half},-}_{\alpha_4}(A_1 y_3) N^{\text{half},-}_{\alpha_4}(A_1 y_3 \frac{t}{q}) N^{\text{half},-}_{\nu_1^T}(\frac{y_3}{A_2}) N^{\text{half},-}_{\nu_2^T}(A_2 y_3) N^{\text{half},-}_{\nu_3^T}(\frac{y_3}{A_1}) N^{\text{half},-}_{\nu_4^T}(A_1 y_3)}{y_3^{\frac{|\nu_1|+|\nu_2|+|\nu_3|+|\nu_4|}{2}} N^{\text{half},-}_{\alpha_4^T}(A_1 y_3) N^{\text{half},-}_{\alpha_4^T}(A_1 y_3 \frac{t}{q})},$$

where $\mathbf{terms}[y_1]$ and $\mathbf{terms}[y_2]$ are defined in Eqs. (4.44) and (4.66), respectively. The extra factors for this theory are given by

$$\begin{aligned} Z^{\text{extra}}_{Sp(2)+1\mathbf{AS}+3\mathbf{F}} &= Z^{\text{pert extra}}_{Sp(2)+1\mathbf{AS}+3\mathbf{F}} \cdot Z^{\text{inst extra}}_{Sp(2)+1\mathbf{AS}+3\mathbf{F}} \\ &= \frac{1}{M(Q_{44}Q_{m_1}Q_{m_3}Q_{f_1}Q_{f_2}, t, q) M(Q_{44}Q_{m_1}Q_{m_3}, t, q)} \cdot \frac{1}{M(Q_{22}Q_{m_{11}}Q_{m_{22}}, q, t) M(Q_{22}Q_{f_3}Q_{f_{34}}Q_{m_{11}}Q_{m_{22}}, q, t)} \\ &= \frac{1}{M(y_1 y_3, t, q) M(\frac{y_1 y_3 q}{t}, t, q)} \cdot \frac{1}{M(u\sqrt{\frac{y_1 y_2}{y_3}}, t, q) M(\frac{t}{q} u \sqrt{\frac{y_1 y_2}{y_3}}, q, t)}. \end{aligned} \tag{4.78}$$

1. Perturbative contribution

We obtain the perturbative part

$$Z^{\text{pert}}_{Sp(2)+1\mathbf{AS}+3\mathbf{F}} = \frac{Z^{\text{pert-I}}_{Sp(2)+1\mathbf{AS}+3\mathbf{F}} \cdot Z^{\text{pert-II}}_{Sp(2)+1\mathbf{AS}+3\mathbf{F}}}{Z^{\text{extra}}_{Q_8} \cdot Z^{\text{pert extra}}_{Sp(2)+1\mathbf{AS}+3\mathbf{F}}} = Z^{\text{pert}}_{Sp(2)+1\mathbf{AS}} \prod_{i=1}^{N_f=3} Z^{pert}_{\mathbf{F}}(Q_{m_i}), \tag{4.79}$$

which can be expanded as

$$\frac{Z^{\text{pert}}_{Sp(2)+1\mathbf{AS}+3\mathbf{F}}}{M(Q_8\sqrt{\frac{t}{q}},t,q)^2} = 1 - \frac{\sqrt{qt}\chi_6^{SU(4)}[y]}{(1-q)(1-t)}A_2 + \frac{qt\chi_6^{SU(3)}[y]^2}{2(1-q)^2(1-t)^2}A_2^2$$
$$+ \frac{(q+t)(q+t+qt+1)+qt(2\chi_{15}^{SU(3)}[y]-\chi_6^{SU(3)}[y]^2)}{(1-q^2)(1-t^2)}A_2^2$$
$$+ \frac{(q+t)-\sqrt{qt}\chi_2^{SU(2)}}{(1-q)(1-t)}\frac{A_1}{A_2} - \frac{\sqrt{qt}(1+qt-\sqrt{qt}\chi_2^{SU(2)})\chi_6^{SU(4)}[y]}{(1-q)^2(1-t)^2}A_1$$
$$+ \frac{(q+t)(qt\chi_3^{SU(2)}-\sqrt{qt}(1+q)(1+t)\chi_2^{SU(2)}+(q+t)(1+qt)+qt)}{(1-q)^2(1+q)(1-t)^2(1+t)}\frac{A_1^2}{A_2^2} + \mathcal{O}(A_1^2;A_2^2),$$

where $\chi_6^{SU(4)}[y] = \sum_{i=1}^3 y_i + y_i^{-1}$ and $\chi_{15}^{SU(4)}[y] = \sum_{i<j} 1 + y_i y_i + \frac{1}{y_i y_j} + \frac{y_i}{y_j} + \frac{y_j}{y_i}$.[5]

2. Instanton contributions

The one-instanton contribution can be expanded as

$$Z^{\text{one-instanton}}_{Sp(2)+1\mathbf{AS}+3\mathbf{F}} = \frac{-\sqrt{qt}}{(1-q)(1-t)}\chi_4^{SU(4)}[y](A_2+A_1) + \frac{q+t}{(1-q)(1-t)}\chi_{\bar{4}}^{SU(4)}[y](A_2^2+A_1^2)$$
$$+ \frac{q+t-\sqrt{qt}\chi_2^{SU(2)}}{(1-q)(1-t)}\chi_{\bar{4}}^{SU(4)}[y]A_2A_1 - \frac{(q+t)(q+t-\sqrt{qt}\chi_2^{SU(2)})}{(1-q)(1-t)\sqrt{qt}}\chi_4^{SU(4)}[y]$$
$$\times (A_2^2A_1 + A_1A_2^2) + \frac{(q+t)^2(q+t-\sqrt{qt}\chi_2^{SU(2)})}{(1-q)q(1-t)t}\chi_{\bar{4}}^{SU(4)}[y]A_2^2A_1^2 + \mathcal{O}(A_1^3,A_2^3), \tag{4.80}$$

where

$$\chi_4^{SU(4)}[y] = \sqrt{y_1y_2y_3} + \frac{\sqrt{y_1}}{\sqrt{y_2}\sqrt{y_3}} + \frac{\sqrt{y_2}}{\sqrt{y_1}\sqrt{y_3}} + \frac{\sqrt{y_3}}{\sqrt{y_1}\sqrt{y_2}},$$
$$\chi_{\bar{4}}^{SU(4)}[y] = \frac{1}{\sqrt{y_1y_2y_3}} + \frac{\sqrt{y_2}\sqrt{y_3}}{\sqrt{y_1}} + \frac{\sqrt{y_1}\sqrt{y_3}}{\sqrt{y_2}} + \frac{\sqrt{y_1}\sqrt{y_2}}{\sqrt{y_3}}.$$

We checked that Eq. (4.80) agrees with the localization result in Appendix B [Eq. (B5)] and by mapping parameters $y_1 = e^{m_1}$, $y_3 = e^{m_3}$, $y_2 = e^{-m_2}$, $Q_8 = e^m$, $A_1 = e^{\alpha_1}$, and $A_2 = e^{\alpha_2}$.

Similarly, we obtain the two-instanton contribution

$$Z^{\text{two-instanton}}_{Sp(2)+1\mathbf{AS}+3\mathbf{F}} = \frac{qt(1+qt)\chi_6^{SU(4)}[y]+(q+t)\chi_{10}^{SU(4)}[y])}{(1-q)^2(1+q)(1-t)^2(1+t)}(A_2^2+A_1^2) + \frac{qt(\chi_6^{SU(4)}[y]+\chi_{10}^{SU(4)}[y])}{(1-q)^2(1-t)^2}A_2A_1$$
$$+ \frac{\sqrt{qt}(2q+\sqrt{qt}+2t)\chi_{15}^{SU(4)}[y]-(q+t)(1+qt)-qt-(q^2+t^2)+qt\chi_{15}^{SU(4)}[y])(\chi_2^{SU(2)}+1)}{(1-q)^2(1-t)^2}$$
$$\times (A_2^2A_1 + A_2A_1^2) + \mathcal{O}(A_1^2;A_2^2),$$

where

$$\chi_{10}^{SU(4)}[y] = \sum_{i=1}^3 y_i + \frac{1}{y_i} + \frac{y_i}{y_jy_k}, \qquad \chi_{15}^{SU(4)}[y] = 3 + \sum_{i\neq j} y_iy_j + \frac{1}{y_iy_j} + \frac{y_i}{y_j}, \quad i = 1,2,3.$$

[5]This definition of character is a bit different here. One can use the LieART package in Ref. [58] to get characters in omega basis and then do a transformation $y_2 \to y_2$, $y_3 \to \sqrt{\frac{y_2y_3}{y_1}}$, $y_1 \to \sqrt{y_1y_2y_3}$ to get this definition. We remind that all characters in this paper are obtained by using LieART.

3. Enhancement of global symmetry

We shift Coulomb branch parameters to the gauge parameters

$$\tilde{A}_1 = A_1 u^{\frac{2}{8-N_f}} = A_1 u^{\frac{2}{5}}, \qquad \tilde{A}_2 = A_2 u^{\frac{2}{8-N_f}} = A_2 u^{\frac{2}{5}}. \tag{4.81}$$

The global symmetry of $Sp(2) + 1\mathbf{AS} + 3\mathbf{F}$ should be $G = SU(2)_{Q_8} \times E_4 = SU(2)_{Q_8} \times SU(5)_{\tilde{y}_i, i=1,\ldots,5}$. Here we define new fugacities $\tilde{y}_1, \ldots, \tilde{y}_5$ for E_4.[6] By observing the diagram in Fig. 27, we notice that the fiber-base duality leads to

$$Q_B \leftrightarrow Q_F, \qquad Q_8 \leftrightarrow Q_8, \qquad Q_{m_2} \leftrightarrow Q_{m_3}, \qquad Q_{m_1} \leftrightarrow Q_{m_1}, \tag{4.82}$$

or it takes the following relations in terms of gauge theory parameters:

$$\tilde{y}_1 \leftrightarrow \tilde{y}_2, \qquad \tilde{y}_3 \leftrightarrow \tilde{y}_4, \qquad \tilde{A}_1 \leftrightarrow \tilde{A}_1, \qquad \tilde{A}_2 \leftrightarrow \tilde{A}_2. \tag{4.83}$$

Combining Eqs. (4.82) and (4.83), we express the Kähler parameters in terms of the gauge theory parameters:

$$Q_F = \tilde{A}_2^2 \tilde{y}_1, \qquad Q_B = \tilde{A}_2^2 \tilde{y}_2, \qquad Q_{k4} = \frac{\tilde{A}_1}{\tilde{A}_2 A_8}, \qquad Q_{m_1} = \frac{\tilde{y}_3 \tilde{y}_4}{\tilde{A}_1}, \qquad Q_{m_2} = \frac{\tilde{y}_3 \tilde{y}_5}{\tilde{A}_1}, \qquad Q_{m_3} = \frac{\tilde{y}_4 \tilde{y}_5}{\tilde{A}_1}. \tag{4.84}$$

In addition to Eq. (4.77), we find the reparameterization of the gauge theory parameters as follows:

$$A_1 = \tilde{A}_1 \sqrt{\tilde{y}_1}, \qquad A_2 = \tilde{A}_2 \sqrt{\tilde{y}_2}, \qquad u = \tilde{y}_1^{-\frac{5}{4}}, \qquad y_1 = \sqrt{\frac{\tilde{y}_3 \tilde{y}_4}{\tilde{y}_2 \tilde{y}_5}}, \qquad y_2 = \sqrt{\frac{\tilde{y}_3 \tilde{y}_5}{\tilde{y}_2 \tilde{y}_4}}, \qquad y_3 = \sqrt{\frac{\tilde{y}_4 \tilde{y}_5}{\tilde{y}_2 \tilde{y}_3}}. \tag{4.85}$$

By expressing the normalized Nekrasov partition function in terms of the parameters $(\tilde{A}_i, \tilde{u}, \tilde{y}_i)$, we see the enhancement of global symmetry as follows:

$$\begin{aligned} Z_{Sp(2)+1\mathbf{AS}+3\mathbf{F}} = 1 &- \frac{\sqrt{qt}\chi_{10}^{E_4}[\tilde{u}]}{(1-q)(1-t)}\tilde{A}_2 + \frac{q+t-\sqrt{qt}\chi_2^{SU(2)}}{(1-q)(1-t)}\frac{\tilde{A}_1}{\tilde{A}_2} + \frac{(qt\chi_2^{SU(2)} - \sqrt{qt}(1+qt))\chi_{10}^{E_4}[\tilde{u}]}{(1-q)^2(1-t)^2}\tilde{A}_1 \\ &+ \frac{((1+q^2t^2)(q+t) - (q^3+t^3))\chi_5^{E_4}[\tilde{y}] + qt(1+qt)\chi_{45}^{E_4}[\tilde{y}] + qt(q+t)\chi_{50}^{E_4}[\tilde{y}]}{(1-q)^2(1+q)(1-t)^2(1+t)}\tilde{A}_2^2 \\ &+ \frac{(q+t)(qt\chi_3^{SU(2)} - \sqrt{qt}(1+q)(1+t)\chi_2^{SU(2)} + (q+t)(1+qt) + qt)}{(1-q)^2(1+q)(1-t)^2(1+t)}\frac{\tilde{A}_1^2}{\tilde{A}_2^2} \\ &+ \frac{\sqrt{qt}(-qt(q+t)\chi_3^{SU(2)} + \sqrt{qt}((1+qt)^2 + (q+t)(1-(q-t)^2))\chi_2^{SU(2)} + \cdots)\chi_{10}^{E_4}[\tilde{u}]}{(1-q)^3(1-t)^3(1+q)(1+t)}\frac{\tilde{A}_1^2}{\tilde{A}_2} \\ &+ \mathcal{O}(\tilde{A}_1^2; \tilde{A}_2^2), \end{aligned} \tag{4.86}$$

where characters are defined as[7]

$$\begin{aligned} &\chi_5^{E_4}[\tilde{y}] = \sum_i \tilde{y}_i, \qquad \chi_{10}^{E_4}[\tilde{y}] = \sum_{i\neq j}\frac{1}{\tilde{y}_i\tilde{y}_j}, \qquad \chi_{45}^{E_4}[\tilde{y}] = 3\sum_i \tilde{y}_i + \sum_{i\neq j\neq k}\frac{\tilde{y}_i\tilde{y}_j}{\tilde{y}_k}, \\ &\chi_{50}^{E_4}[\tilde{y}] = 2\sum_i \tilde{y}_i + \sum_{i\neq j\neq k}\frac{\tilde{y}_i\tilde{y}_j}{\tilde{y}_k} + \sum_{i\neq j}\frac{1}{\tilde{y}_i\tilde{y}_j}, \quad i,j,k = 1,\ldots,5. \end{aligned}$$

[6]For $E_4 = SU(4)$, $\tilde{y}_1\tilde{y}_2\tilde{y}_3\tilde{y}_4\tilde{y}_5 = 1$.
[7]Here, we choose orthogonal basis in LieART.

F. $Sp(2)+1\mathbf{AS}+4\mathbf{F}$

1. The un-Higgsed T_4 diagram

There are many equivalent webs for this theory as depicted in Fig. 28. We choose the first web for computation, as it contains a Higgsed T_4 diagram, which has not been discussed in the previous examples. We find T_2 tuning still works for this Higgsed T_4 diagram, which implies that T_2 tuning could be used for generic Higgsed T_N diagrams. The un-Higgsed diagram for the first web in Fig. 28 is shown in Fig. 29. Following the discussion in Sec. III B, we find the tuned Kähler parameters are as follows:

$$Q_1 = Q_2 = Q_3 = Q_4 = Q_{f_1} = Q_{f_2} = Q_{f_{33}} = Q_{f_4} = Q_{f_9} = Q_{f_{10}} = \sqrt{\frac{q}{t}},$$
$$Q_5 = Q_6 = Q_{f_5} = Q_{f_6} = \sqrt{\frac{t}{q}}, \qquad Q_{F_1} = Q_{F_2} = \cdots = Q_{F_{13}} = \sqrt{\frac{q}{t}}. \tag{4.87}$$

With the help of auxiliary lines, the relations between Kähler parameters and gauge theory parameters (A_i, u, y_i) can be determined as follows:

$$Q_F = {A_2}^2, \qquad Q_{k4} = \frac{A_1}{A_2 Q_8}, \qquad Q_B = \frac{u{A_2}^2}{\sqrt{y_1 y_2 y_3 y_4}}, \qquad Q_{m_i} = \frac{y_i}{A_1}, \tag{4.88}$$

where $y_i = e^{-im_i}$, $i = 1, 2, 3, 4$, are mass parameters. Just like $Sp(2)_0 + 1\mathbf{AS} + N_f\mathbf{F}(N_f = 1, 2, 3)$, geometric transition-related terms (3.20) given by tuning Kähler parameters provide constraints on various Young diagrams $\nu_i = \emptyset$, $i = 5, \ldots, 13$. Hence, the summation part of the partition function was reduced as

$$Z^{\text{sum}}_{Sp(2)+1\mathbf{AS}+4\mathbf{F}} = \sum_{\substack{\nu_1,\nu_2,\nu_3,\nu_4,\\ \alpha_1,\alpha_2,\alpha_3,\alpha_4}} Z^{\mathbf{sum}}_{\mathbf{Sp(2)}+1\mathbf{AS}} \cdot \mathbf{terms}[y_4]' \cdot \prod_{i=1}^{3} \mathbf{terms}[y_i],$$
$$\mathbf{terms}[y_4]' = \frac{y_4^{\frac{|\nu_1|+|\nu_2|+|\nu_3|+|\nu_4|}{2}} N^{\text{half},-}_{\nu_2}\left(\frac{y_4}{A_2}\right) N^{\text{half},-}_{\nu_4}\left(\frac{y_4}{A_1}\right) N^{\text{half},-}_{\nu_1^T}(A_2 y_4) N^{\text{half},-}_{\nu_3^T}(A_1 y_4)}{N^{\text{half}}_{\nu_2}\left(\frac{u}{A_2}\frac{t^2}{q^2}\sqrt{\frac{y_1y_2y_4}{y_3}}\right) N^{\text{half},-}_{\nu_4}\left(\frac{u}{A_1}\frac{t^2}{q^2}\sqrt{\frac{y_1y_2y_4}{y_3}}\right) N^{\text{half},-}_{\nu_1^T}\left(u\frac{A_2t^2}{q^2}\sqrt{\frac{y_1y_2y_4}{y_3}}\right) N^{\text{half},-}_{\nu_3^T}\left(u\frac{A_1t^2}{q^2}\sqrt{\frac{y_1y_2y_4}{y_3}}\right)}. \tag{4.89}$$

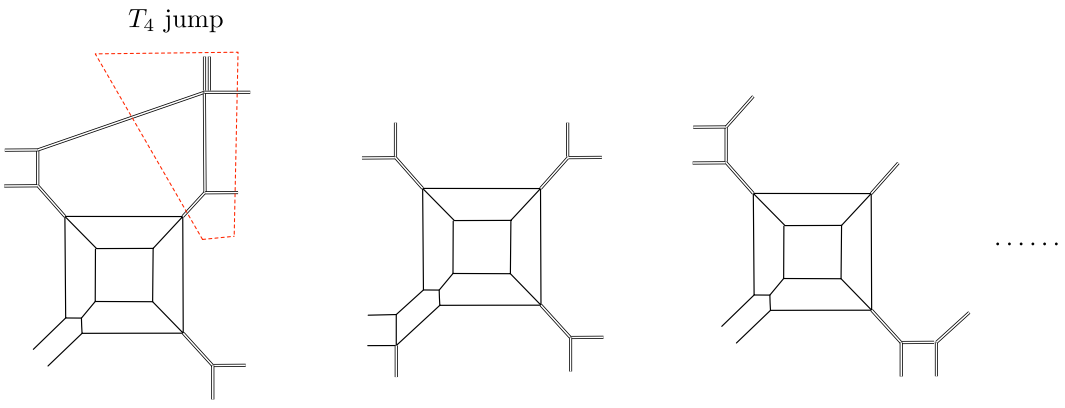

FIG. 28. Some equivalent webs related through Hanany-Witten moves for $Sp(2) + 1\mathbf{AS} + 4\mathbf{F}$.

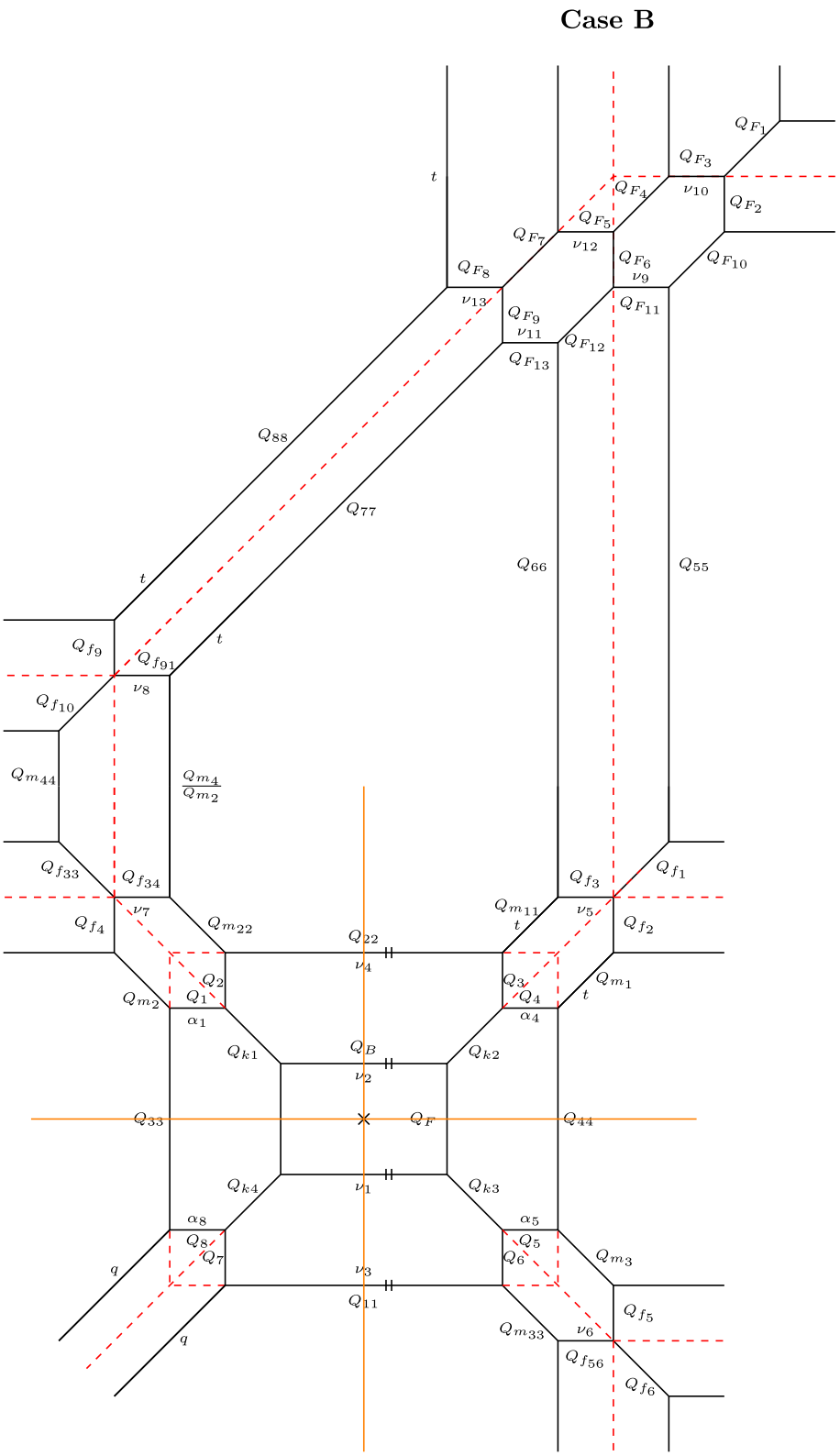

FIG. 29. An un-Higgsed diagram for $Sp(2) + 1\mathbf{AS} + 4\mathbf{F}$. The type of tuned parameters on the right top are found to be type case B. The red dashed lines in the diagram are auxiliary lines.

2. Perturbative contribution

We obtain the perturbative part

$$Z^{\text{pert}}_{Sp(2)+1\mathbf{AS}+4\mathbf{F}} = \frac{Z^{\text{pert-I}}_{Sp(2)+1\mathbf{AS}+4\mathbf{F}} \cdot Z^{\text{pert-II}}_{Sp(2)+1\mathbf{AS}+4\mathbf{F}}}{Z^{\text{extra}}_{Q_8} \cdot Z^{\text{pert extra}}_{=}} = Z^{\text{pert}}_{Sp(2)+1\mathbf{AS}} \prod_{i=1}^{N_f=4} Z^{\text{pert}}_{\mathbf{F}}(Q_{m_i}), \tag{4.90}$$

where $Z^{\text{extra}}_{=}$ is given by

$$\begin{aligned} Z^{\text{extra}}_{=} &= Z^{\text{pert extra}}_{Sp(2)+1\mathbf{AS}+4\mathbf{F}} \cdot Z^{\text{inst extra}}_{Sp(2)+1\mathbf{AS}+4\mathbf{F}} \\ &= \frac{1}{M(y_1y_3,t,q)M(\frac{q}{t}y_1y_3,t,q)M(\frac{y_4}{y_2},q,t)M(\frac{t}{q}\frac{y_4}{y_2},q,t)} \\ &\quad\times \frac{1}{M(u\sqrt{\frac{y_2y_4}{y_1y_3}},t,q)M(u\frac{q}{t}\sqrt{\frac{y_2y_4}{y_1y_3}},t,q)M(u\sqrt{y_1y_2y_3y_4},t,q)M(u\frac{q}{t}\sqrt{y_1y_2y_3y_4},t,q)}. \end{aligned}$$

The normalized perturbative part can be expanded as[8]

$$\begin{aligned} \frac{Z^{\text{pert}}_{Sp(2)+1\mathbf{AS}+4\mathbf{F}}}{M(Q_8\sqrt{\frac{t}{q}},t,q)^2} &= 1 - \frac{\sqrt{qt}\chi^{SO(8)}_{8_v}[y]}{(1-q)(1-t)}A_2 - \frac{\sqrt{qt}(1+qt-\sqrt{qt}\chi^{SU(2)}_2)\chi^{\text{SO}(8)}_{8_v}[y]}{(1-q)^2(1-t)^2}A_1 \\ &\quad + \left(\frac{qt\chi^{SO(8)}_{8_v}[y]^2}{2(1-q)^2(1-t)^2} + \frac{qt(2\chi^{\text{SO}(8)}_{28}[y]-\chi^{\text{SO}(8)}_{8_v}[y]^2)+\cdots}{2(1-q^2)(1-t^2)}\right)A_2^2 + \frac{(q+t)-\sqrt{qt}\chi^{SU(2)}_2}{(1-q)(1-t)}\frac{A_1}{A_2} \\ &\quad + \frac{(q+t)(qt\chi^{SU(2)}_3 - \sqrt{qt}(1+q)(1+t)\chi^{SU(2)}_2 + (q+t)(1+qt)+qt)}{(1-q)^2(1+q)(1-t)^2(1+t)}\frac{A_1^2}{A_2^2} \\ &\quad + \frac{\sqrt{qt}(-qt(q+t)\chi^{\text{SU}(2)}_3 + \sqrt{qt}((1+qt)^2+(q+t)(1-(q-t)^2))\chi^{SU(2)}_2+\cdots)\chi^{SO(8)}_{8_v}[y]}{(1-q)^3(1+q)(1-t)^3(1+t)} \\ &\quad \times\frac{A_1^2}{A_2} + \mathcal{O}(A_1^2;A_2^2), \end{aligned} \tag{4.91}$$

where $\chi^{SO(8)}_{8_v}[y] = \sum_i^4 y_i + y_i^{-1}$ and $\chi^{SO(8)}_{28}[y] = \sum_{i\neq j} y_iy_i + \frac{1}{y_iy_j} + \frac{y_i}{y_j}$, $i = 1,\ldots,4$.

3. Instanton contributions

For the un-Higgsed diagram in Fig. 29, Z^M contains instanton-dependent terms $Z^{\text{nonpert-I}} \neq 1$. We remove instanton extra factors and find that the terms in the first term of Eq. (4.8) are the following, which could contribute to the instanton part:

$$\begin{aligned} \frac{Z^{\text{nonpert-I}}_{Sp(2)+1\mathbf{AS}+4\mathbf{F}}}{Z^{\text{inst extra}}_{Sp(2)+1\mathbf{AS}+4\mathbf{F}}} &= \frac{M\left(u\sqrt{\frac{y_1y_2}{y_3y_4}},q,t\right)M\left(u\frac{t}{q}\sqrt{\frac{y_1y_2}{y_3y_4}},q,t\right)M\left(u\sqrt{\frac{y_1y_4}{y_2y_3}},q,t\right)M\left(u\frac{t}{q}\sqrt{\frac{y_1y_4}{y_2y_3}},q,t\right)}{M\left(\frac{u}{A_1}\frac{t^{5/2}}{q^{5/2}}\sqrt{\frac{y_1y_2y_4}{y_3}},t,q\right)M\left(uA_1\frac{t^{5/2}}{q^{5/2}}\sqrt{\frac{y_1y_2y_4}{y_3}},t,q\right)} \\ &\quad\times\frac{M\left(u\sqrt{\frac{y_2y_4}{y_1y_3}},q,t\right)M\left(u\frac{t}{q}\sqrt{\frac{y_2y_4}{y_1y_3}},q,t\right)M\left(u\sqrt{y_1y_2y_3y_4},t,q\right)M\left(u\sqrt{y_1y_2y_3y_4},q,t\right)}{M\left(uA_2\frac{t^{5/2}}{q^{5/2}}\sqrt{\frac{y_1y_2y_4}{y_3}},t,q\right)M\left(\frac{u}{A_2}\frac{t^{5/2}}{q^{5/2}}\sqrt{\frac{y_1y_2y_4}{y_3}},t,q\right)}. \end{aligned} \tag{4.92}$$

[8]In orthogonal basis of LieART.

In addition, after taking into account the contributions of Z^{sum} given in Eq. (4.89), we obtain the one-instanton contribution, which can be expressed as

$$\begin{aligned} Z^{\text{one-instanton}}_{Sp(2)+1\mathbf{AS}+4\mathbf{F}} &= \frac{-\sqrt{qt}}{(1-q)(1-t)}\chi^{SO(8)}_{8_c}[y](A_2+A_1)+\frac{q+t}{(1-q)(1-t)}\chi^{\text{SO}(8)}_{8_s}[y](A_2^2+A_1^2) \\ &+\frac{q+t-\sqrt{qt}\chi_2^{SU(2)}}{(1-q)(1-t)}\chi^{SO(8)}_{8_s}[y]A_2A_1-\frac{(q+t)(q+t-\sqrt{qt}\chi_2^{SU(2)})}{(1-q)(1-t)\sqrt{qt}}\chi^{\text{SO}(8)}_{8_c}[y] \\ &\times(A_2^2A_1+A_1A_2^2)+\frac{(q+t)^2(q+t-\sqrt{qt}\chi_2^{SU(2)})}{(1-q)q(1-t)t}\chi^{SO(8)}_{8_s}[y]A_2^2A_1^2+\mathcal{O}(A_1^3;A_2^3), \end{aligned} \tag{4.93}$$

where

$$\begin{aligned} \chi^{SO(8)}_{8_c}[y] &= \sum_{i\neq j\neq k\neq l}\frac{\sqrt{y_i}}{\sqrt{y_j}\sqrt{y_k}\sqrt{y_l}}+\frac{\sqrt{y_j}\sqrt{y_k}\sqrt{y_l}}{\sqrt{y_i}}, \quad i,j,k,l=1,\ldots,4, \\ \chi^{SO(8)}_{8_s}[y] &= \sum_{i\neq j\neq k\neq l}\sqrt{y_iy_jy_ky_l}+\frac{1}{\sqrt{y_iy_jy_ky_l}}+\sqrt{\frac{y_iy_j}{y_ky_l}}, \quad i,j,k,l=1,\ldots,4. \end{aligned} \tag{4.94}$$

In order to compare with localization result (B5) with $N_f=4$, we define $Q_8=e^m$, $A_1=e^{\alpha_1}$, $A_2=e^{\alpha_2}$, and $y_i=e^{m_i}$ $(i=1,\ldots,4)$ to make characters manifest.

4. Cross AS subweb

One can perform Hanany-Witten moves to make one D7-brane downward to infinity, which could cross the **AS** subwebs as depicted in Fig. 30. For this diagram, T_2 tuning is still correct and leads to the correct partition function. One can count the number of different types of Higgsed T_2 subwebs and would find that there are three case B, one case C, and three case D on this diagram. Apart from the same tuned Kähler parameters (4.76) for $Sp(2)+1\mathbf{AS}+3\mathbf{F}$, there are two additional tuned Kähler parameters associated with the case B type of Higgsed T_2 subweb on the left bottom of this diagram, as shown in Fig. 31:

$$Q_{g_1}=Q_{g_2}=\sqrt{\frac{t}{q}}. \tag{4.95}$$

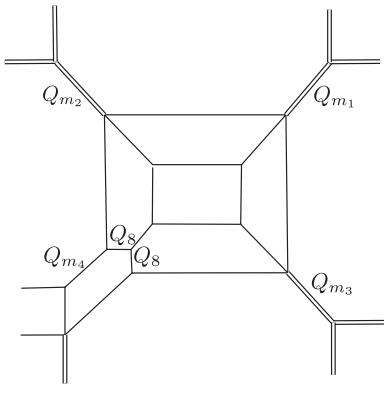

FIG. 30. Hanany-Witten moving of flavors could create overlapped lines on the subweb that represents antisymmetric matter **AS**.

G. $Sp(3)_0+1\mathbf{AS}$

For higher rank cases, as there are more Young diagrams to be summed over, the computation is more involved. Since the computation is straightforward, we skip the computations. Instead, as a representative example for higher rank cases, we discuss $Sp(3)_0+1\mathbf{AS}$ and the structure of the partition function.

Before discussing massive **AS** cases of the partition function for $Sp(3)_0+1\mathbf{AS}$, let us first discuss the massless limit of **AS** with $Q_8=\sqrt{\frac{t}{q}}$. Then the partition function factorizes:

$$\begin{aligned} Z_{Sp(3)+1\mathbf{AS}} &= Z_{\text{first layer}}\cdot Z_{\text{second layer}}\cdot Z_{\text{third layer}} \\ &= Z_{SU(2)}(Q_F,Q_B)\cdot Z_{SU(2)} \\ &\times\left(Q_FQ_{k4}{}^2\frac{t}{q},Q_BQ_{k_4}{}^2\frac{t}{q}\right) \\ &\cdot Z_{SU(2)}(Q_FQ_{h_4}{}^2Q_{k_4}{}^2,Q_BQ_{h_4}{}^2Q_{k_4}{}^2), \end{aligned} \tag{4.96}$$

where we choose Q_F, Q_B, Q_{k4}, and Q_{h_4} as independent parameters. At the massless limit, the diagram turns out to be isolated webs as depicted in Fig. 32. Turning on the mass parameter for **AS** leads to the left web in Fig. 33. The associated tuned Kähler parameters to its un-Higgsed diagram are given by

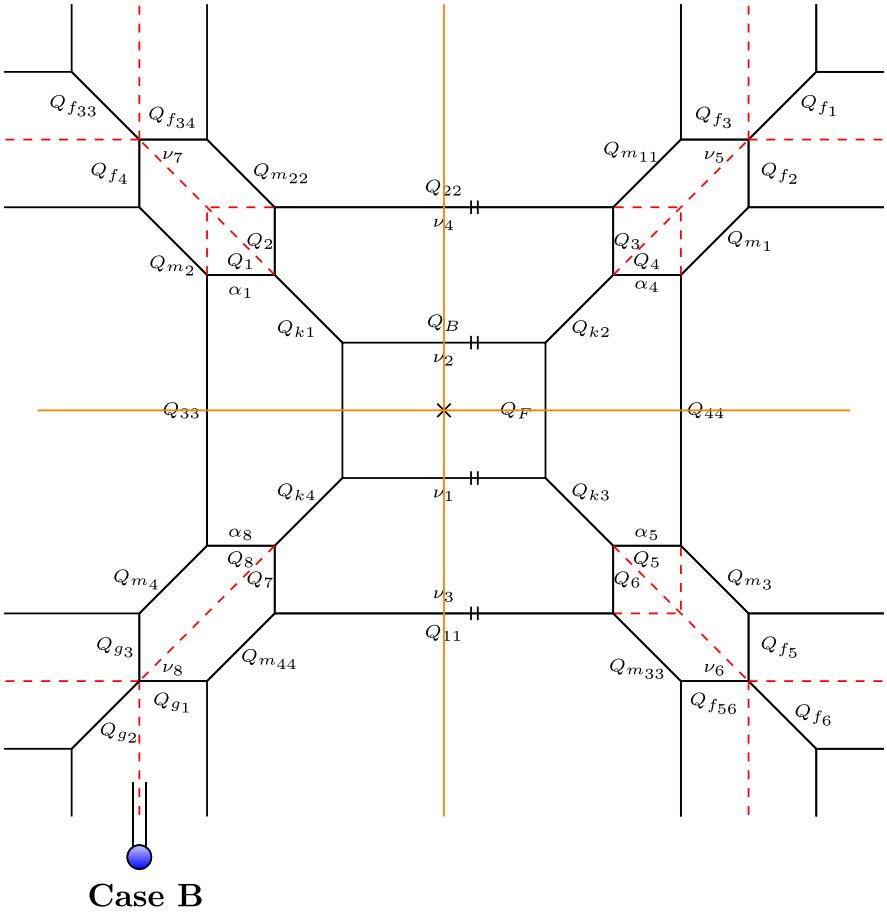

FIG. 31. The un-Higgsed diagram of the web depicted in Fig. 30. The Higgsed T_2 subdiagram on the left bottom is of type case B.

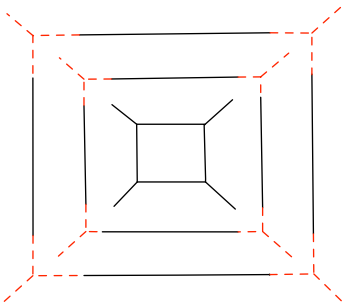

FIG. 32. When **AS** is massless, the web of $Sp(3)+1\mathbf{AS}$ factorizes and, thus, $Sp(3)+1\mathbf{AS}$ equals $SU(2)\times SU(2)\times SU(2)$.

$$Q_1 = Q_2 = Q_3 = Q_4 = Q_{f_{11}} = Q_{f_{12}} = Q_{f_{13}} = Q_{f_{14}} = Q_{f_{21}} = Q_{f_{22}} = Q_{f_{23}} = Q_{f_{24}} = \sqrt{\frac{q}{t}},$$
$$Q_5 = Q_6 = Q_{f_{31}} = Q_{f_{32}} = Q_{f_{33}} = Q_{f_{34}} = Q_{f_{43}} = Q_{f_{44}} = \sqrt{\frac{t}{q}}. \tag{4.97}$$

Gauge theory parameters (A_i, u) should be assigned to the following independent Kähler parameters:

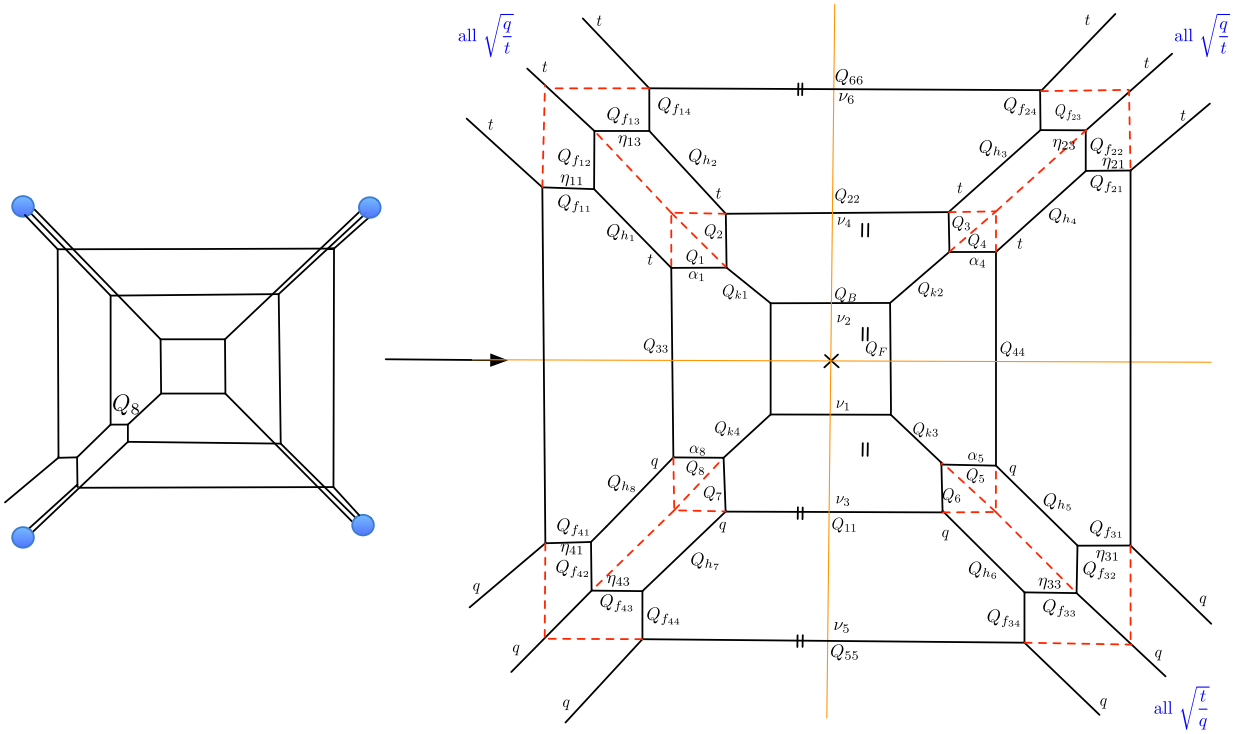

FIG. 33. The left web is for the massive **AS** with mass fugacity Q_8. The right diagram is its un-Higgsed diagram. In the right diagram, we have assigned the virtual lines and the values for some tuned parameters. All tuned parameters above the horizontal orange line are given the value $\sqrt{q/t}$, and all tuned parameters below this line are given $\sqrt{t/q}$.

$$Q_F = {A_2}^2, \qquad Q_{k4} = \frac{A_1}{A_2 Q_8}, \qquad Q_{h_4} = \frac{A_3}{A_1}\sqrt{\frac{t}{q}}, \qquad Q_B = {A_2}^2 u. \tag{4.98}$$

1. Perturbative contribution

We find

$$Z^{\text{pert-I}}_{Sp(3)+1\mathbf{AS}} = \frac{M\left(\frac{A_1}{A_2 Q_8}\sqrt{\frac{t}{q}}, t, q\right) M\left(\frac{A_1 A_2}{Q_8}\sqrt{\frac{t}{q}}, t, q\right) M\left(\frac{A_3}{A_1 Q_8}\sqrt{\frac{t}{q}}, t, q\right) M\left(\frac{A_1 A_3}{{Q_8}^2}, q, t\right)}{M\left({A_1}^2, t, q\right) M\left(\frac{A_1}{A_2}, t, q\right) M\left(A_1 A_2, t, q\right) M\left({A_2}^2, t, q\right) M\left(A_1 A_3, t, q\right) M\left({A_3}^2, t, q\right)}$$
$$\times \frac{M\left({Q_8}^2, t, q\right) M\left(Q_8\sqrt{\frac{t}{q}}, t, q\right)}{M\left(\frac{Q_8 A_3}{A_1}\sqrt{\frac{q}{t}}, t, q\right) M\left({A_2}^2, q, t\right) M\left(\frac{{A_1}^2}{Q_8}\sqrt{\frac{t}{q}}, q, t\right) M\left(\frac{{A_3}^2}{{Q_8}^2}\frac{t}{q}, q, t\right)}, \tag{4.99}$$

$$Z^{\text{pert-II}}_{Sp(3)+1\mathbf{AS}} = \frac{\text{numerator}}{\text{denormator}},$$
$$\text{numerator} = M\left(\frac{Q_8 A_3}{A_1}\sqrt{\frac{q}{t}}, t, q\right) M\left(\frac{A_1^2}{Q_8}\sqrt{\frac{t}{q}}, q, t\right) M\left(\frac{A_1 A_3}{Q_8}\sqrt{\frac{t}{q}}, t, q\right) M\left(\frac{A_3}{A_2 Q_8}\sqrt{\frac{t}{q}}, t, q\right)$$
$$\times M\left(\frac{A_2 A_3}{Q_8}\sqrt{\frac{t}{q}}, t, q\right) M\left(Q_8\sqrt{\frac{t}{q}}, t, q\right)^2 M\left(\frac{Q_8 A_1}{A_2}\sqrt{\frac{t}{q}}, t, q\right) M\left(Q_8 A_1 A_2\sqrt{\frac{t}{q}}, t, q\right)$$
$$\times M\left(\frac{Q_8 A_3}{A_1}\sqrt{\frac{t}{q}}, t, q\right) M\left(Q_8 A_1 A_3\sqrt{\frac{t}{q}}, t, q\right) M\left(\frac{Q_8 A_3}{A_2}\sqrt{\frac{t}{q}}, t, q\right) M\left(Q_8 A_2 A_3\sqrt{\frac{t}{q}}, t, q\right) \times M\left(\frac{{A_3}^2}{{Q_8}^2}\frac{t}{q}, q, t\right),$$

$$\begin{aligned}\text{denormator} = {} & M(A_1{}^2,q,t)M\left(\frac{A_1}{A_2},q,t\right)M((A_1A_2,q,t))M\left(\frac{A_3}{A_1},q,q\right)M\left(\frac{A_3}{A_2},t,q\right)\\ & \times M(A_2A_3,t,q)M(Q_8{}^2,t,q)M\left(Q_8{}^3\sqrt{\frac{q}{t}},t,q\right)M\left(\frac{A_3}{A_1}\frac{t}{q},t,q\right)M\left(A_1A_3\frac{t}{q},t,q\right)\\ & \times M\left(\frac{A_3}{A_2}\frac{t}{q},t,q\right)M\left(A_2A_3\frac{t}{q},t,q\right)M\left(A_3{}^2\frac{t}{q},t,q\right)M\left(\frac{A_1A_3}{Q_8{}^2}\frac{t}{q},t,q\right).\end{aligned} \tag{4.100}$$

Then the full perturbative partition function is given by

$$Z^{\text{pert}}_{Sp(3)+1\mathbf{AS}} = \frac{Z^{\text{pert-I}}_{Sp(3)+1\mathbf{AS}}\cdot Z^{\text{pert-II}}_{Sp(3)+1\mathbf{AS}}}{Z^{\text{extra}}_{Q_8}}, \tag{4.101}$$

where the extra factor in the denominator is

$$Z^{\text{extra}}_{Q_8} = \frac{1}{M(Q_8{}^3\sqrt{\frac{q}{t}},t,q)}. \tag{4.102}$$

In order to match with localization computation in Eq. (B1) when $N=3$, one needs to permute $A_1\to A_2$, $A_2\to A_3$, and $A_3\to A_1$.

2. Instanton contribution

We obtain the one-instanton contribution expanded as

$$\begin{aligned}Z^{\text{one-instanton}}_{Sp(3)+1\mathbf{AS}} = {} & \frac{q+t}{(1-q)(1-t)}(A_1^2+A_2^2+A_3^2)+\frac{q+t-\sqrt{qt}\chi_2^{SU(2)}}{(1-q)(1-t)}(A_2A_3+A_1A_3+A_1A_2)\\ & +\frac{(q+t)^2(q+t-\chi_2^{SU(2)})}{(1-q)(1-t)\sqrt{qt}}(A_1^2A_3^2+A_1^2A_3^2+A_2^2A_3^2)\\ & +\frac{(q+t)(q^2+3qt+t^2-2\sqrt{qt}(q+t)\chi_2^{SU(2)}+qt\chi_3^{SU(2)})}{(1-q)(1-t)qt}(A_1A_2A_3^2+A_1A_2^2A_3+A_1^2A_2A_3)\\ & +\frac{(q+t)^3(q^2+3qt+t^2-2\sqrt{qt}(q+t)\chi_2^{SU(2)}+qt\chi_3^{SU(2)})}{(1-q)(1-t)q^2t^2}A_1^2A_2^2A_3^2+\mathcal{O}(A_1^2;A_2^2;A_3^2),\end{aligned} \tag{4.103}$$

which is equal to the localization result (B5).

V. CONCLUSION

In this paper, we computed the Nekrasov partition function for 5D $\mathcal{N}=1$ $Sp(2)$ gauge theories with an antisymmetric hypermultiplet and $N_f\le 4$ flavors using the refined topological vertex method based on a 5-brane web diagram with the nonzero mass of the antisymmetric matter. The corresponding 5-brane web diagram has jumps on the (p,q) plane (or its dual diagram is generically nontoric) and can be regarded as a Higgsed 5-brane web diagram. To implement the topological vertex method on these 5-brane webs, we considered its un-Higgsed 5-brane web and properly tuned the Kähler parameters associated with the Higgsed edges. As such Higgsing can be considered locally as Higgsing on a 5-brane web diagram for T_2 theory, we developed systematic tunings of Kähler parameters for a T_2 diagram, so that such T_2 tuning can be applicable to various Higgsed 5-brane web diagrams. It is also straightforward to extend the T_2 turning to T_N tuning. As an example of T_3 tuning, we considered 5D $\mathcal{N}=1$ $Sp(3)$ gauge theory with an antisymmetric hypermultiplet. We checked that our results agree with known results based on the ADHM method, up to two instanton contributions.

By redefining the parameters of the theory to make the fiber-base duality manifest [47], the partition functions expressed in terms of new parameters explicitly show enhanced global symmetry $E_{N_f+1}\times SU(2)_{\text{antisym}}$, yielding the Gopakumar-Vafa invariants of 5D $Sp(2)$ gauge theories with an antisymmetric hypermultiplet and $N_f\le 4$ flavors.

Though we did not present the result with a higher number of flavors due to prolonged computation time with higher flavors, it is straightforward to compute the partition function for $Sp(2)$ theory with $N_f = 5, 6, 7, 8$ and for higher rank $Sp(N)$ gauge theory.

Along with new findings of a 5-brane web for 5D superconformal theories with various matter fields, it would be interesting to compute the partition functions using the topological vertex method on the corresponding 5-brane webs of various matters and see enhanced global symmetries. Another interesting direction to pursue is to check various dualities of 5D rank 2 superconformal theories [28] based on 5-brane webs [55] by computing the partition functions based on each 5-brane web.

Here, we discussed the T_2 tuning of the Kähler parameters for jumps. It would also be interesting to study other physical systems such as defects by tuning Kähler parameters to other values and find the corresponding tuning method.

ACKNOWLEDGMENTS

We thank Jin Chen, Hirotaka Hayashi, Hee-Cheol Kim, Kimyeong Lee, and Wenbin Yan for useful discussions. We also thank Futoshi Yagi for carefully reading the draft as well as valuable discussions. S. C. is grateful to ICTS for Asian string winter school, Institute of High Energy Physics (IHEP) for localization summer school, and Babak Haghighat for long-term visiting YMSC. S. C. is supported by the TEAM program of the Foundation for Polish Science cofinanced by the European Union under the European Regional Development Fund (POIR.04.04.00-00-5C55/17-00). S.-S. K. gratefully acknowledges Korea Institute for Advanced Study (KIAS) and Yau Mathematical Sciences Center (YMSC) at Tsinghua University for kind hospitality for his visit and also acknowledges Asia Pacific Center for Theoretical Physics (APCTP) for hosting the Focus program "Strings, Branes and Gauge Theories." S.-S. K. is supported by the UESTC Research Grant No. A03017023801317.

APPENDIX A: USEFUL IDENTITIES

The Cauchy identities take the following forms:

$$\sum_{\eta} s_{\eta/\lambda}(\mathbf{x}) s_{\eta/\mu}(\mathbf{y}) = \prod_{i,j=1}^{\infty} (1 - x_i y_j)^{-1} \sum_{\eta} s_{\mu/\eta}(\mathbf{x}) s_{\lambda/\eta}(\mathbf{y}), \tag{A1}$$

$$\sum_{\eta} s_{\eta^T/\lambda}(\mathbf{x}) s_{\eta/\mu}(\mathbf{y}) = \prod_{i,j=1}^{\infty} (1 + x_i y_j) \sum_{\eta} s_{\mu^T/\eta^T}(\mathbf{x}) s_{\lambda^T/\eta}(\mathbf{y}), \tag{A2}$$

where the skew Schur functions satisfy

$$s_{\emptyset/\mu}(\mathbf{x}) = \delta_{\emptyset\mu} = \delta_{\emptyset\mu^T}, \qquad |\mu| = |\mu^T|, \tag{A3}$$

$$s_{\nu/\emptyset}(\mathbf{x}) = s_{\nu}(x), \qquad s_{\mu/\nu}(\lambda \mathbf{x}) = \lambda^{|\mu|-|\nu|} s_{\mu/\nu}(\mathbf{x}), \tag{A4}$$

$$\sum_{\nu} (-1)^{|\nu|} s_{\mu/\nu}(\mathbf{x}) s_{\nu^T/\lambda^T}(\mathbf{x}) = (-1)^{|\mu|} \delta_{\mu\lambda}. \tag{A5}$$

Using this, one can perform the Young diagram sums along nonpreferred directions.

The following functions are the functions defined with topological vertex (see also Refs. [56,59]):

$$\begin{aligned}
\tilde{Z}_{\nu}(t,q) &:= \prod_{(i,j)\in\nu} (1 - q^{\nu_i - j} t^{\nu_j^T - i + 1})^{-1}, \\
||\tilde{Z}_{\mu}(t,q)||^2 &:= \tilde{Z}_{\mu^T}(t,q) \tilde{Z}_{\mu}(q,t), \\
N_{\mu\nu}(Q;t,q) &:= \prod_{i,j=1}^{\infty} \frac{1 - Q q^{\nu_i - j} t^{\mu_j^T - i + 1}}{1 - Q q^{-j} t^{-i+1}} \\
&= \prod_{(i,j)\in\nu} (1 - Q q^{\nu_i - j} t^{\mu_j^T - i + 1}) \prod_{(i,j)\in\mu} (1 - Q q^{-\mu_i + j - 1} t^{-\nu_j^T + i}), \\
N_{\nu}^{\mathrm{half},+}(Q;t,q) &:= N_{\emptyset\nu}\left(Q\sqrt{\frac{q}{t}}, t, q\right), \\
N_{\nu}^{\mathrm{half},-}(Q;t,q) &:= N_{\nu\emptyset}\left(Q\sqrt{\frac{q}{t}}, t, q\right), \\
M(Q,t,q) &:= \prod_{i,j=1}^{\infty} (1 - Q q^i t^{j-1}) = \exp\left(-\sum_{n=1}^{\infty} \frac{Q^n \left(\frac{q}{t}\right)^{\frac{n}{2}}}{n(q^{\frac{n}{2}} - q^{-\frac{n}{2}})(t^{\frac{n}{2}} - t^{-\frac{n}{2}})}\right).
\end{aligned} \tag{A6}$$

We note that, for some functions, we used slightly different convention from the notations in Ref. [56]:

$$N_{\mu\nu}(Q;t^{-1},q^{-1}) = \mathcal{N}_{\mu\nu}(Q,t,q),$$
$$M(Q;t,q) = \frac{1}{\mathcal{M}(Q,t,q)}, \tag{A7}$$

where the functions on the right-hand side are those defined in Ref. [56]. Other useful identities are as follows:

$$||\tilde{Z}_\mu(t,q)||^2 = ||\tilde{Z}_{\mu^T}(q,t)||^2, \tag{A8}$$

$$N_\nu^{\text{half},+}(Q;t^{-1},q^{-1}) = N_{\nu^T}^{\text{half},-}(Q;q^{-1},t^{-1}), \tag{A9}$$

$$N_\nu^{\text{half},+}(Q;t^{-1},q^{-1}) = N_{\emptyset\nu}\left(Q\sqrt{\frac{t}{q}},t^{-1},q^{-1}\right), \tag{A10}$$

$$N_\nu^{\text{half},-}(Q;t^{-1},q^{-1}) = N_{\nu\emptyset}\left(Q\sqrt{\frac{t}{q}},t^{-1},q^{-1}\right), \tag{A11}$$

$$N_{\nu\nu}(1;t^{-1},q^{-1}) = \frac{(-1)^{|\nu|}q^{-\frac{||\nu||^2}{2}}t^{-\frac{||\nu^T||^2}{2}}(\frac{q}{t})^{\frac{|\nu|}{2}}}{\tilde{Z}_{\nu^T}(q,t)\tilde{Z}_\nu(t,q)}, \tag{A12}$$

$$N_{\nu\nu}\left(\frac{t}{q};t^{-1},q^{-1}\right) = \frac{(-1)^{|\nu|}q^{-\frac{||\nu^T||^2}{2}}t^{-\frac{||\nu||^2}{2}}(\frac{t}{q})^{\frac{|\nu|}{2}}}{\tilde{Z}_{\nu^T}(q,t)\tilde{Z}_\nu(t,q)}. \tag{A13}$$

The following relations are useful, when one expands terms in the partition functions with respect to Q:

$$M\left(Q\sqrt{\frac{t}{q}},t,q\right) = M\left(Q\sqrt{\frac{q}{t}},q,t\right), \tag{A14}$$

$$M(Q^{-1},t,q) = M\left(Q\frac{t}{q},t,q\right) = M(Q,q,t), \tag{A15}$$

$$N_{\mu\nu}\left(\sqrt{\frac{t}{q}}Q^{-1};t^{-1},q^{-1}\right) = (-Q)^{-|\mu|-|\nu|}t^{\frac{-||\mu^T||^2+||\nu||^2}{2}}q^{\frac{||\mu||^2-||\nu||^2}{2}}N_{\nu\mu}\left(\sqrt{\frac{t}{q}}Q;t^{-1},q^{-1}\right). \tag{A16}$$

APPENDIX B: RESULT FROM LOCALIZATION

In Refs. [49,50], the partition function for $Sp(N)+1\mathbf{AS}+N_f\mathbf{F}$ was computed via localization based on the ADHM method, which takes the following form:

$$Z^{\text{perturbative}}_{Sp(N)+1\mathbf{AS}+N_f\mathbf{F}} = Z^{\text{pert}}_{\text{vector}}\cdot Z^{\text{pert}}_{\mathbf{AS}}(y)\cdot\prod_{i=1}^{N_f}Z^{\text{pert}}_{\mathbf{F}}(y_i). \tag{B1}$$

For $Sp(2)+1\mathbf{AS}+N_f\mathbf{F}$,

$$\begin{aligned}
Z^{\text{pert}}_{\mathbf{F}}(y_i) &= M\left(\frac{A_1}{y_i}\sqrt{\frac{t}{q}},t,q\right)M\left(A_1y_i\sqrt{\frac{t}{q}},t,q\right)M\left(\frac{A_2}{y_i}\sqrt{\frac{t}{q}},t,q\right)M\left(A_2y_i\sqrt{\frac{t}{q}},t,q\right),\\
Z^{\text{pert}}_{\mathbf{AS}}(y) &= M\left(yA_1A_2\sqrt{\frac{t}{q}},t,q\right)M\left(\frac{A_1A_2}{y}\sqrt{\frac{t}{q}},t,q\right)M\left(y\frac{A_1}{A_2}\sqrt{\frac{t}{q}},t,q\right)M\left(\frac{A_1}{yA_2}\sqrt{\frac{t}{q}},t,q\right)\\
&\quad\times M\left(y\sqrt{\frac{t}{q}},t,q\right)^2,
\end{aligned} \tag{B2}$$

$$\begin{aligned}
Z^{\text{pert}}_{\text{vector}} &= \frac{1}{M(A_1A_2,t,q)M(A_1A_2,q,t)M(\frac{A_1}{A_2},t,q)M(\frac{A_1}{A_2},q,t)}\\
&\quad\times\frac{1}{M({A_1}^2,t,q)M({A_1}^2,q,t)M({A_2}^2,t,q)M({A_2}^2,q,t)}.
\end{aligned} \tag{B3}$$

For $Sp(3)+1\mathbf{AS}+N_f\mathbf{F}$,

$$
\begin{aligned}
Z^{\text{pert}}_{\mathbf{F}}(y_i) &= \prod_{\alpha=1}^{3} M\left(\frac{A_\alpha}{y_i}\sqrt{\frac{t}{q}},t,q\right)M\left(A_\alpha y_i\sqrt{\frac{t}{q}},t,q\right),\\
Z^{\text{pert}}_{\mathbf{AS}}(y) &= M\left(y\sqrt{\frac{t}{q}},t,q\right)^3\prod_{1\le\alpha<\beta\le 3} M\left(yA_\alpha A_\beta\sqrt{\frac{t}{q}},t,q\right)M\left(\frac{A_\alpha A_\beta}{y}\sqrt{\frac{t}{q}},t,q\right)\\
&\quad\times M\left(\frac{yA_\alpha}{A_\beta}\sqrt{\frac{t}{q}},t,q\right)M\left(\frac{A_\alpha}{yA_\beta}\sqrt{\frac{t}{q}},t,q\right),\\
Z^{\text{pert}}_{\text{vector}} &= \frac{1}{\prod_{1\le\alpha<\beta\le 3}M(A_\alpha A_\beta,t,q)M(A_\alpha A_\beta,q,t)M(\frac{A_\alpha}{A_\beta},t,q)M(\frac{A_\alpha}{A_\beta},q,t)}\\
&\quad\times\frac{1}{\prod_{\alpha=1}^{3}M(A_\alpha^2,t,q)M(A_\alpha^2,q,t)}.
\end{aligned}
\tag{B4}
$$

The one-instanton contribution does not involve an integral and is given by

$$
\begin{aligned}
Z^{\text{one-instanton}}_{Sp(N)+1\mathbf{AS}+N_f\mathbf{F}} &= \frac{1}{2}\left(\frac{\prod_{i=1}^{N_f}2\sinh\frac{m_i}{2}}{2\sinh\frac{\epsilon_+\pm\epsilon_-}{2}}\cdot\frac{\prod_{i=1}^{N}2\sinh\frac{m\pm\alpha_i}{2}-\prod_{i=1}^{N}2\sinh\frac{\pm\alpha_i+\epsilon_+}{2}}{2\sinh\frac{m\pm\epsilon_+}{2}\prod_{i=1}^{N}2\sinh\frac{\pm\alpha_i+\epsilon_+}{2}}\right.\\
&\quad\left.+\frac{\prod_{i=1}^{N_f}2\cosh\frac{m_i}{2}}{2\sinh\frac{\epsilon_+\pm\epsilon_-}{2}}\cdot\frac{\prod_{i=1}^{N}2\cosh\frac{m\pm\alpha_i}{2}-\prod_{i=1}^{N}2\cosh\frac{\pm\alpha_i+\epsilon_+}{2}}{2\sinh\frac{m\pm\epsilon_+}{2}\prod_{i=1}^{N}2\cosh\frac{\pm\alpha_i+\epsilon_+}{2}}\right),
\end{aligned}
\tag{B5}
$$

where m_i are masses for fundamental flavors and m is the mass for an antisymmetric hypermultiplet.

[1] N. Seiberg, Five-dimensional SUSY field theories, non-trivial fixed points and string dynamics, Phys. Lett. B **388**, 753 (1996).

[2] O. Aharony and A. Hanany, Branes, superpotentials and superconformal fixed points, Nucl. Phys. **B504**, 239 (1997).

[3] O. Aharony, A. Hanany, and B. Kol, Webs of (p,q) five-branes, five-dimensional field theories and grid diagrams, J. High Energy Phys. 01 (1998) 002.

[4] D. R. Morrison and N. Seiberg, Extremal transitions and five-dimensional supersymmetric field theories, Nucl. Phys. **B483**, 229 (1997).

[5] M. R. Douglas, S. H. Katz, and C. Vafa, Small instantons, Del Pezzo surfaces and type I-prime theory, Nucl. Phys. **B497**, 155 (1997).

[6] O. J. Ganor, D. R. Morrison, and N. Seiberg, Branes, Calabi-Yau spaces, and toroidal compactification of the $N = 1$ six-dimensional E(8) theory, Nucl. Phys. **B487**, 93 (1997).

[7] K. A. Intriligator, D. R. Morrison, and N. Seiberg, Five-dimensional supersymmetric gauge theories and degenerations of Calabi-Yau spaces, Nucl. Phys. **B497**, 56 (1997).

[8] N. C. Leung and C. Vafa, Branes and toric geometry, Adv. Theor. Math. Phys. **2**, 91 (1998).

[9] A. Iqbal, All genus topological string amplitudes and five-brane webs as Feynman diagrams, arXiv:hep-th/0207114.

[10] A. Iqbal and A.-K. Kashani-Poor, Instanton counting and Chern-Simons theory, Adv. Theor. Math. Phys. **7**, 457 (2003).

[11] A. Iqbal and A.-K. Kashani-Poor, SU(N) geometries and topological string amplitudes, Adv. Theor. Math. Phys. **10**, 1 (2006).

[12] T. Eguchi and H. Kanno, Topological strings and Nekrasov's formulas, J. High Energy Phys. 12 (2003) 006.

[13] T. J. Hollowood, A. Iqbal, and C. Vafa, Matrix models, geometric engineering and elliptic genera, J. High Energy Phys. 03 (2008) 069.

[14] M. Taki, Refined topological vertex and instanton counting, J. High Energy Phys. 03 (2008) 048.

[15] M. Aganagic, A. Klemm, M. Marino, and C. Vafa, The topological vertex, Commun. Math. Phys. **254**, 425 (2005).

[16] H. Awata and H. Kanno, Instanton counting, Macdonald functions and the moduli space of D-branes, J. High Energy Phys. 05 (2005) 039.

[17] A. Iqbal, C. Kozcaz, and C. Vafa, The refined topological vertex, J. High Energy Phys. 10 (2009) 069.

[18] H. Awata and H. Kanno, Refined BPS state counting from Nekrasov's formula and Macdonald functions, Int. J. Mod. Phys. A **24**, 2253 (2009).

[19] A. Iqbal and C. Kozçaz, Refined topological strings on local P2, J. High Energy Phys. 03 (2017) 069.

[20] H. Hayashi, H.-C. Kim, and T. Nishinaka, Topological strings and 5d T_N partition functions, J. High Energy Phys. 06 (2014) 014.
[21] O. Bergman, D. Rodríguez-Gómez, and G. Zafrir, 5-Brane Webs, Symmetry enhancement, and duality in 5d supersymmetric gauge theory, J. High Energy Phys. 03 (2014) 112.
[22] O. Bergman and G. Zafrir, Lifting 4d dualities to 5d, J. High Energy Phys. 04 (2015) 141.
[23] H. Hayashi, S.-S. Kim, K. Lee, M. Taki, and F. Yagi, A new 5d description of 6d D-type minimal conformal matter, J. High Energy Phys. 08 (2015) 097.
[24] O. Bergman and G. Zafrir, 5d fixed points from brane webs and O7-planes, J. High Energy Phys. 12 (2015) 163.
[25] G. Zafrir, Brane webs, 5d gauge theories and 6d $\mathcal{N} = (1, 0)$ SCFT's, J. High Energy Phys. 12 (2015) 157.
[26] H. Hayashi, S.-S. Kim, K. Lee, and F. Yagi, 6d SCFTs, 5d dualities and Tao web diagrams, J. High Energy Phys. 05 (2019) 203.
[27] P. Jefferson, H.-C. Kim, C. Vafa, and G. Zafrir, Towards classification of 5d SCFTs: Single gauge node, arXiv: 1705.05836.
[28] P. Jefferson, S. Katz, H.-C. Kim, and C. Vafa, On geometric classification of 5d SCFTs, J. High Energy Phys. 04 (2018) 103.
[29] F. Benini, S. Benvenuti, and Y. Tachikawa, Webs of five-branes and $N = 2$ superconformal field theories, J. High Energy Phys. 09 (2009) 052.
[30] S.-S. Kim, M. Taki, and F. Yagi, Tao probing the end of the world, Prog. Theor. Exp. Phys. (**2015**), 083B02.
[31] H. Hayashi, S.-S. Kim, K. Lee, M. Taki, and F. Yagi, More on 5d descriptions of 6d SCFTs, J. High Energy Phys. 10 (2016) 126.
[32] G. Zafrir, Brane webs and $O5$-planes, J. High Energy Phys. 03 (2016) 109.
[33] H. Hayashi, S.-S. Kim, K. Lee, and F. Yagi, 5-brane webs for 5d $\mathcal{N} = 1$ G_2 gauge theories, J. High Energy Phys. 03 (2018) 125.
[34] H. Hayashi and G. Zoccarato, Exact partition functions of Higgsed 5d T_N theories, J. High Energy Phys. 01 (2015) 093.
[35] H. Hayashi and G. Zoccarato, Topological vertex for Higgsed 5d T_N theories, J. High Energy Phys. 09 (2015) 023.
[36] T. Dimofte, S. Gukov, and L. Hollands, Vortex counting and lagrangian 3-manifolds, Lett. Math. Phys. **98**, 225 (2011).
[37] M. Taki, Surface operator, bubbling Calabi-Yau and AGT relation, J. High Energy Phys. 07 (2011) 047.
[38] M. Aganagic and S. Shakirov, Knot homology and refined Chern-Simons index, Commun. Math. Phys. **333**, 187 (2015).
[39] M. Aganagic and S. Shakirov, Refined Chern-Simons theory and topological string, arXiv:1210.2733.
[40] S.-S. Kim and F. Yagi, Topological vertex formalism with O5-plane, Phys. Rev. D **97**, 026011 (2018).
[41] S. Benvenuti, A. Hanany, and N. Mekareeya, The Hilbert series of the one instanton moduli space, J. High Energy Phys. 06 (2010) 100.
[42] C. A. Keller, N. Mekareeya, J. Song, and Y. Tachikawa, The ABCDEFG of instantons and W-algebras, J. High Energy Phys. 03 (2012) 045.
[43] A. Hanany, N. Mekareeya, and S. S. Razamat, Hilbert series for moduli spaces of two instantons, J. High Energy Phys. 01 (2013) 070.
[44] C. A. Keller and J. Song, Counting exceptional instantons, J. High Energy Phys. 07 (2012) 085.
[45] S. Cremonesi, G. Ferlito, A. Hanany, and N. Mekareeya, Coulomb branch and the moduli space of instantons, J. High Energy Phys. 12 (2014) 103.
[46] H.-C. Kim, J. Kim, S. Kim, K.-H. Lee, and J. Park, 6d strings and exceptional instantons, Phys. Rev. D **103**, 025012 (2021).
[47] V. Mitev, E. Pomoni, M. Taki, and F. Yagi, Fiber-base duality and global symmetry enhancement, J. High Energy Phys. 04 (2015) 052.
[48] Shurcancellation, https://github.com/shichenguw/shurcancellation.
[49] H.-C. Kim, S.-S. Kim, and K. Lee, 5-dim superconformal index with enhanced en global symmetry, J. High Energy Phys. 10 (2012) 142.
[50] C. Hwang, J. Kim, S. Kim, and J. Park, General instanton counting and 5d SCFT, J. High Energy Phys. 07 (2015) 063; 04 (2016) 094(A).
[51] O. Bergman, D. Rodríguez-Gómez, and G. Zafrir, Discrete θ and the 5d superconformal index, J. High Energy Phys. 01 (2014) 079.
[52] H. Hayashi, S.-S. Kim, K. Lee, and F. Yagi, Discrete theta angle from an O5-plane, J. High Energy Phys. 11 (2017) 041.
[53] A. Sen, F theory, and orientifolds, Nucl. Phys. **B475**, 562 (1996).
[54] D. Gaiotto and H.-C. Kim, Duality walls and defects in 5d $\mathcal{N} = 1$ theories, J. High Energy Phys. 01 (2017) 019.
[55] H. Hayashi, S.-S. Kim, K. Lee, and F. Yagi, Dualities and 5-brane webs for 5d rank 2 SCFTs, J. High Energy Phys. 12 (2018) 016.
[56] L. Bao, V. Mitev, E. Pomoni, M. Taki, and F. Yagi, Non-lagrangian theories from brane junctions, J. High Energy Phys. 01 (2014) 175.
[57] S.-S. Kim and F. Yagi, 5d E_n Seiberg-Witten curve via toric-like diagram, J. High Energy Phys. 06 (2015) 082.
[58] R. Feger and T. W. Kephart, LieART—A *mathematica* application for Lie algebras and representation theory, Comput. Phys. Commun. **192**, 166 (2015).
[59] B. Haghighat, A. Iqbal, C. Kozcaz, G. Lockhart, and C. Vafa, M-Strings, Commun. Math. Phys. **334**, 779 (2015).